PREDICTION AND CONTROL
of
FROST FORMATION IN AN AIR TO AIR
HEAT EXCHANGER

A Thesis
Submitted to the Faculty of Graduate Studies
in Partial Fulfillment of the Requirements
for the Degree of
Master of Science
in the
Department of Agricultural Engineering
University of Saskatchewan

by
Myles Richard Leo Bantle

Saskatoon, Saskatchewan

Dedication

This work is dedicated to
my sister, Jacqueline, whose
presence and support encouraged
me through the hard times

and to my grandfather, Leo, who
was my first teacher of engineering.

ABSTRACT

Air-to-air heat exchangers can be used to preheat ventilating air and hence increase the winter ventilation rate in livestock barns; however, frost accumulation is a major problem in this application. Currently available frost control systems operate based on some combination of time, core pressure drop, or exhaust air temperature. These systems do not result in an optimal rate of heat transfer, independent of barn temperature and relative humidity.

In this project, a frost control strategy based on the measured instantaneous rate of heat transfer was studied. The control strategy involved measuring the temperature rise of the cold air stream and controlling the rate of heat transfer by positioning a damper to regulate the mass flow rate of the cold air stream.

As an aid to the design of the controller, a simulation model was developed. The model was based on an existing steady-state model of a condensing heat exchanger. The model was enhanced and changed in order that it could predict the thermal performance of a heat exchanger over time as frost formed in the heat exchanger.

Experiments were conducted with a 472 L/s plate-type commercial heat exchanger. The experiments were used to calibrate the heat exchanger simulation, to validate the simulation model, and to test the proposed frost control strategy.

The simulation model was useful in developing the control strategy and in establishing the control parameters for the prototype controller. Also, the simulation showed that it was not possible to continuously maintain a constant rate of heat transfer which approached the maximum

possible heat transfer rate available from the heat exchanger. The simulation did show that a time average rate of heat transfer approaching the maximum possible heat transfer rate was possible. The calibrated heat transfer model did satisfactorily predict the general trends of the controlled heat exchanger operation. However, there were enough differences between the experimental results and simulation results that significant redevelopments to the simulation heat and mass transfer model will be necessary to obtain good agreement.

In the prototype tests, the prototype controller was confirmed to operate satisfactorily under four widely differing input conditions. Three control parameters were identified as being critical to the design of a heat transfer optimizing controller; the amount of heat transfer degradation permitted before a defrost is initiated, the maximum cold air stream mass flow rate through the heat exchanger permitted just following a defrost; and the rate at which the supply air flow rate is changed.

The proposed control strategy directly measures the instantaneous rate of heat transfer. This enables the optimal average heat recovery to be obtained over a wide range of input conditions. Further development is necessary to establish the optimal control parameters and to complete development of a marketable heat exchanger frost controller.

ACKNOWLEDGEMENTS

The author wishes to express his gratitude to Mr. Ron Otsig who developed and built parts of the data acquisition system and Mr. Louis Roth who assisted in preparing the laboratory test equipment and who prepared the sketches which appear in the thesis manuscript.

The author is indebted to Mr. Miles Jorgenson, Mr. Glen Frehlick and the Prairie Agricultural Machinery Institute, Humboldt for permitting and assisting in the laboratory tests which would not have been possible without the use of their facilities.

The author's supervisor, Professor Ernest Barber, requires special recognition for providing the guidance and freedom that made this project possible. His assistance and patience in preparing the thesis manuscript were much appreciated.

Mrs. Carole Fontaine deserves special thanks for typing and editing the thesis manuscript.

This project was funded by Agriculture Canada Grant #85041 "Microprocessor-based control of heat exchangers" to Professor Ernest Barber.

TABLE OF CONTENTS

1. HEAT EXCHANGERS IN AGRICULTURE 1

1.1 Early Heat Exchanger Research 1

1.2 Thermosiphon Heat Exchanger 2

1.3 Rock Bed Heat Exchangers 3

1.4 McGinnis Shell and Tube Heat Exchanger 4

1.5 Recent Work with Agricultural Heat Exchangers 5

1.6 Frost Control in Agricultural Heat Exchangers 7

2. OBJECTIVES 10

3. HEAT EXCHANGER COMPUTER MODEL 16

3.1 Literature Review 16
3.1.1 Dry Heat Exchanger Model 16
3.1.2 Condensing Heat Exchanger Models 17
3.1.3 Frost Formation 22
3.1.3.1 Early Work 22
3.1.3.2 Frost Models 23
3.1.3.3 Frost Growth Equations 25
3.1.3.4 Density and Thermal Conductivity of Frost 28
3.1.3.5 Pressure Loss 29

3.2 Heat Exchanger Model 32
3.2.1 Condensing Heat Exchanger 32
3.2.2 Convective Heat Transfer Coefficients 35
3.2.3 Frost Formation in the Heat Exchanger 41
3.2.4 Pressure Drop and Mass Flow Equations 47
3.2.5 Air/Water Mixture Thermophysical Properties 49

3.3 Simulation 51

4. FROST CONTROLLER DEVELOPMENT 54

4.1 Background Development 54

4.2 Optimizing Controller 56

4.3 Frost Controller Tested 63

5. PROTOTYPE TESTS 69

5.1 Experimental Test Conditions 69

5.2 Experimental Equipment 70
5.2.1 Overall Test Setup 70
5.2.2 Air Flow Measurement 75
5.2.2.1 Supply Air Mass Flow Measurement 75
5.2.2.2 Exhaust Air Mass Flow Measurement 77
5.2.3 Temperature Measurement 79
5.2.3.1 Air Temperature Measurement 79
5.2.3.2 Core Temperature Measurement 81
5.2.3.3 PAMI Temperature Measurement 83
5.2.4 Bypass Damper System Calibration 84
5.2.5 Condensate Measurement 86
5.2.6 Duct Insulation 86
5.2.7 Measurement of Pressure Drop Across the Core 87
5.2.8 Control and Data Acquisition System 88

5.3 Experimental Test Procedure 89

6. RESULTS, COMPARISONS AND DISCUSSION 91

6.1 Results of Optimizing Controller Operation 91

6.2 Results of Defrost Controller Operation 93

6.3 Comparison of Simulation Results and Experimental Results 100

6.4 Additional Experimental Results 114
6.4.1 Core Temperature Distribution 114
6.4.2 Condensate Accumulation 115
6.4.3 Heat Transfer Rate Balance 116

7. CONCLUSIONS AND RECOMMENDATIONS 120

REFERENCES 124

APPENDIX A Simulation Flow Charts 131

APPENDIX B AD590KF Temperature Sensor Calibration 144

APPENDIX C Test Procedure 149

APPENDIX D Simulation Results 153

APPENDIX E Experimental Results 162

APPENDIX F Simulation Listing 171

LIST OF TABLES

TABLE	DESCRIPTION	PAGE
2.1	Heat Exchanger Physical Data	13
4.1	RUN 0 Input Conditions	59
4.2	RUN 0 Controller Parameters	59
4.3	Summary of Controller Settings	67
5.1	Experimental Test Conditions	71
5.2	Venturi Calibration	77
5.3	Velocity Distribution	80
6.1	Heat Exchanger Thermodynamic Potential	96
6.2	Controller Operating Fraction	97
6.3	Comparison of Maximum and Average Heat Transfer Rates	100
6.4	Outside Air Mass Flow Rate During the Heat Transfer Monitoring State	103
6.5	Time Controller Operated in the Heat Transfer Monitoring State	104
6.6	Average Heat Transfer Rate Comparison	112
6.7	Outlet Air Stream Temperature Comparison	112
6.8	Core Temperature Comparison	113
6.9	Minimum Return Air Stream Mass Flow Rate and Maximum Pressure Drop Across the Hot Side of the Heat Exchanger	114
6.10	Average Condensate Release	115
6.11	Heat Transfer Rate Balance	119

LIST OF FIGURES

FIGURE	DESCRIPTION	PAGE
2.1	Heat Exchanger and Bypass	11
2.2	Heat Exchanger Overall Dimensions	14
2.3	Heat Exchanger Air Streams	15
3.1	Heat Exchanger Processes	33
3.2	Heat Exchanger Surface Contours	38
3.3	Frost Calculation Locations	42
3.4	Frost Front and Condensation Front With No Entrance Effects	46
3.5	Frost Front and Condensation Front With Entrance Effects	46
4.1	Optimizing Controller	57
4.2	Outside Air Mass Flow Rate	60
4.3	Heat Transfer Rate	60
4.4	Return Air Mass Flow Rate	61
4.5	Hot Side Pressure Drop	61
4.6	Controller Flow Chart	68
5.1	Experiment Test Setup	72
5.2	Dimensioned Experiment Test Setup	73
5.3	Core Temperature Sensors	82
5.4	Damper System Calibration	85
6.1	Optimizing Controller: Measured Outside Air Mass Flow Rate	92
6.2	Optimizing Controller: Measured Heat Transfer Rate	92
6.3	RUN 1: Measured Heat Transfer Rate	94
6.4	RUN 2: Measured Heat Transfer Rate	94

LIST OF FIGURES (continued)

FIGURE	DESCRIPTION	PAGE
6.5	RUN 3: Measured Heat Transfer Rate	95
6.6	RUN 4: Measured Heat Transfer Rate	95
6.7	Heat Transfer Rate with Nonoptimized Defrost Controller	99
6.8	Heat Transfer Rate with Optimized Defrost Controller	99
6.9	RUN 4: Predicted Outside Air Mass Flow Rate	106
6.10	RUN 4: Measured Outside Air Mass Flow Rate	106
6.11	RUN 4: Predicted Heat Transfer Rate	107
6.12	RUN 4: Measured Heat Transfer Rate	107
6.13	RUN 4: Predicted Outlet Air Stream Temperatures	108
6.14	RUN 4: Measured Outlet Air Stream Temperatures	108
6.15	RUN 4: Predicted Core Temperature	109
6.16	RUN 4: Measured Core Temperatures	109

1. HEAT EXCHANGERS IN AGRICULTURE

The heat produced in a confinement livestock facility by the animals and the lighting equipment is removed by outside air infiltration, by heat conduction through the building shell and by exhausted ventilation air. During most of the year the heat balance ventilation rate is sufficient to maintain moisture and odor control in the building, but during the winter the heat produced by the animals and the lighting equipment is not always sufficient to permit proper ventilation for moisture and odor control while still maintaining an acceptable indoor air temperature. Farmers have dealt with this problem either by permitting the building environment to be cold, wet and foul smelling or by providing supplemental heat which permits higher ventilation rates. The use of heat exchangers provides an alternative to costly supplemental heat.

1.1 Early Heat Exchanger Research

Giese and Downing (1950) and Giese and Ibrahim (1950) developed and tested a shell and tube heat exchanger. The exchanger consisted of a large outside duct with a number of pipes running down the centre of the duct. The heat exchanger was run in two configurations. The first configuration was a parallel flow arrangement where the fresh air flowed in the small tubes. The second arrangement was a counterflow arrangement where the exhaust air was carried in the small tubes.

The plate type of heat exchanger was then investigated in an attempt to achieve greater heat transfer capacity, to reduce the space requirement and to meet a number of other economic considerations.

The plate type of heat exchanger, consisting of a number of highly conductive plates which separate the hot and cold fluids, had been successfully used in industry and was therefore considered possibly useful in agriculture.

The exchanger developed by Giese and Bond (1952) was constructed from sheets of corrugated aluminum roofing separated by leather spacers. Thirty-two sheets of corrugated aluminum were used. Each sheet was 660 mm X 1829 mm. The heat transfer surface was estimated to be 34 m^2. Giese and Bond concluded that an improved heat exchanger design had been developed since it was more compact than the earlier shell and tube exchanger.

1.2 Thermosiphon Heat Exchanger

After the work of Giese in the early 1950s, little new work was done with agricultural heat exchangers until the mid 1970s when Larkin et al. (1975) introduced the use of a thermosiphon heat exchanger in a poultry house.

The thermosiphon heat exchanger was a bank of finned heat pipes. The evaporator portion of the heat pipe was in the hot (exhaust) air stream and the condenser portion was in the cold (supply) air stream. The evaporation and condensation of the working fluid transfered the heat from the hot air stream to the cold air stream. This arrangement was viable because the thermal conductivity of the heat pipe was several orders of magnitude greater than a solid copper bar of equivalent diameter.

The thermosiphon heat exchanger was simple, easy to clean and compact. These advantages made the thermosiphon more attractive than the

plate type heat exchanger for use in livestock facilities. The thermosiphon heat exchanger was probably not widely used because it was more expensive than a plate type heat exchanger with equivalent capacity.

The problems associated with the thermosiphon heat exchanger were fouling and freezing of the exhaust air passages (Larkin et al., 1975). The freeze-up problem was remedied by installing a thermostat which switched the inlet fan off when the exhaust side temperature decreased below 1.7°C. The performance of the controller was described in detail by Larkin et al. (1975).

Larkin and Turnbull (1977) discussed the effects of core fouling on the heat exchanger performance. They showed that with proper choice of exhaust air filters and the correct maintenance of the filters dust fouling would degrade the heat exchanger performance by only six percent.

The economic benefits of the thermosiphon heat exchanger were calculated by Larkin and Turnbull (1979). The general conclusion of the economic analysis was that for facilities of sufficiently high inside temperature and sufficiently high ventilation requirements the thermosiphon heat exchanger was economically viable.

1.3 Rock Bed Heat Exchangers

Rock bed heat exchangers are regenerative heat exchangers. The simplest regenerative heat exchanger system consists of two regenerators. The hot air stream flows through one regenerator warming the regenerative material while the cold air stream flows through the other regenerator cooling its regenerative material. The heat exchanger provides heat continuously by alternating the air streams between the two regenerators.

Witz et al. (1976) studied the performance of a rock bed heat exchanger used to heat a building which housed beef animals. The heat exchanger performed well for outside temperatures above -26°C but frost accumulation became a problem at colder temperatures. Witz et al. found that by applying salt to the rocks the frost accumulation problem could be solved.

Lampman and Moysey (1984) performed field tests on a rock bed exchanger which consisted of two 1200 mm square insulated boxes. This exchanger was installed in a swine barn. The depth of the rocks in the boxes was 300 mm. The measured and calculated heat exchanger sensible effectivenesses were compared and adequate agreement was found. Sensible effectiveness values of 60% or better were achieved. Lampman and Moysey pointed out, as Witz et al. did, the problem of frost accumulation.

1.4 McGinnis Shell and Tube Heat Exchanger

A 2350 L/s shell and tube heat exchanger was developed by McGinnis et al. (1983). The heat exchanger shell was 1.2 m x 1.2 m x 2.5 m. Within the shell were 196 polyethylene tubes 50 mm in diameter and 1.5 m long. The exhaust air was circulated through the tubes while supply air flowed around the outside of the tubes.

The unit was installed in a 1000 hog finishing barn and tested during the winter of 1980. During the testing it was found that fouling was not a problem since condensation in the unit tended to clean the tubes. The recommended cleaning schedule according to McGinnis et al. (1983) was an inside washing once during, and once at the end of the heating season.

The heat exchanger tested did experience ice formation but the vertical tube orientation and the smooth tube walls tended to facilitate the dispersal of the ice. As well, the heat exchanger was fitted with an

automatic defrost controller that would stop the supply air flow if the pressure in the exhaust plenum exceeded 100 Pa. However, for the tests conducted the automatic defrost was not utilized. The measured effectiveness of the heat exchanger was around 30 percent. McGinnis et al. (1983) also made measurements on a 36 tube prototype heat exchanger. The effectiveness of this unit averaged 32 percent over the test period.

McGinnis (1984) developed a mathematical model of a shell and tube, crossflow-counterflow heat exchanger. The model was developed by dividing the heat exchanger into a number of control volumes. For each control volume, an energy balance and a mass balance were written. The energy balance was performed by equating the change in enthalpy of the two air streams with the heat transferred between the two airstreams. The mass balance equation was used to compute the rate of condensation which in turn was used in the energy balance equations to compute the outlet temperature of the supply air stream and the outlet temperature of the exhaust air stream. The temperatures were computed in an interative fashion. The development of the heat transfer coefficients and the diffusion coefficients was discussed by McGinnis.

Limited test results were presented to compare the model and the working unit. Comparison of the heat exchanger effectiveness and the heat recovery rate indicated good agreement between the model and the working unit.

1.5 Recent Work with Agricultural Heat Exchangers

Sokhansanj et al. (1980) presented a method to size a heat exchanger for a particular barn. The inter-relationship of ventilation rate, heat exchanger size and supplemental heat required was shown. Criteria were developed to evaluate the economic value of different

heat exchangers for a turkey growing building.

A compact, cross-flow heat exchanger was developed and tested by Swift et al. (1981). The heat exchanger drew exhaust air from a 100-cow dairy barn and provided warmed fresh air to an attached calf nursery. The heat exchanger was run significantly unbalanced which almost eliminated freeze up problems. Experimental results showing the outlet air stream temperatures, the heat exchanger effectiveness and the heat transfer rate were given.

A central ventilation heat recovery system for an eight room farrowing-nursery facility was developed and studied by Meyer et al. (1983). In addition to the eight rooms housing the livestock, two other rooms were used for ventilation. One room, the heat exchanger room, contained eight 300 mm diameter polytubes. The polytubes carried fresh air from the attic through the length of the exchanger room. At the same time warm inside air was drawn through the heat exchanger room and exhausted to the outdoors; thus, the heat exchanger room was merely a large heat exchanger. The tempered cold air from the heat exchanger room was moved through a second room and then distributed to the eight rooms housing the livestock. Meyer et al. cited advantages of the polytube heat exchanger including greater surface area, fewer leaks, lower costs and higher effectiveness compared to a hollow wall heat exchanger.

Plans for home built heat exchangers for agricultural facilities are available. Hodgkinson and Small (1984) outlined a design procedure for a home built heat exchanger which has a single cold air passage and a single warm air passage. The thermal performance of three different home built heat exchangers was reported by Hodgkinson and Small.

Most engineers cite energy savings as the primary justification for the use of heat exchangers. Thornton (1983) after surveying 46 Alberta farmers found that only four percent of them bought heat exchangers to save energy. Most bought heat exchangers to dry out the barn and to improve ventilation. Thornton also monitored the performance of three commercial heat exchangers and one home built heat exchanger. He provided specific comments about the operation of the four heat exchangers individually and general comments applicable to all the heat exchangers.

Saskatchewan Agriculture (1983) provided a bulletin which addressed a wide range of topics regarding the use of heat exchangers in livestock facilities. Their bulletin discussed:

(1) principles of ventilating and heating livestock buildings,
(2) different types of heat exchangers available,
(3) commercially available heat exchangers,
(4) heat exchanger effectiveness,
(5) sizing a heat exchanger,
(6) air distribution in the barn, and
(7) economics of heat exchangers.

The bulletin contains sufficient breadth to make it a very good place to start when considering the use of a heat exchanger in a livestock facility.

1.6 Frost Control in Agricultural Heat Exchangers

The literature dealing with agricultural heat exchangers over and over mentions the problems associated with frost accumulation. Three general methods have been identified to control the frost accumulation.

The methods identified were outside air preheat, air flow rate imbalance and defrost cycle.

Sufficiently preheating the outside air ensures that all the surfaces of the heat exchanger core are above 0°C. Since all the core surfaces are above 0°C no frost can accumulate. The primary drawback of this method is that the thermodynamic potential of the heat exchanger is reduced. The advantage of this method is that the heat exchanger operates continuously without interruption.

The air flow rate imbalance method, similar to the preheat method, keeps the surfaces of the heat exchanger core above 0°C. The surfaces are kept above 0°C by reducing the cold air stream flow rate. The cold air stream flow rate can be reduced by restricting the flow or by bypassing some of the flow. The Blackhawk, Koenders and Better Air commercial heat exchangers control frost accumulation by air flow rate imbalance. The air flow rates are imbalanced by manually dampering down the flow of cold air. Mackay Equipment Sales Ltd., Saskatoon, using a Z-Duct commercial heat exchanger experimented with a different air flow rate imbalance method. Their method imbalanced the air flow rates by bypassing a portion of the cold air stream around the heat exchanger. The amount of bypass was automatically controlled based on the outlet temperature of the hot air stream. Van Lambalgen et al. (1986) studied this control strategy and showed that it does not control frost accumulation. The major drawback of the air flow rate imbalance method except for the Mackay Equipment Sales Ltd. system is that more air is withdrawn from the building than is returned and thus the additional outside air must be brought in through separate vents.

Defrosting the heat exchanger periodically keeps in check the

adverse effects of frost. The major problem with defrosting is deciding how long to let the frost form before defrosting and secondly how long to let the heat exchanger defrost. The simplest method of defrost is a timed defrost cycle. Del-Air commercial heat exchangers use a timed defrost. Defrosting is accomplished by reversing the cold air fan motor for eight minutes every hour. This method is simple but is not very efficient except under the worst frost forming conditions. A much more efficient method is to measure the pressure drop aross the hot side of the heat exchanger and initiate defrost whenever the pressure drop exceeds some threshold value. The defrost is terminated when the pressure drop reduces to the pressure drop of an unfrosted heat exchanger. Van Lambalgen et al. (1986) tested a pressure controlled defrost system and found it very efficient but expensive to implement. Defrost can be accomplished by reducing the cold air stream flow rate or by increasing the cold air stream temperature.

The three general methods for controlling frost accumulation mentioned above have all been used in agricultural heat exchangers in some form or another but no controller has yet been developed which is both inexpensive and efficient.

2. OBJECTIVES

The winter ventilation of intensive livestock houses can be very costly. Consequently, most livestock houses are ventilated at very low rates during the winter. Ventilation at such low rates generally results in less than ideal conditions for the animals housed. Heat exchangers can be used to permit higher ventilation rates without higher heating costs, but heat exchanger use is not without problems. Frost tends to accumulate in the exhaust air passages of the heat exchanger. The accumulation of frost causes the exhaust air flow through the heat exchanger to be restricted and the effective conductivity of the heat exchanger plates to be reduced.

The main objective of this study was to investigate the frost formation process in a heat exchanger and to design and test a suitable frost control strategy that would maximize the overall rate of heat transfer in a heat exchanger. Although several methods are available for controlling the heat transfer in a heat exchanger, imbalanced air flow rates was selected. The air flow rates were imbalanced by modulating a damper which bypassed a portion of the cold air stream around the heat exchanger (see Figure 2.1).

Specifically, the following two hypotheses were tested:

(1) An existing computer model developed by Besant and Bugg (1981), with modification, will simulate the thermal performance of a heat exchanger operating under frost forming conditions and under frost control.

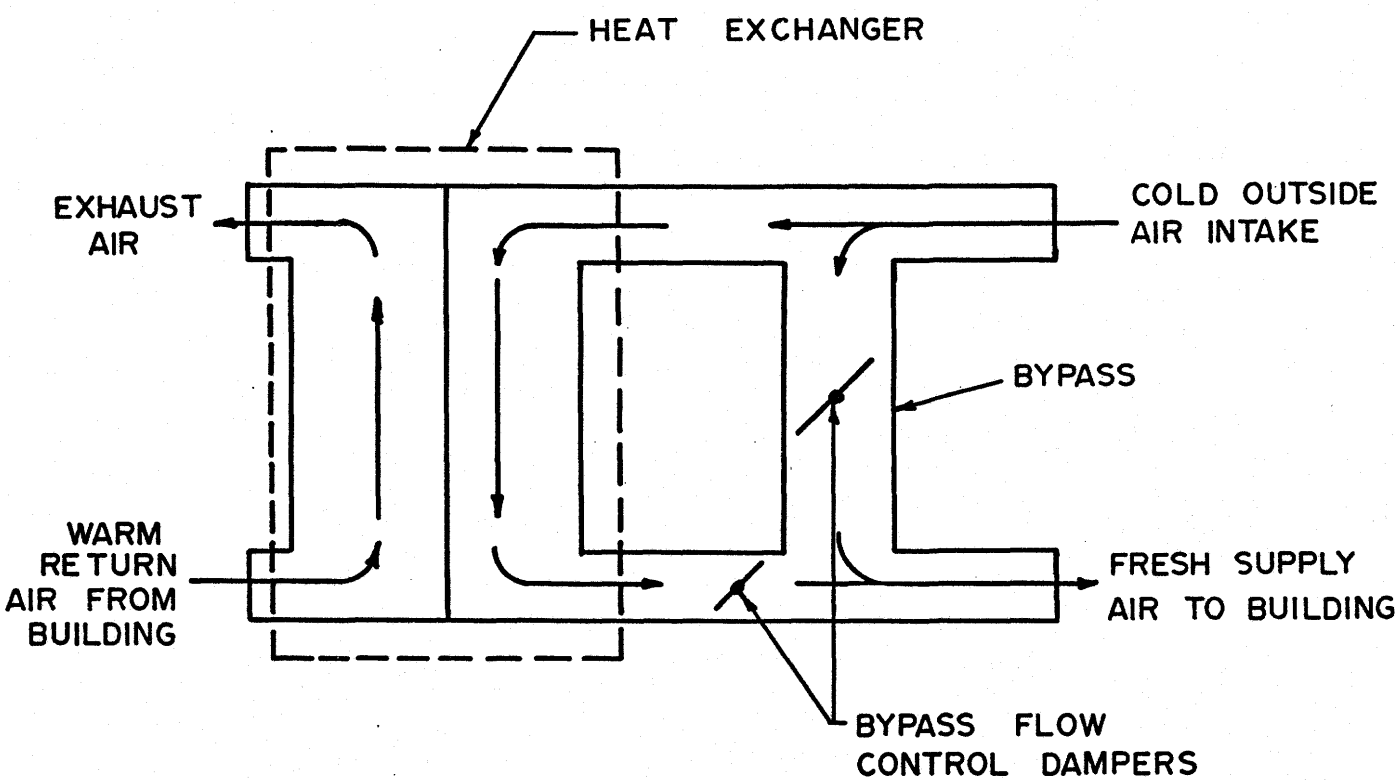

FIGURE 2.1

Heat Exchanger and Bypass

(2) A controller can be designed and implemented on a plate type commercial heat exchanger operating under frosting conditions that will find and continuously maintain a constant rate of heat transfer. The constant rate of heat transfer achieved will approach the maximum thermodynamic potential of the heat exchanger and will increase the efficiency of the heat exchanger compared to commonly used frost control strategies.

The heat exchanger chosen to be modelled and tested was a 472 L/s capacity Z-Duct commercial heat exchanger. This heat exchanger was selected because an 1180 L/s capacity heat exchanger of identical construction was installed in the University of Saskatchewan Campus Dairy Barn. This larger heat exchanger could have been used to field test the controller. The exact physical properties of the heat exchanger are given in Table 2.1. Figure 2.2 shows the heat exchanger overall dimensions. Figure 2.3 labels the different airstreams entering and leaving the heat exchanger.

TABLE 2.1

Heat Exchanger Physical Data

DESIGNER	DesChamps Laboratories Inc. 5-B Merry Lane E. Hanover, N.J.
MANUFACTURER	Fabrication Z-Air Inc. 690 Place Trans-Canada Longueuil, Quebec
MODEL	74-1000AA6 DAV
SPECIFICATIONS*	Spacing of Exchanger Surfaces 5.4 mm Fouling Factor 0.0 m^2 K/W Thickness of Exchanger Surfaces** 0.152 mm Conductivity of Core Material** 208 W/mK Length of Exchanger Surfaces 0.880 m Width of Exchanger Surfaces 0.408 m Number of Hot Passages 49 Number of Cold Passages 50 Number of Heat Exchange Surfaces 98

* Measured unless otherwise noted.
** Private communication with DesChamps Laboratories Inc.

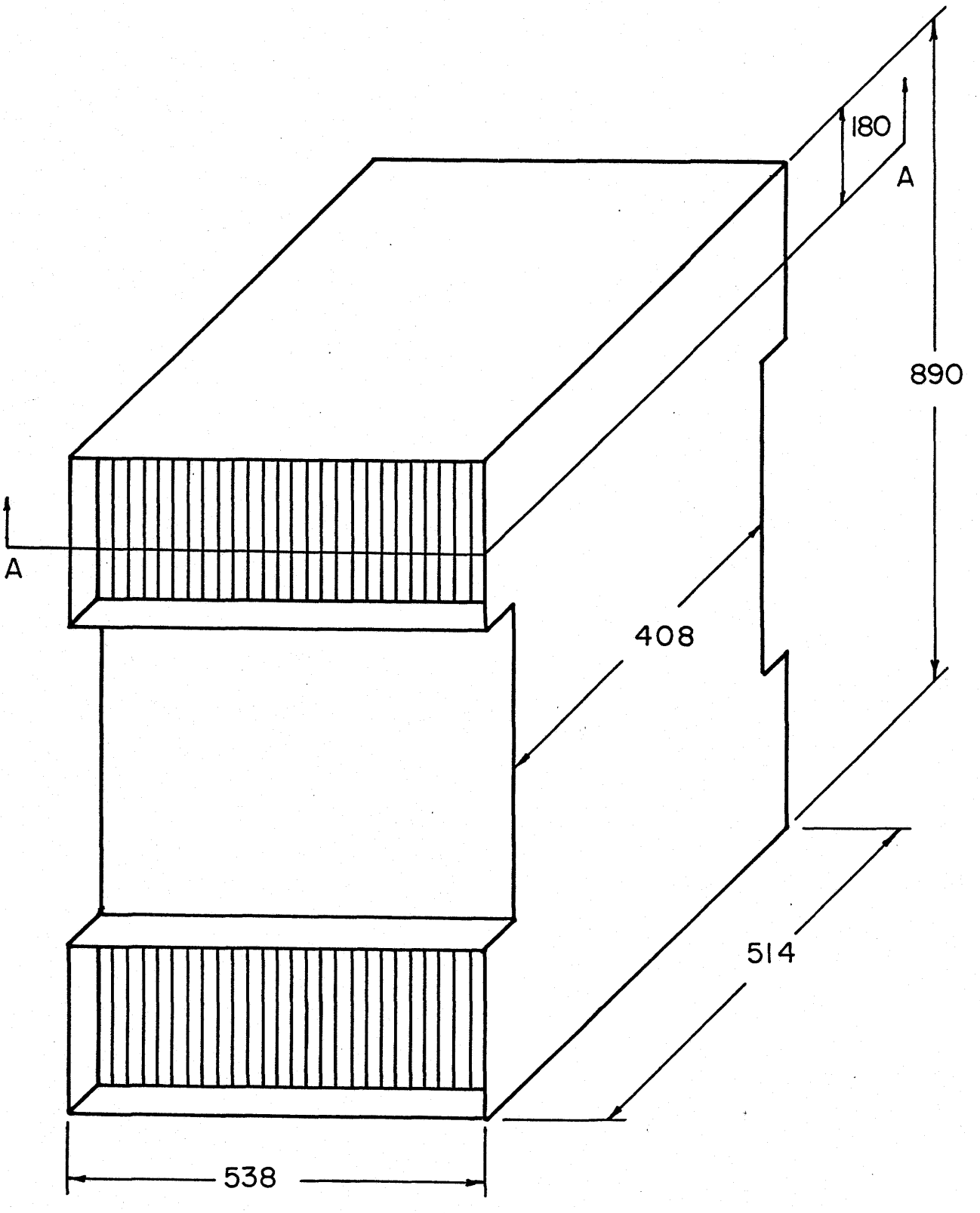

FIGURE 2.2

Heat Exchanger Overall Dimensions

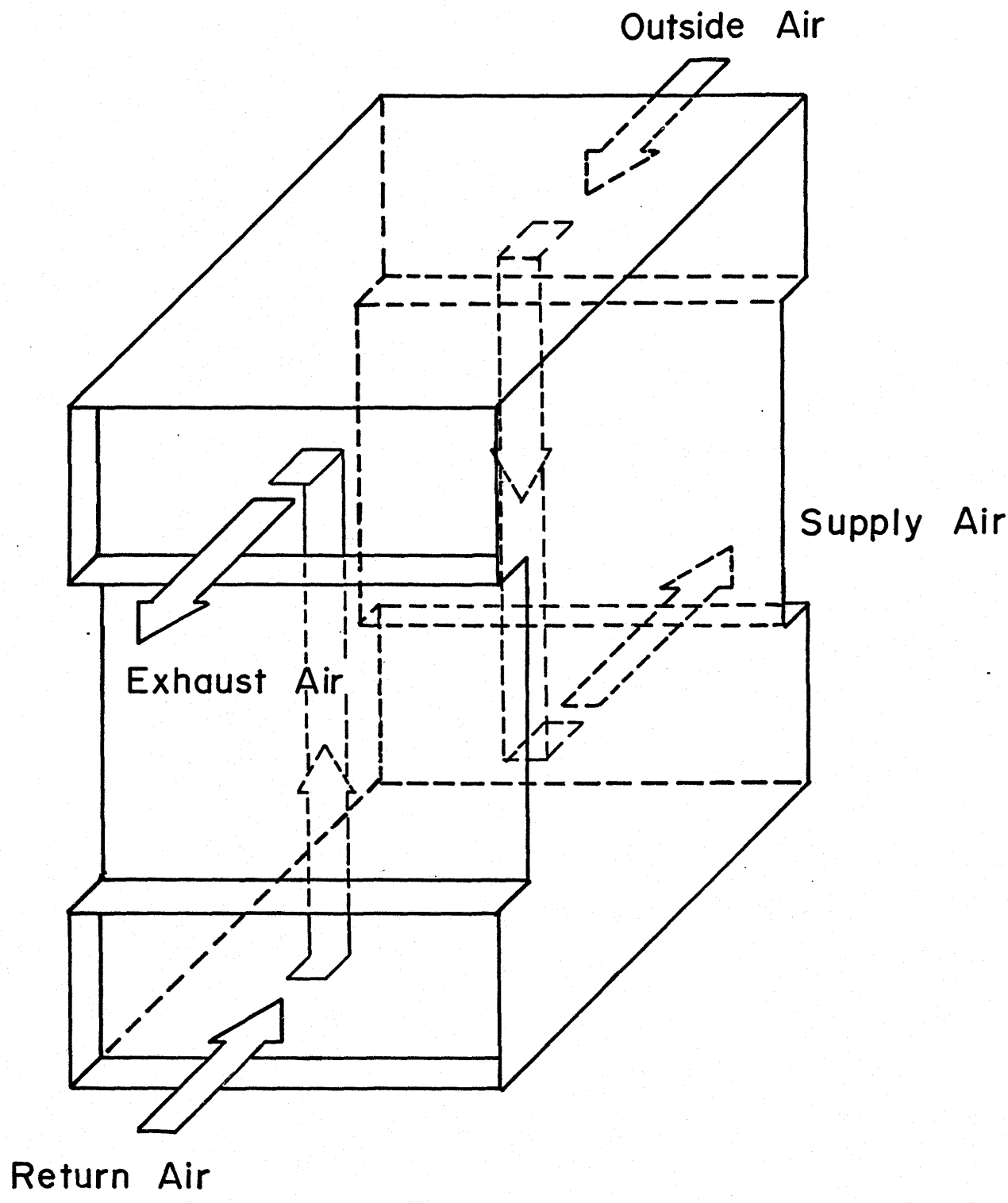

FIGURE 2.2

Heat Exchanger Air Streams

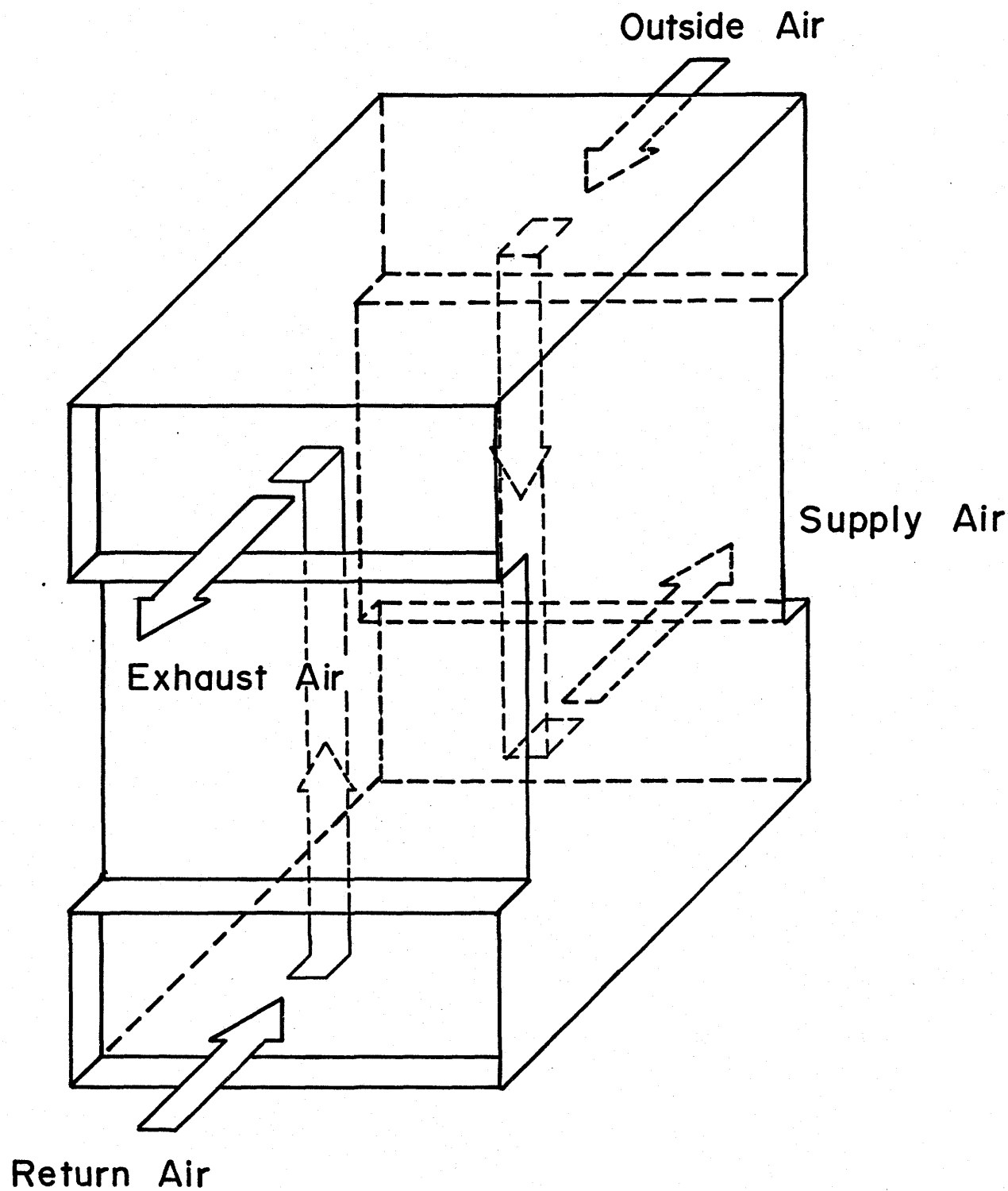

FIGURE 2.3

Heat Exchanger Air Streams

3. HEAT EXCHANGER COMPUTER MODEL

3.1 Literature Review

Summarized below is the literature that was found to relate to the development of a frosting and condensing heat exchanger model.

3.1.1 Dry Heat Exchanger Model

Calculation of the heat transferred between two single phase fluids in a counterflow heat exchanger is well known and can be found in most introductory heat transfer texts such as Karlekar and Desmond (1977).

The ability of the heat exchanger to transfer heat is determined by the overall heat transfer coefficient.

$$\frac{1}{U} = \frac{1}{h_h} + \frac{t_p}{k_p} + \frac{1}{h_c} + R_F \qquad 3.1$$

where

U = overall heat transfer coefficient ($W/m^2\ K$)

h_h = convection heat transfer coefficient on the hot side ($W/m^2\ K$)

h_c = convection heat transfer coefficient on the cold side ($W/m^2\ K$)

t_p = separating wall thickness (m)

k_p = separating wall thermal conductivity ($W/m\ K$)

R_F = fouling factor ($m^2\ K/W$)

The heat transferred by a heat exchanger can be calculated if the heat exchanger effectiveness is known. The heat exchanger effectiveness is defined as:

$$\varepsilon = \frac{\left[\begin{array}{c}\text{temperature change of the fluid} \\ \text{with minimum capacity rate}\end{array}\right]}{\left[\begin{array}{c}\text{the largest temperature} \\ \text{difference in the heat exchanger}\end{array}\right]}$$

The effectiveness of a counterflow heat exchanger with only sensible heat transfer is calculated using equation 3.2.

$$\varepsilon = \frac{1 - \exp\left\{-\left[UA/C_{min}\right]\left[1 - \left[C_{min}/C_{max}\right]\right]\right\}}{1 - \left[C_{min}/C_{max}\right]\exp\left\{-\left[UA/C_{min}\right]\left[1 - \left[C_{min}/C_{max}\right]\right]\right\}} \qquad 3.2$$

where

ε = heat exchanger effectiveness

U = overall heat transfer coefficient ($W/m^2\ K$)

A = heat transfer area (m^2)

C_{min} = minimum heat capacity rate (W/K)

C_{max} = maximum heat capacity rate (W/K)

The heat transfer rate is calculated using equation 3.3.

$$Q = \varepsilon\, C_{min}\, (T_{h,i} - T_{c,i}) \qquad 3.3$$

where

Q = heat transfer rate (W)

ε = heat exchanger effectiveness

C_{min} = minimum heat capacity rate (W/K)

$T_{h,i}$ = temperature of the hot fluid at the inlet (K)

$T_{c,i}$ = temperature of the cold fluid at the inlet (K)

Knowing the heat capacity rates, the heat transfer rate, and the inlet fluid temperatures, then the outlet fluid temperatures can be calculated.

3.1.2 Condensing Heat Exchanger Models

Calculation of the heat transfer rate in a condensing heat exchanger can proceed in roughly two directions. The heat transfer rate can be calculated using the log mean enthalpy difference and Colburn j factors or by using control volume equations.

Guillory and McQuiston (1973) showed how the log mean enthalpy difference and the Colburn j factors could be used to design a condensing coil.

Guillory and McQuiston started their analysis by pointing out that the most common methods used to design dehumidifying coils involve an analogy between the dry coil operation and the wet coil operation.

$$Q_t = h_t A \Delta t_m \qquad 3.4$$

where

Q_t = heat transferred by a dry coil (W)

h_t = sensible convective heat transfer coefficient (W/m^2 K)

A = heat transfer area (m^2)

Δt_m = log mean temperature difference (K)

Karlekar and Desmond (1977) derived the log mean temperature difference.

$$Q_i = h_i A \Delta i_m \qquad 3.5$$

where

Q_i = heat transferred by a wet coil (W)

h_i = enthalpy convective heat transfer coefficient ($kg/m^2 sec$)

A = heat transfer area (m^2)

Δi_m = log mean enthalpy difference (J/kg)

As Guillory and McQuiston pointed out, this method can be justified on theoretical grounds since the differential energy conservation equation for sensible heat transfer and the differential energy conservation equation for total energy transfer in a system involving mass diffusion

are mathematically identical. The sensible convective heat transfer coefficient in Equation 3.4 was related to the enthalpy convective heat transfer coefficient using Equation 3.6.

$$h_i = h_{t/C_p} \qquad 3.6$$

where

h_i = enthalpy convective heat transfer coefficient ($kg/m^2 sec$)

h_t = sensible convective heat transfer coefficient ($W/m^2\ K$)

C_p = specific heat at constant pressure (J/kg K)

But measurements made by Guillory and McQuiston (1973) showed that for the range of Reynolds numbers tested the use of dry heat transfer data in the design of wet exchangers can result in the heat transfer area being overestimated and the pressure drop being underestimated. McQuiston (1976), Tree and Helmer (1976), McQuiston (1978a) and McQuiston (1978b) presented the Colburn j factors for parallel plate exchangers and for a variety of plate-fin-tube coils. These studies indicated that the heat and mass transfer coefficients could be affected by the presence of condensation.

Anonymous (1965) and Demetri and Siegel (1970) describe a finite difference model developed from the control volume equations that predicted the dynamic thermal performance of a compact heat exchanger with condensation occurring. The model divided the heat exchanger into two parts. One part, called the precooling region, was where both the hot and cold fluid were in a single phase. The second part, called the condensing region, was where one of the fluids was condensing. Though it was not entirely clear it appeared that the boundary between the precooling region and the condensing region occurred at the point where

the condensing fluid bulk temperature reached the dewpoint. The energy equations and the specific heat equation in the wet region were different from those used in the dry region. The energy equations had an extra term which accounted explicitly for the condensation. The specific heat equation contained an enhancement to recognize the increase in specific heat due to the condensation. An extension of the work of Anonymous (1965) and Demetri and Siegel (1970) was given by Duleba and Lloyd (1977).

Another heat exchanger model which broke the heat exchanger into a wet region and a dry region was developed by Besant and Bugg (1981). The model consisted of seven equations that were solved simultaneously. Three of the equations described the heat transfer in the dry region and three other equations described the heat transfer in the wet region. The seventh equation of the set defined the interface between the dry and the wet regions. The heat transfer coefficient in the wet region was calculated by multiplying the dry heat transfer coefficient by an enhancement factor to account for the condensation.

$$h_{wet} = \left(\frac{di}{dT}\right) \frac{h_{dry}}{C_p(1+W)} \qquad 3.7$$

where

h_{wet} = enhanced convective heat transfer coefficient (W/m^2 K)

i = moist air stream enthalpy (J/kg)

T = moist air stream temperature (K)

h_{dry} = convective heat transfer coefficient for a noncondensing flow (W/m^2 K)

C_p = specific heat of the moist air stream (J/kg K)

W = humidity ratio

Maclaine-cross and Banks (1981) developed a linear approximate model for wet surface heat exchangers. The model was based on ten assumptions, the most important assumptions being:

(1) the specific enthalpy of moist air was a linear function of the air temperature and the air humidity ratio;
(2) the moisture content of the air in equilibrium with the water surface was a linear function of the surface temperature.

Equations for the moist air wet bulb depression and the moist air wet bulb outlet temperature were developed. The model of Maclaine-cross and Banks provided a simplified method for calculating the outlet conditions from a wet plate heat exchanger.

Kettleborough and Hsieh (1983) also developed a model for a wet plate heat exchanger. Their model was formulated by dividing the plate area into a number of small elements. Each element was divided into three control volumes: one represented the air stream to which the liquid water evaporated, another represented the separating plate and water film and the third control volume represented the unsaturated air stream. For each control volume a heat and mass balance was done. The analysis assumed that the sensible heat transfer coefficient in the wet passages had approximately the same characteristics as the sensible heat transfer coefficient in the dry passages. The mass transfer coefficient was determined using the Lewis relation. Kettleborough and Hsieh solved the equations on a computer and showed their calculations to be eight percent higher than measurements made by Pescod (1968) and Chan (1973).

Heat transfer through an impermeable wall between a condensing flow and a noncondensing flow results in a problem when using the control volume equations. The heat transfer involving the condensing flow

should be analyzed using enthalpy potential but the heat transfer involving the dry fluid should be analyzed using temperature potential. Kreid et al. (1978) presented a method whereby the heat transfer parameters in the dry region were modified so that the enthalpy potential was applied throughout the heat exchanger. Besant and Bugg (1981) took an opposite approach and modified the heat transfer parameters in the wet region so that the temperature potential was applied throughout the heat exchanger.

3.1.3 Frost Formation

The difficulty in modelling the frost formation in a heat exchanger was well expressed by Gates et al. (1967):

> The analytical problems involved in analyzing a cooling coil under frosting conditions are made quite complex by the continually changing geometry due to the increase in frost layer thickness. In addition, the problem is three dimensional and transient in nature. (p. I.2.1)

The literature which was available on frost properties and frost formation is discussed below.

3.1.3.1 Early Work

Beatty et al. (1951) predicted the frost height by representing the frost layer as a conduction resistance of uniform conductivity. The heat delivered to the frost-air interface was assumed to be all conducted through the frost layer.

$$h_i (i_a - i_f) = k_f \frac{(t_f - t_s)}{x} \qquad 3.8$$

where

h_j = coefficient of enthalpy transfer (kg/sec)

i_a = bulk air stream enthalpy (J/kg)

i_f = enthalpy of saturated air at the frost-air interface temperature (J/kg)

k_f = thermal conductivity of frost (Wm/K)

t_f = temperature at air-frost interface (K)

t_s = temperature of metal surface (K)

x = frost thickness (m)

Stoecker (1957), when studying a finned coil operating under frost forming conditions, indicated that the factors most affected by frost formation are the heat transfer coefficient and the pressure drop across the coil. The tests performed by Stoecker showed that the overall heat transfer coefficient increased initially and then slowly decreased as the frost accumulated. For constant volume flow the pressure drop across the core increased at an increasing rate with time. Stoecker (1960) examined the frost forming on a bare tube under natural convection. He observed that the first frost that formed was granular and fluffy but that as time progressed the frost became increasingly like ice.

The work of Beatty and Stoecker represents some of the early work addressing the problems associated with frost formation in refrigeration and air conditioning equipment.

3.1.3.2 Frost Models

Yonko and Sepsy (1967) proposed a frost model which modelled the frost as a cubic lattice of uniform spherical ice particles in a surrounding gas. The thermal conductivity as a function of frost density

was predicted by Yonko and Sepsy's model and found to agree reasonably well with the measurements made by other researchers. Biguria and Wenzel (1970) predicted the thermal conductivity of frost using equations developed by other researchers for the conductivity of a two-phase composite material. Both Yonko and Sepsy, and Biguria and Wenzel modelled the frost layer as a composite material without considering the processes occurring in the frost.

Brian et al. (1969) used heat and mass balance equations to predict the frost density and height. The difficulty with the model was that initial values of frost density and frost thermal conductivity had to be inputted. Brian et al. (1970) extended the model to permit density gradients in the frost layer.

Parish and Sepsy (1972) numerically modelled the frost forming on a cylinder. They assumed the frost layer was composed of cylindrical shells. Each shell was broken into a number of annular segments. The frost properties were assumed uniform in each segment. Using this frost model and three boundary equations, the energy, momentum, diffusion and continuity equations, the frost height was numerically solved for.

Yamakawa and Ohtani (1972) proposed two frost models. In both models the frost layer was considered composed of frost columns and the frost thermal conductivity was input. In one model, the conductivity of the frost columns was an average experimentally measured frost conductivity. In the other model the frost columns were ice and the thermal conductivity was taken as the thermal conductivity of ice multiplied by a correction factor. For both models, the frost layer properties were predicted by applying heat and mass transfer equations.

Jones and Parker (1975) proposed a model that treated the frost layer as a porous substance. Water vapor was considered to be transported to the surface like any other surface but the vapor transported through the surface was divided into two parts. Some of the vapor diffused into the layer and increased the frost density while the remainder collected on the surface and increased the frost height. The unique feature of their model was that it did not require constant inputs such as airstream humidity ratio but could accommodate nonconstant inputs.

Hayashi et al. (1977) studied the frost layer growth by considering the frost layer to be a collection of ice columns. Hayashi et al. assumed that after the initial frost columns were deposited the frost grew from the base of the columns and the top of the columns without increasing the column diameter. Yamakawa and Ohtani (1972), who also used an ice column frost model, had assumed the diameters of the frost columns increased as the frost grew.

An equation for the frost growth rate was developed by Schneider (1978). In order to develop this equation he assumed that the frost was a collection of needles through which all the latent heat of sublimation was conducted.

3.1.3.3 Frost Growth Equations

The simplified frost model of Scheider (1978) lead to an equation for the frost height on a cooled tube.

$$x_F = 0.465\left[\frac{k_l}{\Delta h_s \rho_l}\,\tau\,(t_F - t_W)\right]^{1/2}\left[\frac{\tau}{3600}\right]^{-0.03}\left[t_F - t_W\right]^{-0.01}\,\Pi^{0.25}\,F_t \qquad 3.9$$

where

x_F = frost thickness (mm)

k_l = thermal conductivity of water-ice (W/mm K)

Δh_s = latent heat of sublimation (J/kg)

ρ_l = density of water-ice (kg/mm^3)

τ = time (s)

t_F = frost surface temperature (K)

t_W = wall temperature (K)

$$\Pi = \frac{P - P'_F}{P' - P'_F} \quad \text{(ratio of supersaturation)} \qquad 3.10$$

where

P = partial vapor pressure of air (Pa)

P' = vapor pressure of saturated air (Pa)

P'_F = pressure of saturated vapor at the frost surface temperature (Pa)

$$F_t = 1 + 0.052 \frac{t - t_M}{t_M - t_W} \qquad 3.11$$

where

t = air temperature (K)

t_M = melting point temperature of water-ice (K)

t_W = wall temperature(K)

Equation 3.9 was derived based on experiments on a cylindrical tube of 47.5 mm O.D. The tests were run over a range of air velocities from 1.2 m/s to 10 m/s, air temperatures from 5°C to 15°C, relative humidities from 50 percent to 100 percent and tube temperatures between -5°C and -30°C. Schneider compared the calculated frost thickness with the experimentally measured values of other researchers and found good

agreement. Schneider observed that the frost thickness was independent of the test surface, vapor pressure difference between the air stream and the frost surface; and the Reynolds number. The key factors he found were the ratio of supersaturation and the capacity of the frost to conduct the heat of sublimation.

White and Cremers (1981) developed equations for frost thickness and density. They pointed out that after an initial transient period the rates of heat transfer and condensation became constant. They also showed that for steady overall heat and mass transfer the density and frost thickness both increased with the square root of time. Measurements were made to show the validity of the square root relation.

Experiments performed by Schulte and Howell (1982) on a flat plate showed that the frost thickness was generally greatest near the leading edge of the plate and decreased along the length of the plate. Schulte and Howell specifically studied the effect of the airstream turbulence intensity on the frost growth rate. They found that the turbulence intensity had no measureable effect on the frost growth rate but that the air stream humidity ratio, the air stream velocity and the plate temperature had a significant effect on the frost growth rate.

A dimensional analysis of the key parameters that influenced frost density and frost growth was done by Tokura et al. (1983). An experimental study was carried out on a cooled vertical plate in free convection and correlations were developed between the different dimensionless parameters.

O'Neal and Tree (1984) studied the effect of various parameters on the rate of frost growth and the frost density on a vertical plate. Tests were performed for plate temperatures from -5°C to -12°C, air humidity ratios from 0.00382 to 0.00514, Reynolds numbers from 4400 to

15900 and air temperatures from 5°C to 12°C. An empirical correlation relating frost height to; time, Reynolds number, plate temperature and air humidity was developed by O'Neal and Tree.

$$x_f = 0.466 \left(\frac{t}{1hr}\right)^{0.663} Re^{0.393} \left(\frac{T_o - T_p}{T_o}\right)^{0.705} \left(\frac{W_a - W_o}{W_o}\right)^{0.098} \qquad 3.12$$

where

x_f = frost height (mm)

t = time (hr)

Re = Reynolds number (based on hydraulic diameter)

T_o = freezing temperature of water (K)

T_p = plate temperature (K)

W_o = humidity ratio of saturated air at 0°C

W_a = humidity ratio of the air stream

3.1.3.4 Density and Thermal Conductivity of Frost

Hosoda and Uzuhashi (1967) developed an experimental equation relating the frost density to the cooling surface temperature and the air stream velocity.

$$\rho = 340 \left| t_p \right|^{-0.445} + 85V \qquad 3.13$$

where

ρ = density of frost (kg/m^3)

t_p = cooling surface temperature (°C)

V = air stream velocity (m/s)

Equation 3.13 was developed for air temperatures between 0°C and 10°C, air humidities between 50 percent and 80 percent, and air velocities of 1 m/s, 3 m/s and 5 m/s.

Yonko and Sepsy (1967) summarized the investigations of frost

thermal conductivity and frost density by other researchers. Yonko and Sepsy also made their own measurements and devised their own correlation of frost thermal conductivity and frost density.

$$k_f = 0.0242 + 7.22E\text{-}04\rho + 1.18E\text{-}06\rho^2 \qquad 3.14$$

where

k_f = frost conductivity (W/m K)

ρ = frost density (kg/m^3)

ρ < 577 kg/m^3

Brian et al. (1969) studied frost formation on a copper plate at -193°C. His studies showed that the rate of the densification of the frost layer was very sensitive to the frost surface temperature; the colder the frost surface, the less dense the frost.

The frost density as a function of airstream velocity, airstream humidity, plate temperature, boundary layer (untripped - artificially tripped) and frost surface temperature was measured by Bigura and Wenzel (1970). They found for moist air flow over a brass plate that the density varied along the plate. As well they found that for the lowest air velocities and the lowest frost surface temperatures the lowest frost densities resulted.

Other investigations of the correlation of frost density with frost thermal conductivity were done by Yamakawa et al. (1972), Gatchilov and Ivanova (1979) and Marinyuk (1980).

3.1.3.5 Pressure Loss

Experimental results showing the pressure drop across a heat exchanger as a function of frost accumulation are not very abundant.

Using coils with fin spacings of 6.4 mm and 2.8 mm Stoecker (1957) measured the constant volume flow rate pressure drop across the coil as a function of the weight of frost on the coil. The measurements indicated that the pressure drop increased at an increasing rate as the weight of frost accumulation increased.

Pressure drop measurements made on extended surface heat exchangers with fin spacings between 2.1 mm and 12.7 mm and with between one and six tube rows lead Gates et al. (1967) to the following equation:

$$\Delta p = \Delta p_i \, 10^{M} \qquad 3.15$$

where

Δp = pressure drop across the coil (Pa)

Δp_i = pressure drop across the coil when unfrosted (Pa)

M = exponent which relates pressure drop with time (hr^{-1})

τ = time (hr)

Gates et al. developed tables of the exponent M for different heat exchanger configurations. The conditions under which this equation applies were not clearly outlined by Gates et al.

The flow-stream pressure-drop through a heat exchanger core can be calculated using a relation given by Kays and London (1984).

$$\Delta p = \frac{G^2 v_1}{2} \left[(K_c + 1 - \sigma^2) + 2 \left(\frac{v_2}{v_1} - 1 \right) + f \frac{A}{A_c} \frac{v_m}{v_1} \right. \qquad 3.16$$

$$\left. - (1 - \sigma^2 - K_e) \frac{v_2}{v_1} \right]$$

where

Δp = pressure difference (Pa)

G = exchanger flow stream mass velocity $(W/A_c)(kg/m^2s)$

v_1 = specific volume of entering fluid (m^3/kg)

v_2 = specific volume of leaving fluid (m^3/kg)

v_m = mean specific volume (m^3/kg)

K_c = contraction loss coefficient for flow at heat exchanger entrance

σ = ratio of free flow area to frontal area (A_c/A_{fr})

f = mean friction factor, defined on the basis of local surface shear stress

A = exchanger total heat transfer area on one side (m^2)

A_c = exchanger minimum free-flow area (m^2)

A_{fr} = exchanger total frontal area (m^2)

K_e = expansion loss coefficient for flow at heat exchanger exit

W = mass flow rate (kg/s)

Using the Kays and London relation, but neglecting the terms containing K_c and K_e, Huffman and Sepsy (1967) developed an expression for the mean friction factor nondimensionalized. Measurements were made and the nondimensionalized friction factor was plotted against nondimensional time. The results obtained were for fin tube exchangers.

Pressure drop measurements were also made by Gatchilov and Ivanova (1979) but with finned air coolers with fin spacings of 7.5 mm, 10 mm and 15 mm. The measurements showed a similar form to those given by Stoecker (1957).

3.2 Heat Exchanger Model

After reviewing the literature, it was clear that no model was available which would simulate the thermal performance of a frosting and condensing heat exchanger. The literature which seemed most useful dealt primarily with the theory of frost formation on flat plates of uniform and constant temperature. However, this literature did not answer what the effect of frost was on the heat and mass transfer coefficients, how the degradation of the return air stream mass flow rate could be predicted as frost accumulated in a heat exchanger and how the frost melting process could be modelled.

The development of the frosting and condensing model started with an available condensing heat exchanger model. A model of the frosting process was developed and inserted into the condensing heat exchanger model. After considerable changes to both the condensing heat exchanger model and the frost model the frosting and condensing heat exchanger model described below resulted.

3.2.1 Condensing Heat Exchanger

Following Demetri and Siegel (1970) and using the model developed by Besant and Bugg (1981) the condensing heat exchanger was modelled by treating the heat exchanger as two separate parts. The heat exchanger was divided at the section where the hot fluid bulk mean temperature reached its dewpoint temperature. One part of the exchanger was dry and the other part of the exchanger was wet. Figure 3.1 shows the processes that were assumed to occur in the heat exchanger [(1-2-3-4) and (8-7-6-5)] and the processes that were known [American Society of Heating, Refrigerating and Air-Conditioning Engineers (1979)] to occur in the heat exchanger [(1-4') and (8-7-6-5)]. The ideal process (1-4) assumed that the air was uniformly and perfectly contacted while in practice (1-4') temperature and water vapor concentration gradients occurred normal to the flow direction.

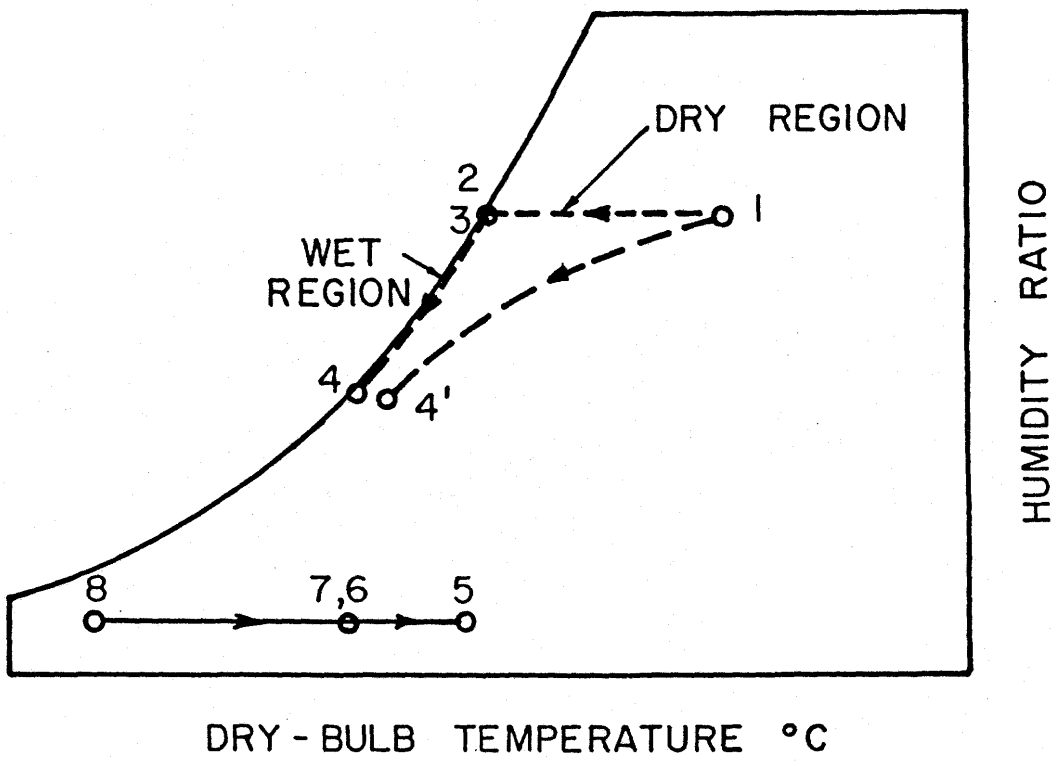

FIGURE 3.1

Heat Exchanger Processes

1 conditions of the moist hot air (return air) entering the heat exchanger

2 condition of the moist hot air leaving the dry region

3 condition of the moist hot air entering the wet region

4 condition of the moist hot air (exhaust air) leaving the heat exchanger

4' actual condition of the moist hot air (exhaust air) leaving the heat exchanger

5 condition of the cold air (supply air) leaving the heat exchanger

6 condition of the cold air entering the dry region

7 condition of the cold air leaving the wet region

8 condition of the cold air (outside air) entering the heat exchanger

An iteration and bisection method was used to find the position of the interface between the wet and dry regions. The position of the interface and the temperature of the cold air stream at the interface were guessed. The guessed interface position and the cold air interface temperature were used to calculate a new cold air interface temperture. If the guessed cold air interface temperature was within 0.1°C of the calculated cold air interface temperature then the iteration was stopped, otherwise the calculated cold air interface temperature became the guessed cold air interface temperature and the iteration was repeated. When the iteration was complete the temperature of the hot air stream at the interface was also known. Since the boundary between the wet and dry region was, by definition, the place where the hot air stream reached the dewpoint temperature, then the hot air stream temperature calculated needed to agree with the hot air stream dewpoint temperature. If the two temperatures did not agree within 0.1°C, then, using the bisection method, a new position of the wet and dry region interface was calculated. Using the last calculated cold air temperature at the interface and the new position of the interface of the wet and dry region the solution process was repeated by solving for the cold air stream temperature at the new interface position.

The heat transferred in each region was calculated by first calculating the heat exchanger effectiveness for the region using Equation 3.2. The overall heat transfer coefficient was computed using Equation 3.1. In the dry region R_F was equal to zero or the thermal resistance of the frost if any was present. In the wet region R_F was equal to the thermal resistance of the water film plus any additional thermal resistance due to frost present. A water film of 0.2 mm was used [Maclaine-cross and Banks (1981)]. Applying Equation 3.3 to each region separately the heat transfer rate in each region was calculated.

The thermophysical properties of the fluids and the heat transfer parameters were calculated at eight locations in the heat exchanger. The eight locations were the four entrances to the two regions and the four exits to the two regions (see Figure 3.1). The properties were evaluated at the mixed mean temperature and no correction was made for the wall to fluid temperature difference. The heat transfer in each region and the outlet temperatures from each region were calculated using the average convective heat transfer coefficients and heat capacity rates of the inlet and the outlet of each side of the two regions.

The specific heat of the hot fluid at the entrance to and the exit from the wet region and the convective heat transfer coefficients at the entrance to and the exit from the wet region were enhanced to account for the condensation.

3.2.2 Convective Heat Transfer Coefficients

Shah and London (1974) present the laminar flow sensible heat transfer coefficient for laminar duct flow forced convection. The boundary conditions were assumed to be midway between constant axial wall heat flux with constant peripheral wall temperature and constant wall temperature peripherally as well as axially. The heat transfer coefficient was the average given for the two boundary conditions.

$$Nu = 7.9 \qquad \begin{matrix} Re < 2300 \\ 2b/2a = 0 \end{matrix} \qquad 3.17$$

where

Nu = Nusselt number

Re = Reynolds number (based on hydraulic diameter)

2b = the plate separation (0.0054 m)

2a = the plate width (0.408 m)

The solution is for fully developed flow (passage length/passage hydraulic diameter >100) but in this case passage length/passage hydraulic diameter was 81.

Besant and Bugg (1981) used a relationship given by Petukhov and Popov (1963) for the Nusselt number for turbulent flow in a tube to calculate the Nusselt number for turbulent flow in a heat exchanger passage.

$$Nu = \frac{fr/8 \; Re \; Pr}{1.07 + 12.7\sqrt{fr/8}\,(Pr^{2/3} - 1)} \qquad 3.18$$

where

Nu = Nusselt number

fr = coefficient of frictional resistance (see Equation 3.19)

Re = Reynolds number

Pr = Prandtl number

$$fr = (1.82 * Log_{10}\,[Re] - 1.64)^{-2} \qquad 3.19$$

The equation has an error of five to six percent for Re from 10^4 to 5.1×10^7 and Pr from 0.5 to 200 assuming constant physical properties. Kays and Leung (1963) and Shibani and Ozisik (1977) developed solutions for the Nusselt number in turbulent flow between parallel plates. Neither solution was used because the boundary conditions used to obtain these solutions did not apply.

Equation 3.17 was used to calculate the heat transfer coefficient for laminar flow and Equation 3.18 was used to calculate the heat transfer coefficient for turbulent flow. In the transition region ($2300 < Re < 10\ 000$), the Nusselt number was calculated by linear interpolation.

Equations 3.17 and 3.18 assume that the fluid is flowing through a smooth walled channel. Figure 3.2 shows a schematic of the actual flow passages. The flow passages have considerable contours which may have resulted in the enhancement of the heat transfer coefficient.

A check was made to see if a correction to the convection heat transfer coefficient should be applied for entrance effects. Assuming the lowest Reynolds number in the heat exchanger was 1000 and using Equation 3.20 [Burmeister (1983)] an estimate of the entrance length was made.

$$\frac{Le}{D_h} \leq 0.05\ Re \qquad 3.20$$

where

Le = entrance length (m)

D_h = hydraulic diameter (m)

Re = Reynolds number

Since, for Re = 1000, the entrance length was approximately 0.54 m, a significant part of the 0.880 m heat exchanger length, a correction for entrance effects was needed. Equation 3.21 given by Rohsenow and Hartnett (1973) was used to correct the average Nusselt number for entrance effects.

$$\frac{Nu_m}{Nu_\infty} = 1 + \frac{C}{L/D} \qquad 3.21$$

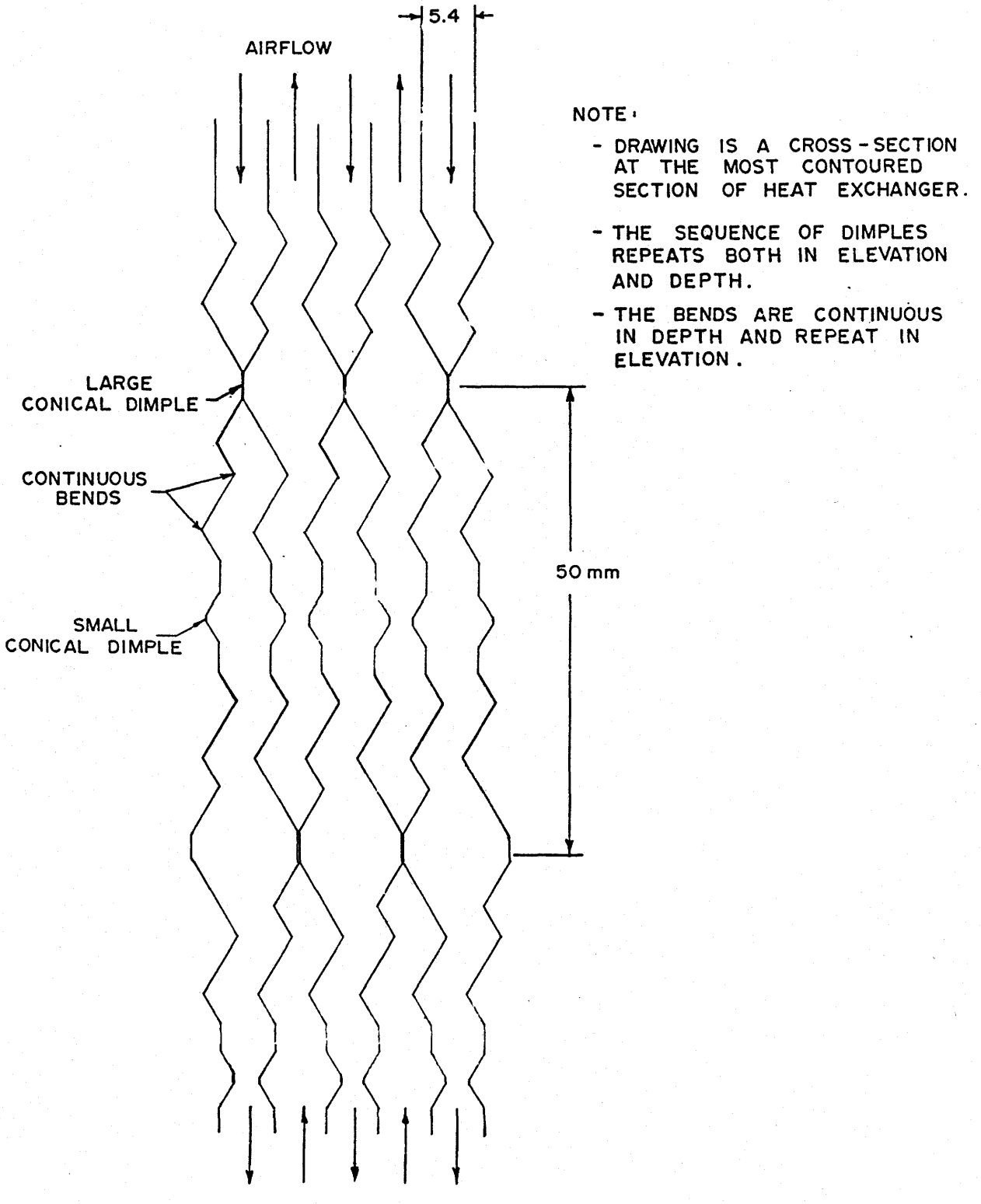

FIGURE 3.2

Heat Exchanger Surface Contours

where

Nu_m = mean Nusselt number

Nu_∞ = Nusselt number for fully developed flow

C = 6 (abrupt contraction entrance)

L = heat exchanger length (m)

D = passage hydraulic diameter (m)

Rather than applying the correction universally to all eight of the convective heat transfer coefficients as the equation implies, the enhancement (C*D/L) was multiplied by four and applied to just the convective heat transfer coefficients at the return air entrance and the outside air entrance. This was done so that the frost growth rate at the return air entrance was more representative than if the correction was applied throughout. Shah and London (1976) added credibility to this approach because they showed that the Nusselt number is significantly enhanced in the first few centimeters of the passage entry.

The convection heat transfer coefficients calculated using Equations 3.17 and 3.18 are for noncondensing flow. At locations 3 and 4 in Figure 3.1 however, condensation was occurring.

Much work has been done in the area of condensation heat transfer. Merte (1973) and Burmeister (1983) both gave comprehensive studies of condensation heat transfer. But despite the wealth of information on condensation heat transfer little has been done regarding the condensation of water vapor from air at atmospheric pressure. Denny et al. (1971) came closest when they studied the effects of noncondensable gas on laminar film condensation of vapor undergoing forced flow along a vertical plate. But the largest air mass fraction considered by Denny et al. was 0.1 which is considerably lower than all air water processes at atmospheric pressure.

The convective heat transfer coefficient in the condensing region was determined by multiplying the dry convection heat transfer coefficient by an enhancement factor. The method given by Threlkeld (1970) was used.

$$\frac{dq}{dA} = \frac{h_c}{C_{p,a}} (i - i_{s,w}) \qquad 3.22$$

where

q = heat transfer (W)

A = heat transfer area (m^2)

h_c = dry convection heat transfer coefficient (W/m^2 K)

$C_{p,a}$ = specific heat at constant pressure of moist air per unit mass of dry air (J/kg K)

i = enthalpy of dry air per unit mass of dry air (J/kg K)

$i_{s,w}$ = enthalpy of saturated moist air per unit mass of dry air evaluated at the water film temperature (J/kg K)

By multiplying the right side of Equation 3.22 by $(T_h - T_w)/(T_h - T_w)$ and separating out the dry heat transfer, the enhancement factor was obtained.

$$e = \frac{1}{C_{p,a}} \frac{(i - i_{s,w})}{(T_h - T_w)} \qquad 3.23$$

where

T_h = the moist air temperature (K)

T_w = the temperature of the water film (K)

Multiplying the dry convection heat transfer coefficient by the enhancement factor gave the convective heat transfer coefficient used in the condensing region (Locations 3 and 4, Figure 3.1).

3.2.3 Frost Formation in the Heat Exchanger

The frost model assumed the frost formation was peripherally and axially identical between all the hot side heat exchanger passages and that the frost height could be calculated based on the plate temperature and the time since the frost began forming regardless of the frost layer past history.

The frost was calculated at 42 locations along the heat exchanger length (see Figure 3.3). Twenty-one of the locations were equally spaced starting at the entrance plane and ending at the exit plant of the dry region. The other 21 locations were equally spaced starting at the entrance plane and ending at the exit plane of the wet region. At each of the 42 points the air temperature on the hot side, the air temperature on the cold side, the convection heat transfer coefficient on the hot side, and the convection heat transfer coefficient on the cold side were calculated by linear interpolation between the region end points. Using the interpolated hot side air temperature, the local thermophysical properties, humidity ratio and Reynolds Number were calculated.

The frost height was calculated at each location using the equation developed by O'Neal and Tree (1984), Equation 3.12. The plate temperature required in Equation 3.12 was calculated using Equation 3.24.

$$T_p = T_c + (T_h - T_c) * \frac{\frac{1}{h_c} + \frac{t_p}{k_p}}{\frac{1}{h_c} + \frac{t_p}{k_p} + \frac{t_f}{k_f} + \frac{t_c}{k_c} + \frac{1}{h_h}} \qquad 3.24$$

where

T_p = plate temperature (K)

T_c = cold air stream temperature (K)

T_h = hot air stream temperature (K)

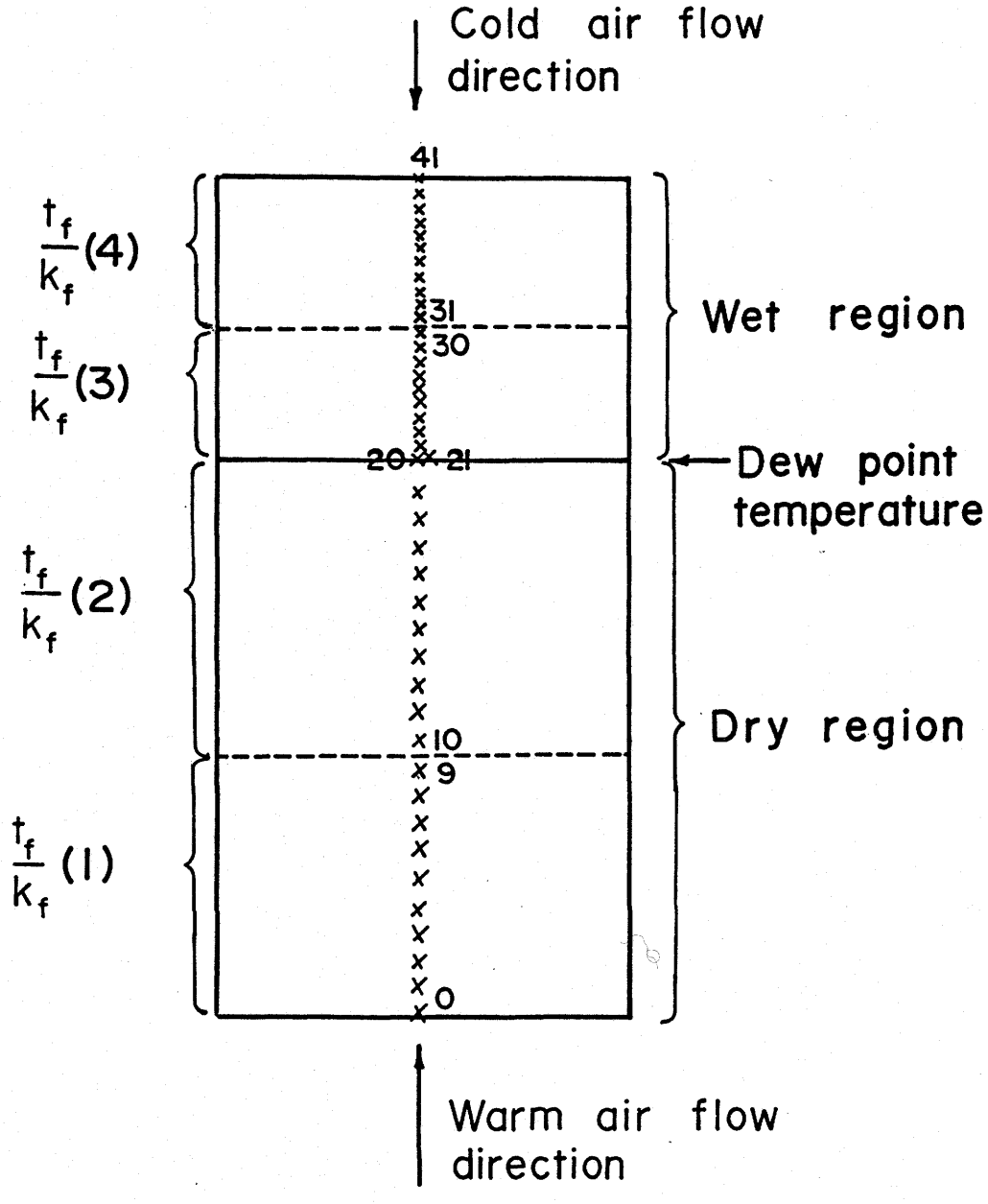

FIGURE 3.3

Frost Calculation Locations

h_c = cold side convective heat transfer coefficient (W/m^2 K)

h_h = hot side convective heat transfer coefficient (W/m^2 K)

t_c = condensate thickness (0.0 in the dry region; 0.002 m in the wet region)

t_f = frost thickness (m)

t_p = plate thickness (m)

k_c = condensate conductivity (0.5745 W/m K)

k_f = frost conductivity (0.01 W/m K)

k_p = plate conductivity (W/m K)

An iterative solution was used to solve for the frost height and the plate temperature. The solution proceeded by first estimating the plate temperature. If the plate temperature was greater than or equal to 273.16 K then the frost height was set to zero. If the plate temperature was less than 273.16 K, the time variable in the frost height equation was advanced and the new frost height was calculated. If the humidity ratio of the hot side air stream was less than the humidity ratio of a saturated air stream whose temperature was 273.16 K then the frost time was not advanced but a new frost height was calculated. The calculated frost height was substituted into Equation 3.24 and a new plate temperature was calculated. If the old plate temperature and the new plate temperature agreed within 0.1°C then a solution for the frost height and the plate temperature was achieved. Otherwise another iteration was performed starting with the new plate temperature.

The use of O'Neal and Tree's equation implied that only frost and no ice formed in the exchanger. This assumption seemed reasonable since the heat exchanger tests were set up so that the condensate flowed into the warmer part of the heat exchanger under the action of gravity.

The frost which accumulated in the heat exchanger acted as a thermal resistance. Despite the wide variety of frost models available, the simple model of Beatty et al. (1951) was used to calculate the frost thermal resistance.

$$R_F = \frac{t_F}{k_F} \qquad 3.25$$

where

R_F = frost thermal resistance (m^2 K/W)

t_F = frost thickness (m)

k_F = frost thermal conductivity (W/m K)

Once the frost thermal resistance at each location was calculated then an average thermal resistance for the dry region and the wet region was computed. The average frost resistance for each region was equal to the average of the average frost resistance of the first 10 locations in the region and the average frost resistance of the last 11 locations in the region. For the purposes of computing the averages all the locations had a weight of one except locations 0, 20, 21 and 41 which had a weight of one-half. These locations had a weight of one-half because they represented only half the area compared to the other locations in the same region (see Figure 3.3).

The effect of the frost thermal resistance was integrated into the condensing heat exchanger model by including an extra term in the overall heat transfer coefficient. The final form of Equation 3.1 was Equation 3.26.

$$\frac{1}{U} = \frac{1}{h_h} + \frac{t_p}{k_p} + \frac{1}{h_c} + \frac{t_c}{k_c} + \left(\frac{t_F}{k_F}\right)_{AVE} \qquad 3.26$$

where

U = overall heat transfer coefficient (W/m^2 K)

h_h = convective heat transfer coefficient on the hot side (W/m^2 K)

t_p = plate thickness (m)

k_p = plate thermal conductivity (W/m K)

h_c = convective heat transfer coefficient on the cold side (W/m^2 K)

t_c = thickness of the water film (0.0 in the dry region: 0.2 mm in the wet region)

k_c = water thermal conductivity (0.5745 W/m K)

t_F = frost thickness (m)

k_F = frost thermal conductivity (0.01 W/m K)

The transient thermal effects of the frost accumulation were neglected. These effects were neglected because the frost conductivity was assumed small and thus the frost density was small.

Thus, the frost height was computed at 42 locations in the heat exchanger. The computed frost height was converted to thermal resistance, an average frost thermal resistance was computed for the wet and dry regions and finally the average frost resistance in each region was integrated into the heat exchanger model through the overall heat transfer coefficient computed for each region.

The heat exchanger model assumed that the frost front and the condensation front were orthogonal to an axis along the length of the heat exchanger. Entrance effects probably significantly skewed the two fronts. Figure 3.4 shows the locations of the assumed fronts while Figure 3.5 shows the fronts when entrance effects were considered.

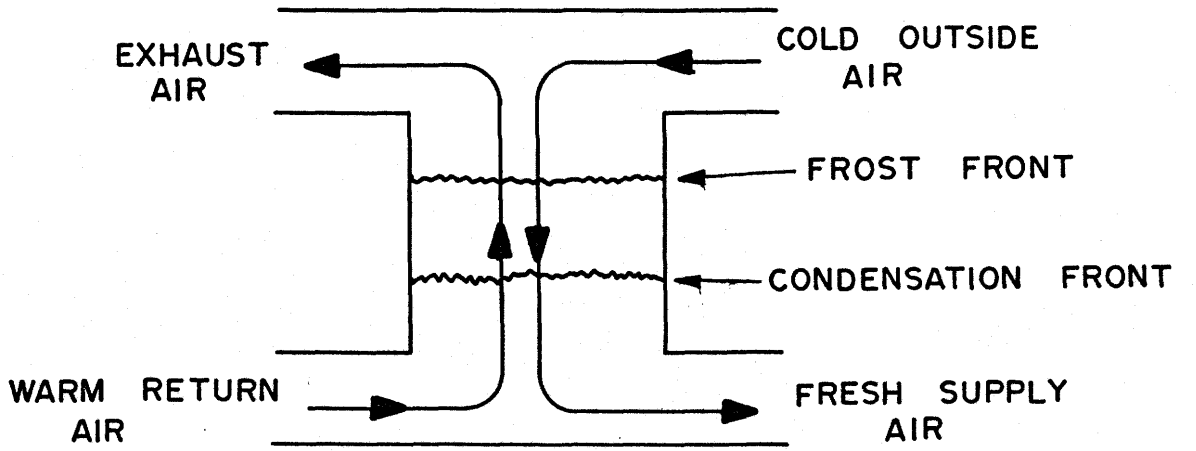

FIGURE 3.4

Frost Front and Condensation Front

With No Entrance Effects

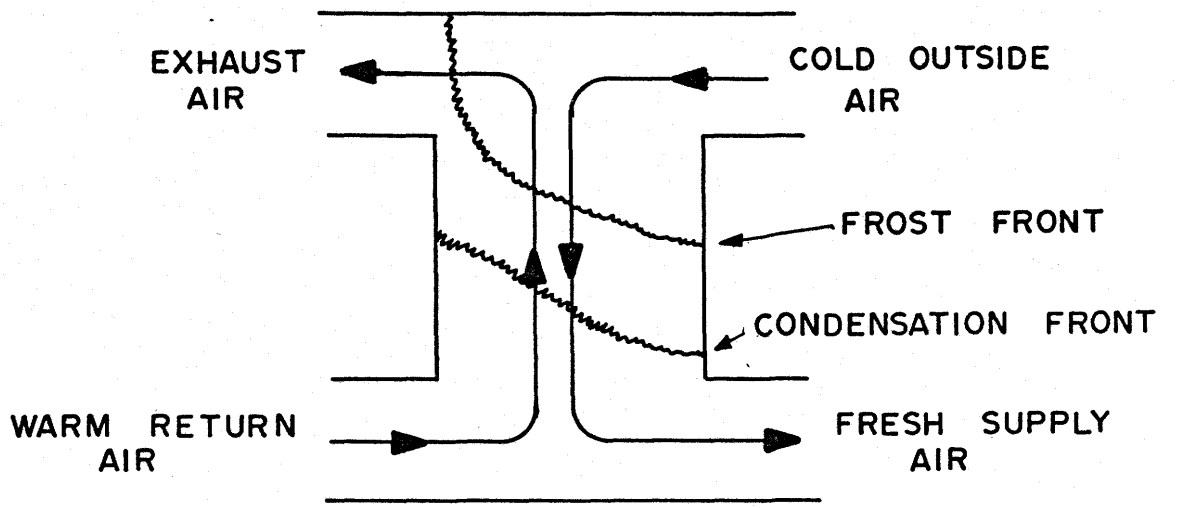

FIGURE 3.5

Frost Front and Condensation Front

With Entrance Effects

Figures 3.1 and 3.3 show an incompatibility between the condensing heat exchanger and the frost forming process because the condensing heat exchanger was analyzed by dividing the heat exchanger into two regions while the frost formation was analyzed by dividing the heat exchanger into 42 locations.

3.2.4 Pressure Drop and Mass Flow Equations

The equation given by Kays and London (1984), Equation 3.16, was used to calculate the pressure drop across the heat exchanger core. The loss coefficients K_c was set equal to 9.225 and the loss coefficient K_e was set equal to 0.400. It must be noted that the term in Equation 3.16 which contained K_c was held constant as frost accumulated when in actual fact it varied slightly as frost accumulated.

The friction factors in Equation 3.16 were calculated in a way similar to the convection heat transfer coefficients. If the Reynolds number was less than 2300 then the friction factor for laminar flow [Shah and London (1974)] was used.

$$f = \frac{24.0}{Re} \quad \text{(Laminar Flow)} \qquad 3.27$$

where

f = fanning friction factor

Re = Reynolds number

If the Reynolds number was greater than 10000 then the equation for turbulent flow given by Petukhov and Popov (1963) was used.

$$fr = (1.82 * \text{Log}_{10}\,[Re] - 1.64)^{-2} \quad \text{(Turbulent Flow)} \qquad 3.19$$

where

fr = coefficient of frictional resistance

Re = Reynolds number

If the Reynolds number was greater than 2300 but less than 10000 a linear interpolation was done between Equation 3.27 (Re = 2300) and Equation 3.19 (Re = 10000).

As frost accumulated in the heat exchanger the minimum free flow area of the heat exchanger decreased and the pressure drop across the exchanger increased. Equation 3.28 gives the heat exchanger minimum flow area.

$$A_C = W * (S - FHMAX) * NH \qquad 3.28$$

where

A_C = exchanger minimum free-flow area (m^2)

W = width of the exchanger (m)

S = exchanger surface spacing (m)

FHMAX = maximum thickness of frost in the exchanger (m).

NH = number of hot passages

Equation 3.28 implied that all the hot side air passages were completely coated with a uniform film of frost FHMAX/2.0 thick.

The frost accumulation not only caused the pressure drop across the heat exchanger to increase but also caused the return air mass flow rate to decrease. In order to develop an equation for the return air mass flow rate, it was assumed that the return air fan developed a constant pressure and that only the heat exchanger pressure volume

characteristics changed as the frost accumulated while the remainder of the duct work carrying the hot side air followed a typical system curve (volume flow rate is proportional to the square root of pressure). Thus, it was possible to develop Equation 3.29 for the return air mass flow rate.

$$M = \left(\frac{P_F - \Delta P}{P_F}\right)^{1/2} * OMFRH * (1 + W) \qquad 3.29$$

where

M = mass flow (kg/s)

P_F = fan static pressure minus the pressure drop across the exchanger when no frost was accumulated (Pa)

ΔP = pressure drop across the heat exchanger minus the pressure drop across the exchanger when no frost was accumulated (Pa)

OMFRH = mass flow at beginning of the test before any frost accumulation had occurred (kg dry air/s)

W = humidity ratio of the return air stream

Using an incremental-search method Equations 3.16 and 3.29 were solved for the return air mass flow rate.

3.2.5 Air/Water Mixture Thermophysical Properties

Kinematic viscosity, Prandtl number, thermal conductivity and specific heat at constant pressure were the thermophysical properties calculated. The properties of the air/water mixture were computed based on mass fraction.

$$Z = \frac{Z_a + WZ_w}{1 + W} \qquad 3.30$$

where

Z = thermophysical property of the mixture

Z_a = thermophysical property of the dry air alone

Z_w = thermophysical property of the water vapor alone

W = humidity ratio

The thermophysical properties of dry air were found by linear interpolation from tables given by Karlekar and Desmond (1977). The thermophysical properties of the water vapor were taken from Haar et al. (1984). The specific heat of steam at 12.5°C and a pressure of 0.014503 bar was used to represent the specific heat of the water vapor at all temperatures. The Prandtl number and thermal conductivity of saturated steam at 12.5°C represented these properties for all temperatures. The specific heat, Prandtl number and thermal conductivity of the water vapor represented a small contribution to the air/water mixture and therefore interpolation was not required. The presence of water vapor significantly affected the kinematic viscosity of the mixture. The kinematic viscosity of saturated steam at 0.01°C and at 30°C was found. For temperatures between 0.01°C and 30°C linear interpolation was used. For temperatures below 0.01°C the value at 0.01°C was used since no tabulated data below 0.01°C were available.

The humidity ratio was calculated using the saturation vapor pressures given in ASHRAE (1985). The humidity ratio, density and enthalpy of the air were found using equations given by Wilhelm (1976). The heat capacity rate was computed using equation 3.31.

$$C = m \frac{di}{dT} \qquad 3.31$$

where

C = heat capacity rate (J/K s)

m = mass flow rate ($kg_{dry\ air}/s$)

i = enthalpy of the air ($J/kg_{dry\ air}$)

T = temperature of the air (K)

di/dT was computed by differentiating the equation for enthalpy given by Wilhelm (1976), Equation 3.32.

$$i = 1.006t + W(2501 + 1.775t) \quad -50°C \leq t \leq 110°C \qquad 3.32$$

where

i = enthalpy of moist air ($KJ/kg_{dry\ air}$)

t = temperature of air (°C)

W = humidity ratio

3.3 Simulation

The condensing and frosting heat exchanger model described above computed the thermal performance of the heat exchanger at any instant in time. In order to study the thermal performance of the heat exchanger over time the heat exchanger model was solved at successive time steps. A model of the frost controller was added to the time series heat exchanger model to complete the simulation. The simulation was written in FORTRAN and run on the University of Saskatchewan College of Engineering, VAX 11/780. The detailed operation of the simulation is described below.

The simulation first read from disk the heat exchanger physical properties, the controller parameters (see Section 4) and the table of temperature versus saturation vapor pressure for water. Before the time series operation of the heat exchanger was started, the program initialized certain variables, the operating conditions were manually inputted and the return air stream dewpoint was calculated.

At the beginning of each time iteration the heat exchanger core temperatures were checked to see if they were all above 0°C and the heat exchanger surfaces were checked to see if they were dry. If both conditions existed and time was greater than zero hours, the frost height, the frost time and the frost thermal resistance were set equal to zero throughout the heat exchanger.

Providing the time was greater than zero hours, the next step was to calculate the frost properties. The frost height and frost thermal resistance were calculated at 42 locations in the heat exchanger (see Figure 3.3). Twenty-one of the locations were in the dry region and 21 of the locations were in the wet region. Four average frost thermal resistances were calculated which were later used in calculating the overall heat transfer coefficient.

Next, using an iteration/bisection method the interface between the wet region and the dry region was calculated. The air temperatures at the interface, at the two outlets and the heat transfer rate in each region were calculated.

If the heat exchanger was completely dry, then the subroutine which calculated the heat transfer rate in the wet region was bypassed and the subroutine which calculated the heat transfer rate in the dry region represented the entire heat exchanger. The condition of a completely

dry heat exchanger usually occurred during defrost.

If the heat exchanger had a wet region, the heat transfer rate in the dry region and the heat transfer rate in the wet region were summed together to give the overall heat transfer rate. At the end of the heat transfer calculations, the time, the outlet air temperature, the heat transfer rate, the core temperature, the percentage of the exchanger which was dry, the two mass flow rates, the location of the frost front, the pressure drop across the hot side of the exchanger and the largest frost height in the heat exchanger were written to the disk and the terminal.

If the time was zero hours and the core temperatures were all above 0°C the simulation was stopped. If not the controller model was permitted to operate. The controller model performed one of three possible functions: exhaust air temperature set, heat transfer rate monitoring or defrost. The controller operation is described in greater detail in Section 4.3.

If the time limit for the simulation had not been exceeded then the time was incremented and control was transferred to the beginning of the time series loop.

Flow charts describing the overall simulation, the dry heat exchange subroutine, the wet heat exchange subroutine and the frost subroutine are given in Appendix A.

4. FROST CONTROLLER DEVELOPMENT

The goal of the frost controller design was to develop a controller which would find and continuously maintain a constant rate of heat transfer which approached the thermodynamic potential of the heat exchanger. The heat transfer rate at the thermodynamic potential of the heat exchanger was the heat transfer rate which occurred when the maximum available rate of flow of outside air passed through the heat exchanger and no frost was accumulated in the heat exchanger core. The controller developed was implemented on a 472 L/s capacity Z-Duct commercial heat exchanger. The frost was controlled using imbalanced air flow rates. The air flow rates were imbalanced by bypassing some of the outside air past the heat exchanger.

4.1 Background Development

At the onset of the control strategy development, it was assumed that the maximum continuous rate of heat transfer occurred when the largest outside air mass flow rate was selected which did not cause frost to accumulate. This could have been achieved by reducing the outside air mass flow rate until the entire heat exchanger core remained above 0°C. But examination of the available literature seemed to indicate that if some frost was present in the heat exchanger the increased surface roughness would significantly increase the heat transfer rate. Huffman and Sepsy (1967) wrote:

> A cursory examination of heat exchanger performance under frosting conditions indicates that in the early stages of frost formation the heat transfer coefficient, including both the air and frost thermal resistance increases, resulting in a from a surface roughening due to the initial frost formation; however, as the frost layer thickens the frost thermal resistance increases, resulting in a decrease in the heat transfer coefficient. Hence, the heat transfer coefficient increases, then decreases with time.

Schulte and Howell (1982), referring to Stoecker (1957) wrote:

> Stoecker verified that a light frost buildup (i.e., 0.91 kg to 1.36 kg (2 to 3 lbs) of overall frost buildup on the close finned coil) actually increases the overall heat transfer coefficient. However, frost buildups over this amount cause the coefficient value to decline.

This evidence suggested that the outside air mass flow should be controlled based on the rate of heat transfer.

A heat flux meter would have been a logical way to monitor the heat transfer rate but developing and installing a sensor that would not affect the thermal performance of the heat exchanger was considered impossible.

Since only sensible heat transfer existed on the cold side of the heat exchanger the heat transfer rate was given by Equation 4.1.

$$Q \alpha \dot{m} (T_{c,in} - T_{c,out}) \qquad 4.1$$

where

Q = rate of heat transfer (kW)

$\dot{m}$ = mass flow rate of dry air (kg/s)

$T_{c,in}$ = temperature of the outside air stream (°C)

$T_{c,out}$ = temperature of the supply air stream (°C)

By monitoring $\dot{m}$, $T_{c,in}$ and $T_{c,out}$ the heat transfer rate could be monitored. This seemed possibly the key in developing a controller that would obtain the maximum continuous rate of heat transfer from the heat exchanger.

Draper and Li (1951) and Li (1952) developed an optimizing controller for an internal combustion engine that would adjust the air supply and the spark ignition to get optimum performance under varying load conditions with constant engine speed and constant fuel flow rate. This kind of optimizing controller seemed precisely what was required. The

given inputs would be the return air stream mass flow rate, the return air stream temperature, the return air stream relative humidity and the outside air stream temperature. The variable input was the outside air mass flow rate.

An alternative to measuring the rate of heat transfer and control based on it was to develop an adaptive controller. An adaptive controller would run a model of the heat exchanger in real time and would predict the optimum outside air mass flow rate. The development of the frosting and condensing heat exchanger model described in Section 3 was started in the hope of developing an adaptive controller but the complexity of the model meant the development of a practical adaptive controller was impossible.

Instead it was decided that an optimizing controller based on the work of Draper and Li would be developed and that a computer model of a condensing and frosting heat exchanger would be developed to aid in the controller development.

4.2 Optimizing Controller

Li (1952) described four different optimizing controllers. The peak-holding controller was selected as the most suited to achieve the maximum rate of heat transfer from the heat exchanger. The peak holding controller monitored the heat transfer rate and changed the outside air mass flow rate through the heat exchanger in a stepwise fashion. The direction of the steps was reversed whenever the heat transfer rate decreased a prescribed amount from the maximum heat transfer rate which had occurred since the last direction change. In this way the controller would seek the maximum rate of heat transfer and continuously operate the heat exchanger within a small error band of the optimum heat transfer rate (see Figure 4.1).

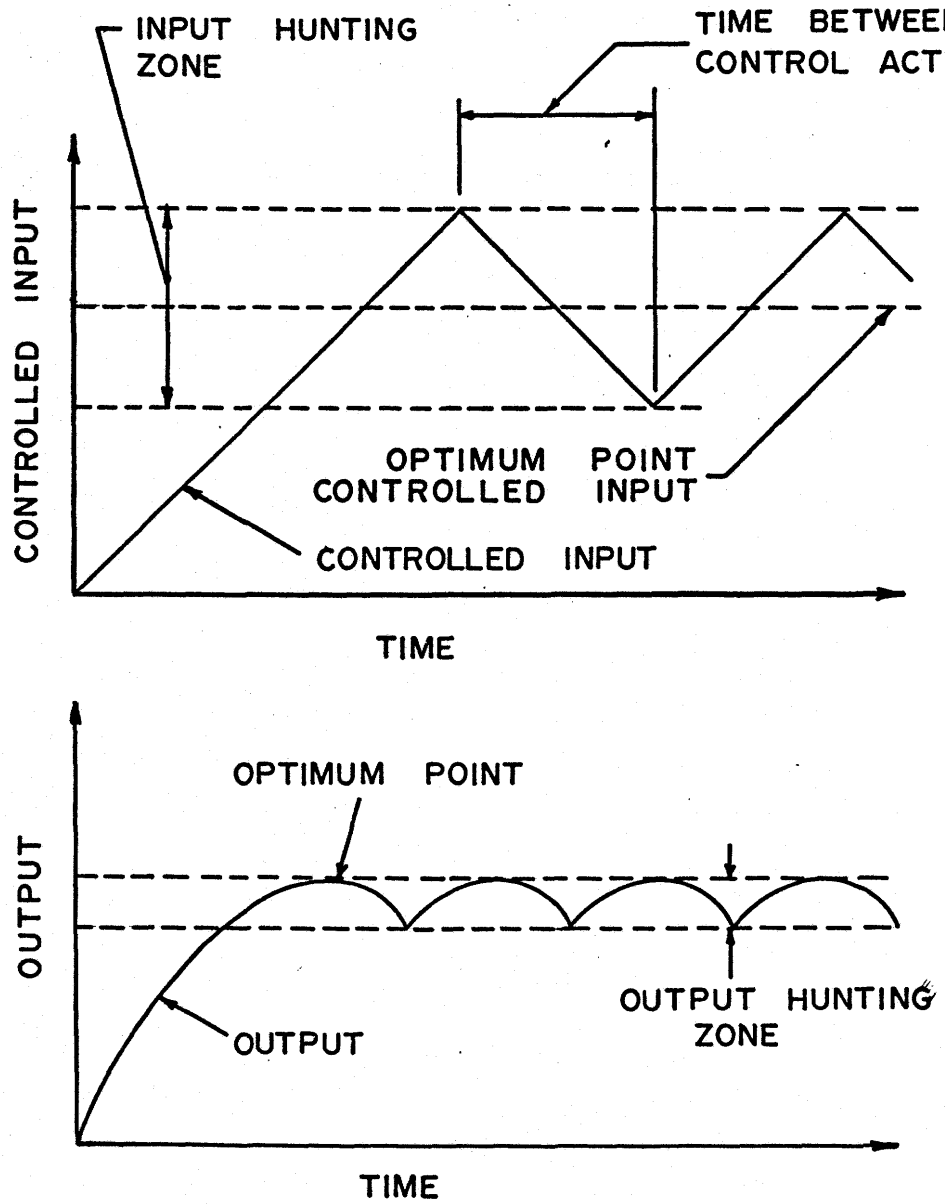

FIGURE 4.1

Optimizing Controller

The starting outside air mass flow rate, the step size, the amount the heat transfer was permitted to decrease before the step direction was reversed, and the length of time between control actions were the independent control parameters identified. An earlier version of the heat exchanger model than was described in Section 3 was used to find the best combination of control parameters for a range of different input conditions. But no matter what combination of controller parameters that were selected, the model showed that the controller would not bring the heat exchanger to a stable state at which it could operate continuously. What was observed was that the return air mass flow rate decreased at a decreasing rate until the return air mass flow rate predicted by the model began to oscillate. Figures 4.1 to 4.4 show respectively the outside air mass flow rate, the heat transfer rate, the return air mass flow rate, and the pressure drop across the hot side of the heat exchanger as a function of time. These figures illustrate the typical heat exchanger performance that was observed with optimizing control. The run was terminated at 5.7 hours because the maximum frost height was nearly one-half the plate spacing and the results were beginning to oscillate. The results were computed for one particular combination of input conditions (see Table 4.1) using the heat exchanger model described in Section 3 with one change and using the best combination of controller parameters (see Table 4.2) determined with the earlier version of the model. The one change made to the model was made to equation 3.28. In equation 3.28 the maximum frost thickness in the exchanger (FHMAX) was multiplied by two. Without this change the heat exchanger model would predict some return air mass flow when the frost accumulation in the heat exchanger passages had blocked the passages. Equation 3.28 was used otherwise in the simulation because it gave the best agreement between the measured pressure drop and the predicted pressure drop.

TABLE 4.1

RUN 0 Input Conditions*

Outside Air Mass Flow Rate (kg/s)	0.43
Outside Air Temperature (°C)	-23.2
Outside Air Relative Humidity (%)	100.0
Return Air Mass Flow Rate (kg/s)	0.33
Return Air Temperature (°C)	12.7
Return Air Relative Humidity (%)	78.3
Atmospheric Pressure (kPa)	95.2

*based on an experimental run.

TABLE 4.2

RUN 0 Controller Parameters

Change in Outside Air Mass Flow Rate (kg/s per step) (Input Hunting Zone [Figure 4.1])	0.01646
Heat Transfer Rate Decrease for Direction Change (kW) (Output Hunting Zone [Figure 4.1])	0.175
Time Between Control Actions (hr)	0.5

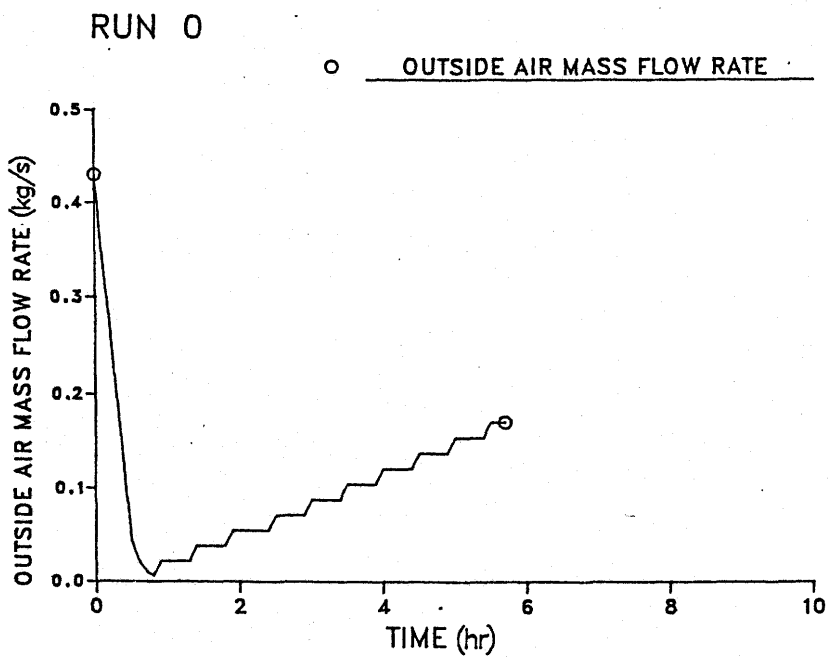

FIGURE 4.2

Outside Air Mass Flow Rate

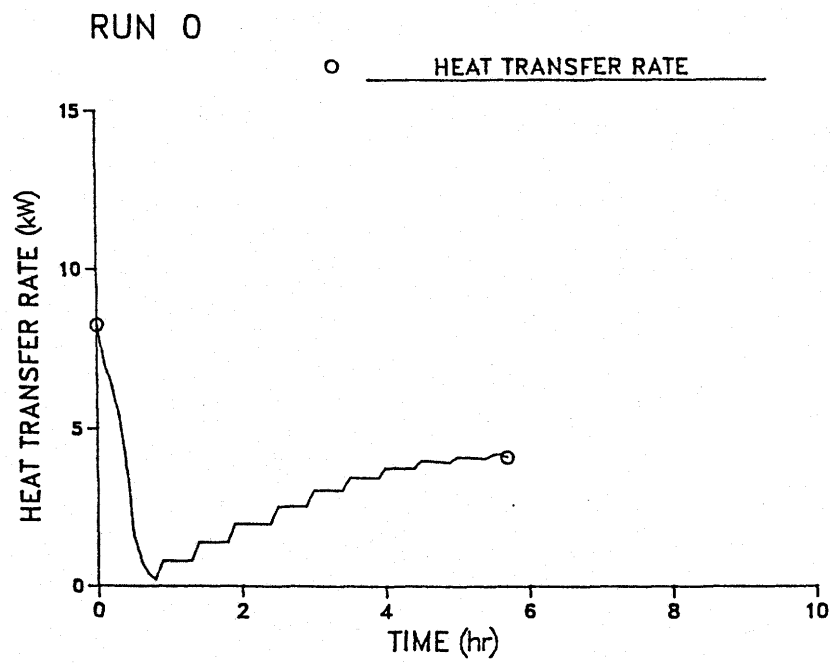

FIGURE 4.3

Heat Transfer Rate

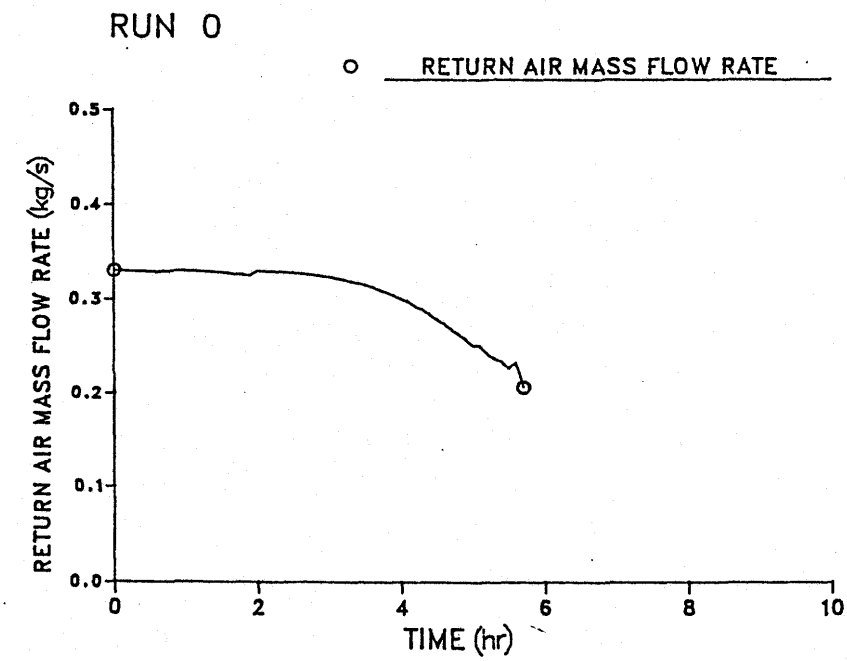

FIGURE 4.4

Return Air Mass Flow Rate

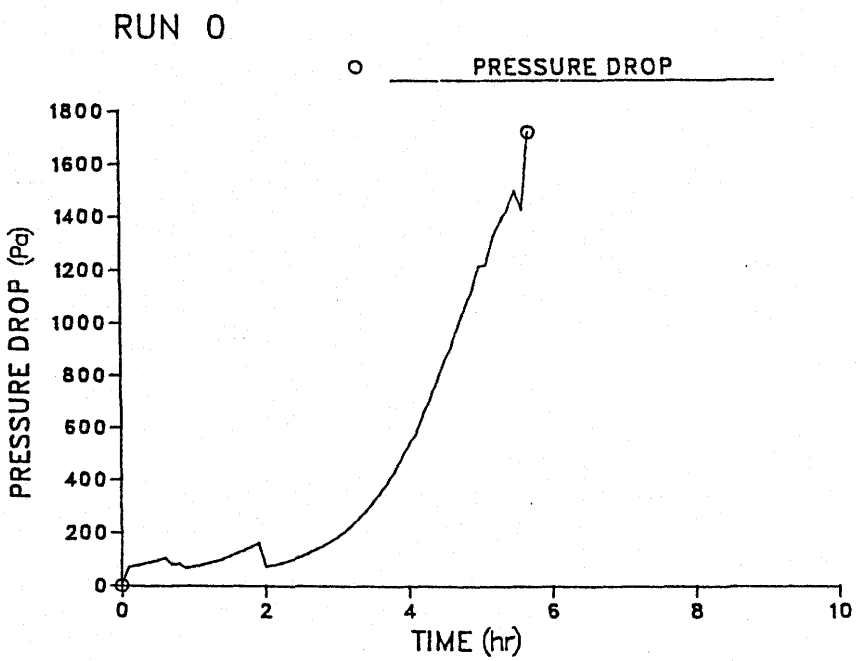

FIGURE 4.5

Hot Side Pressure Drop

The simulation results indicated that a stable state could not be found at which the heat exchanger could be operated continuously. But close examination of the equation given by O'Neal and Tree (1984) for frost growth on a plate, Equation 3.12, shows clearly that some frost accumulation and a stable state cannot coexist. Repeating Equation 3.12:

$$x_f = 0.466 \left(\frac{t}{1hr}\right)^{0.663} Re^{0.393} \left(\frac{T_o - T_p}{T_o}\right)^{0.705} \left(\frac{W_a - W_o}{W_o}\right)^{0.098} \qquad 3.12$$

where

x_f = frost height (mm)

t = time (hr)

Re = Reynolds number (based on hydraulic diameter)

T_o = freezing temperature of water (K)

T_p = plate temperature (K)

W_o = humidity ratio of saturated air at 0°C

W_a = humidity ratio of the air stream

Since the Reynolds number was greater than zero and the return airstream humidity ratio was greater than the humidity ratio of saturated air at 0°C then if the time approached infinity (continuous operation) then the heat exchanger core temperature must approach 0°C. But this corresponds to exactly the first control strategy that was proposed but which was discarded because other researchers had pointed out that some frost accumulation enhances the heat transfer rate. Thus it is not possible to develop a controller which continuously maintains a constant rate of heat transfer approaching the maximum thermodynamic potential of the heat exchanger.

Hypothesis Two given in Section 2 was rejected. A small amount of frost accumulation is beneficial but maintaining a small amount of frost indefinitely is not possible. By using a defrost cycle the heat

exchanger could be operated in the range of maximum performance but then defrosted when the frost accumulation significantly degraded the heat exchanger performance. A defrost control strategy was finally selected as the best possible frost control strategy to be tested. Recognizing that timed defrost and pressure controlled defrost were not without problems, it was decided that measuring the instantaneous rate of heat transfer and using this to initiate defrost could lead to a superior heat exchanger frost controller.

4.3 Frost Controller Tested

The defrost controller permitted the heat exchanger to be operated in the range of maximum performance. Once the frost accumulation degraded the rate of heat transfer a prescribed amount the frost was removed by a defrost cycle. Control was achieved by modulating the amount of outside air which passed through the heat exchanger. A bypass duct and a system of dampers were used to modulate the amount of outside air which flowed through the exchanger. The performance of the heat exchanger was monitored using Equation 4.1. The controller operated by continuously following a series of three phases: exhaust air temperature set, heat transfer rate monitoring and defrost. The operation of the defrost controller was simulated using the exchanger model given in Section 3 before it was tested. A description of the defrost controller tested (experiment controller) and the defrost controlled simulated (simulation controller) is presented below.

The experiment controller and the simulation controller were digital controllers that performed a control action every 360 seconds. The control action of the experiment controller and the simulation controller differed at start up. The experiment controller started 1080

seconds earlier than the simulation controller. During the first 720 seconds the bypass damper was completely open and three measurements of all the data channels were made.

The first common control action was to completely close the bypass. This permitted the heat exchanger performance to be measured at full flow (baseline measurement). After the baseline measurement a defrost was initiated. The defrost involved bypassing more and more outside air until the core temperature exceeded 0°C. The core temperature was computed in the experimental tests by averaging the three temperatures measured by the three temperature sensors mounted in the cold air passages of the heat exchanger. These sensors were mounted so that they very nearly measured the coldest core temperatures in the heat exchanger. The modulation of the outside air flow rate was controlled using a proportional controller. An alternate control method would have been to open the bypass damper completely in a single step. This method was not used because it was felt that with proportional control the bypass damper would not in some cases completely open during defrost and thus some minimum rate of heat transfer would be maintained even during defrost. Equation 4.2a was the proportional control equation used in the simulation and Equation 4.2b was the proportional control equation used in the experimental runs.

$$dm = (1.0 - T_C) * G * OMFRC \qquad 4.2a$$

where

dm = change in outside air mass flow rate (kg/s)

T_C = core temperature at the outside air inlet (°C)

G = controller gain (0.020 $°C^{-1}$)

OMFRC = cold air mass flow rate with no bypass (kg/s)

$$dd = (1.0 - T_C) * C5 * D \qquad 4.2b$$

where

dd = change in damper position (steps)

T_c = core temperature calculated by averaging the temperature at three positions close to the outside air inlet (°C)

C5 = controller gain [0.020 $°C^{-1}$ RUN 1, 0.0149 $°C^{-1}$ RUN 2, RUN 3, RUN 4 (see Section 5.2.4)]

D = position range of the bypass damper [280 steps RUN 1, 209 steps RUN 2, RUN 3, RUN 4 (see Section 5.2.4)]

It should be noted that the simulation controller set the core temperature to 0.1°C if the outside air mass flow rate through the heat exchanger was less than 0.007 kg/s. Without this change the simulation predicted very long defrost times which did not seem reasonable.

Once the heat exchanger had been defrosted then the flow of cold air through the heat exchanger was increased. The mass flow rate of cold air was increased until the exhaust air temperature was within 1.0°C of 2.5°C. The mass flow rate of outside air was increased using proportional control action. The maximum available outside air mass flow rate was not automatically selected because it was assumed that if the exhaust air stream temperature reached less than 0°C the exhaust air passages would freeze closed very quickly due to ice accumulation. Equation 4.3a was the control equation used in the simulation and Equation 4.3b was the control law used in the experiments.

$$dm = (2.5 - T_e) * G * OMFRC \qquad 4.3a$$

where

dm = change in mass flow rate (kg/s)

T_e = exhaust air stream temperature (°C)

G = controller gain (0.020 $°C^{-1}$)

OMFRC = cold air mass flow rate with no bypass (kg/s)

$$dd = (2.5 - T_e) * C5 * D \qquad 4.3b$$

where

dd = change in damper position (steps)

T_e = exhaust air stream temperature (°C)

C5 = controller gain [0.020 $°C^{-1}$ RUN 1, 0.0149 $°C^{-1}$ RUN 2, RUN 3, RUN 4 (see Section 5.2.4)]

D = position range of the bypass damper [280 steps RUN 1, 209 steps RUN 2, RUN 3, RUN 4 (see Section 5.2.4)]

This phase of the control action was called exhaust air temperature set.

The last phase of the controller operation was monitoring the heat transfer rate. During this phase the mass flow rate of the cold air stream was unchanged. Thus the temperature change of the cold air stream was a direct measure of the heat transfer rate. The maximum heat transfer rate and the maximum temperature change occurred at the start of the phase and both decreased as the frost accumulated. When the temperature rise of the cold airstream had reduced by 2.5°C a defrost was initiated and the control cycle repeated.

In order to accommodate fluctuations of the outside airstream temperature and the return air stream temperature a correction factor was applied to the cold airstream temperature change.

$$T5 = (T_S - T_O) - 0.68 * (T_R - T_O) \qquad 4.4$$

where

$T5$ = normalized cold air stream temperature change (°C)

T_S = supply air stream temperature (°C)

T_O = outside air stream temperature (°C)

T_R = return air stream temperature (°C)

Equation 4.4 was developed assuming that the heat exchanger effectiveness was 68 percent and the cold air stream had the minimum heat capacity rate. The manufacturer stated that at rated flow the heat exchanger effectiveness is 68 percent. The correction term in Equation 4.4 was developed using Equation 3.3.

A summary of the controller settings used are given in Table 4.3. The controller flow chart is given in Figure 4.6.

TABLE 4.3

Summary of Controller Settings

Control error for the cold airstream temperature change (°C)	-2.5
Exhaust airstream set point temperature (°C)	2.5
Control gain* ($°C^{-1}$)	0.0200 0.0149
Defrost set point temperature (°C)	0.0
Time interval between control actions (s)	360

* [0.0200 $°C^{-1}$ RUN 1, 0.0149 $°C^{-1}$ RUN 2, RUN 3, RUN 4 (See Section 5.2.4)].

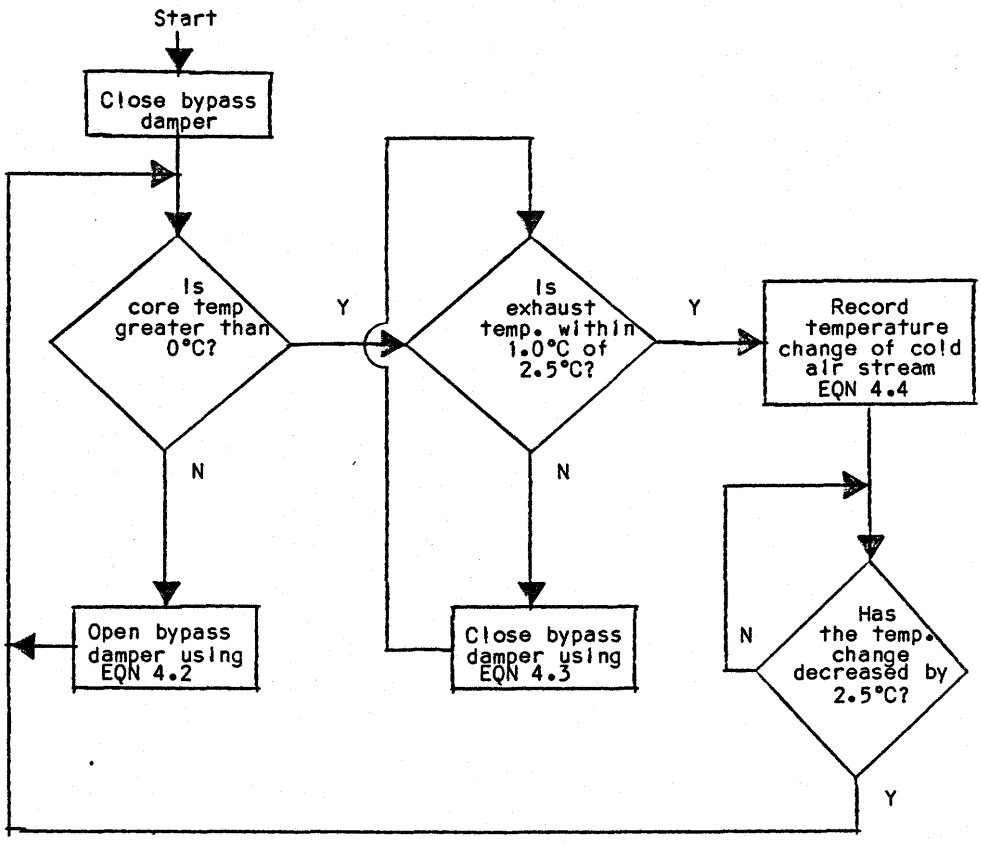

FIGURE 4.6

Controller Flow Chart

5. PROTOTYPE TESTS

The prototype tests were conducted at the Prairie Agricultural Machinery Institute (PAMI), Humboldt, Saskatchewan. PAMI have experience in, and equipment for, testing heat exchangers.

A Z-Duct Model 74-1000AA6 commercial heat exchanger was used in the tests. The laboratory test results were compared with the thermal performance predicted by the computer model in order to test Hypothesis One given in Section Two.

Prototype tests were also conducted to see if a heat transfer optimizing frost control strategy could be implemented on a commercial heat exchanger installation tested in a laboratory environment.

5.1 Experimental Test Conditions

The test conditions were selected by identifying all of the independent input variables and the range of each of these variables.

The independent inputs are those that affect the formation of frost in a heat exchanger. Those factors affecting the formation of frost on a uniform temperature single parallel plate heat exchanger were given by O'Neal and Tree (1984) (Equation 3.12) as Reynolds number, plate temperature, air stream humidity ratio and the length of time since the start of frost formation. Since the heat exchanger to be tested was a series of plates, similar factors were likely to influence frost formation in it. Thus air stream mass flow rates, fluid temperatures at the inlets, return air relative humidity and length of time since start of frost formation were the independent variables identified.

The large number of independent inputs meant a large number of trials would be required to identify all the effects of the independent variables. The outside air mass flow and the return air mass flow were fixed at the maximum the test setup would develop. This led to imbalanced air flows which is not how the manufacturer suggests the heat exchanger be used. The outside air temperature was also fixed by the maximum cooling capacity of the refrigeration plant. The heat exchanger was operated with imbalanced flow at maximum flow and the coldest outside air temperature because all these factors were expected to enhance the rate of frost formation. The return air temperature and the return air relative humidity were the only remaining independent inputs. In most livestock houses the room air temperature will be between 10°C and 22°C and the room air humidity will be between 50% and 90%. The permutation of these two independent inputs at their two extremes suggested the four trials that were done. Table 5.1 summarizes the actual test conditions used.

The length of each test was chosen so that several defrost cycles could be observed during the test.

5.2 Experimental Equipment

5.2.1 Overall Test Setup

The test setup is shown in Figure 5.1. The dimensions of the test setup are shown in Figure 5.2. In order to describe the test setup the air flow through the system will be traced.

Air entered on the exhaust side through the conditioning box where the relative humidity and temperature were adjusted to the test requirements. The air then passed through the fan to boost the static

TABLE 5.1

Experimental Test Conditions

PARAMETER	UNITS	RUN 1	RUN 2	RUN 3	RUN 4
OUTSIDE AIR MASS FLOW RATE	kg/s	0.43	0.44	0.45	0.45
OUTSIDE AIR TEMPERATURE	°C	-23.8	-24.8	-26.9	-26.4
OUTSIDE AIR RELATIVE HUMIDITY	%	100.0	100.0	100.0	100.0
RETURN AIR MASS FLOW RATE	kg/s	0.31	0.32	0.33	0.33
RETURN AIR TEMPERATURE	°C	24.0	25.3	12.8	13.1
RETURN AIR RELATIVE HUMIDITY	%	77.9	41.7	76.9	45.5
TEST DURATION*	hr	4.5	8.0	7.0	10.0
ATMOSPHERE PRESSURE	kPa	93.2	94.4	95.2	95.1

*The test duration was selected in order to provide at least three complete controller cycles. Repeating the control cycle three times was felt to sufficiently demonstrate continuous operation of the controller.

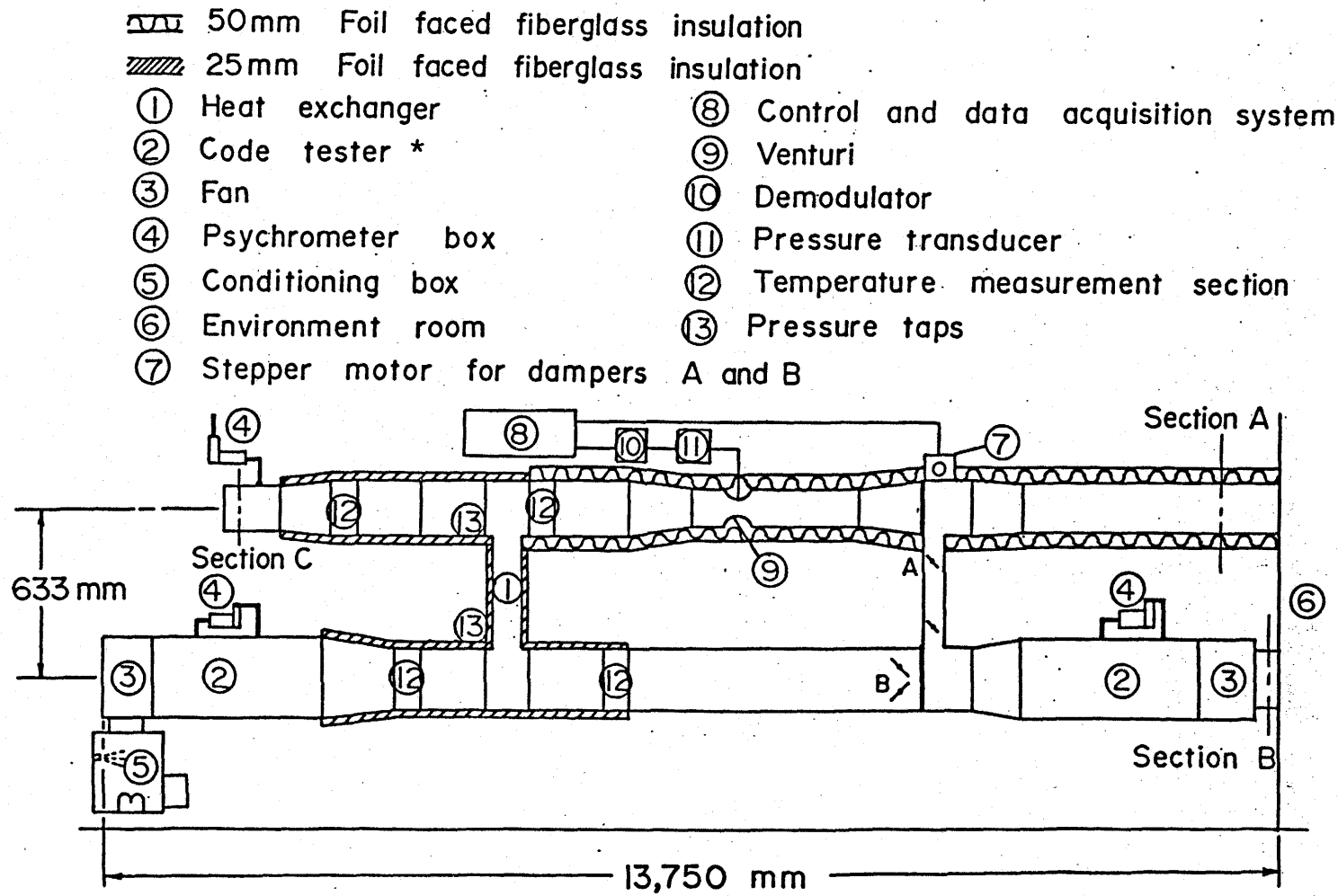

FIGURE 5.1
Experiment Test Setup

* Device used to mix the air stream, sample the air stream psychometric properties and measure the air stream mass flow rate.

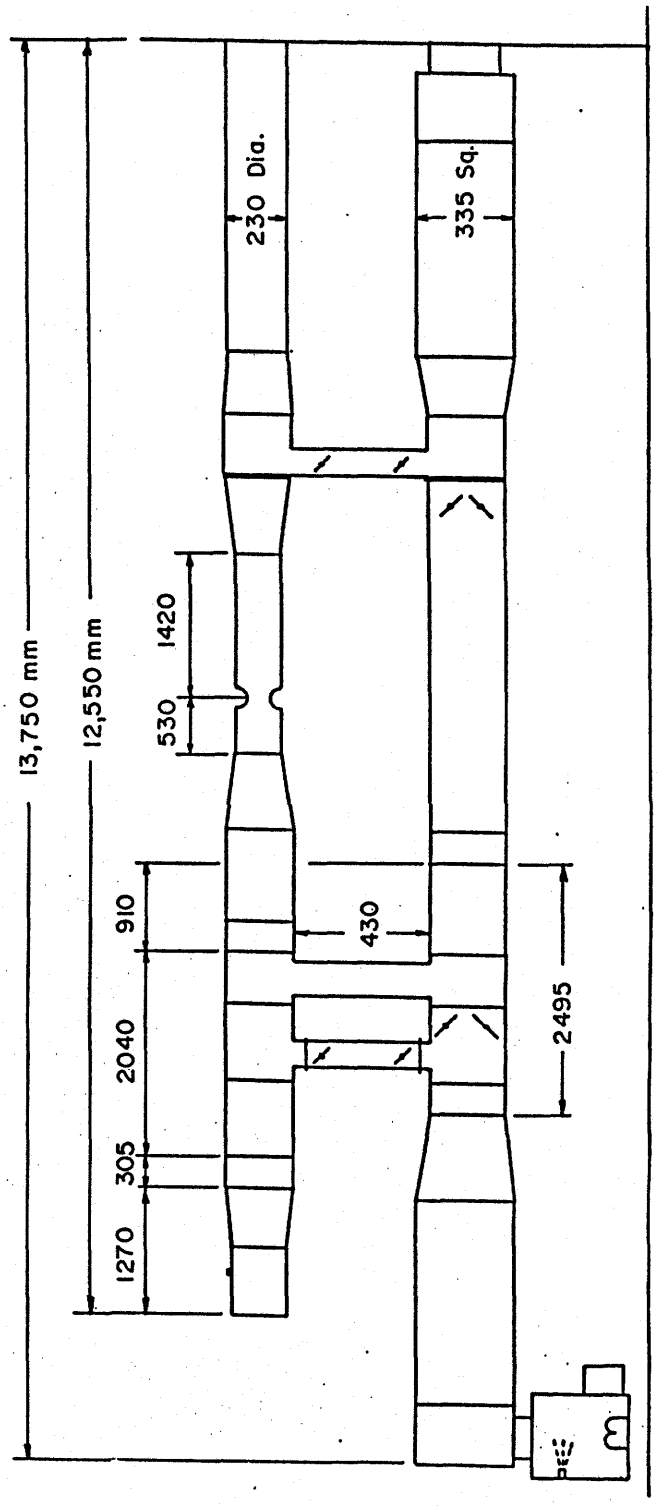

FIGURE 5.2

Dimensioned Experiment Test Setup

pressure. Next the air passed through the code tester where the air wet and dry bulb temperatures and the air volume flow rate were measured. The air then passed through a straight section of duct to a temperature measurement section where eight individual temperatures were measured on an equal area grid. The air then passed through the exhaust side of the heat exchanger. After leaving the heat exchanger the air passed through a second temperature measurement section. Following the temperature mesurement section a sample of air was drawn into a psychrometer box where the wet and dry bulb temperature of the air were measured. The air was then exhausted back into the laboratory.

The cold air entered on the supply side from the environment room. This cold air could proceed either through the bypass or through the heat exchanger. Air going to the heat exchanger, entered a flow tube where the volume flow was accurately measured using a venturi flow meter. The air then passed through a temperature measurement section and into the supply side of the heat exchanger. After leaving the heat exchanger the air passed through another temperature measurement section. After passing through a long section of duct this air was mixed with the air which passed through the bypass. The mixed air was drawn through a code tester and a fan and then was exhausted back into the environment room.

In addition to the four temperature measurement sections shown in Figure 5.1 a number of individual temperature sensors were placed in the heat exchanger core.

Most of the temperatures and the supply side volume flow rates were recorded by a control and data acquisition system (described in Section 5.2.8). These data were used by the controller to drive a stepper motor which modulated the bypass dampers.

5.2.2 Air Flow Measurement

5.2.2.1 Supply Air Mass Flow Measurement

The supply air mass flow rate was measured using a venturi (Fielding Crossman and Associates Limited, Willowdale, Ontario). The venturi was designed to measure mass flow rates very accurately between 170 m^3/hr and 1700 m^3/hr. A device with such a large range was selected because it was known that the outside air mass flow would be modulated over a large range by the frost controller.

Figure 5.1 shows the venturi mounted in the overall test set up. The venturi was inserted in size 6, schedule 40 pipe and supported between ANSI Class 125 flanges. The venturi was mounted following the guidelines given by Bean (1971) except that the upstream pipe length was 9.2 diameters rather than the recommended 10 diameters. A converging section immediately preceeded the pipe supporting the venturi and a diverging section immediately followed the pipe supporting the venturi (see Figure 5.1).

The differential pressure output from the venturi was measured by a pressure transducer and demodulator (DP103 Pressure Transducer and CD101 Demodulator, Validyne, Northridge, California). The demodulator gave a 0-5V signal which was accepted by the controller.

Given the differential pressure developed by the venturi, the atmospheric pressure and the fluid temperature, the mass flow rate was calculated. Following Bean (1971), an equation relating mass flow to differential pressure, atmospheric pressure and temperature was developed.

$$m = 1.610 \times 10^{-3} \sqrt{\frac{h_w \, Pa}{T + 273.15}} \qquad 5.1$$

where m = mass flow rate (kg/s)

h_w = differential pressure (mm w.c.)

Pa = atmospheric pressure (Pa)

T = air temperature (°C)

To verify the correct operation of the venturi, the mass flow rate was measured using a pitot static traverse at four different flow rates. Since the venturi had never been used before, its operation was verified to ensure it was being used correctly. Each traverse consisted of 20 readings taken along two diameters at centers of equal area. This followed the recommendation of ASHRAE (1985). The traverse was performed in a 200 mm inside diameter pipe connected upstream of Section A in Figure 5.1. The traverse was done 8.6 diameters from the pipe entrance and 7.4 diameters from the pipe exit. Care was taken to ensure no leakage occurred between the traverse section and the venturi section.

Table 5.2 shows the calibration results obtained. The errors in the traverse measurements were computed using ASHRAE (1976). The error calculations included the error in temperature, atmospheric pressure, manometer reading and pipe diameter.

Duct leakage will cause a difference in the mass flow measured and the mass flow through the heat exchanger. To reduce the leakage a bead of silicone caulking was placed between all the mating surfaces. As well almost all of the connections were cleat connections. To verify that no leakage was occurring a pitot static traverse was performed. The traverse was performed by connecting the pipe used to calibrate the

venturi at Section B in Figure 5.1. A traverse consisting of 10 readings was taken along one diameter at centers of equal area. The measurements were made 8.6 diameters from the pipe entrance and 7.4 diameters from the pipe exit. The mass flow measured was 0.427 kg/s $\pm$ 0.024 kg/s. To verify that no leakage was occurring this measurement was compared with the mass flow measured by the venturi. The venturi mass flow was 0.44 kg/s. Thus, within the measurement error the duct leakage was taken as negligible.

TABLE 5.2

VENTURI CALIBRATION

TOTAL	AVERAGE TEMPERATURE (°C)	TRAVERSE MASS FLOW (kg/s)	VENTURI MASS FLOW (kg/s)	TRAVERSE ERROR (kg/s)
1	21.2	0.423	0.42	$\pm$0.011
2	21.4	0.354	0.35	$\pm$0.010
3	21.5	0.258	0.25	$\pm$0.010
4	21.6	0.084	0.08	$\pm$0.014

5.2.2.2 Exhaust Air Mass Flow Measurement

The exhaust air mass flow rate was measured by a nozzle station. The nozzle station, consisting of four nozzles was designed and built by PAMI [Begin and Frehlich (1982)] and is part of their standard heat exchanger test equipment.

The differential pressure output from the nozzle station was read by a manometer (Type 4 and Type 5 Air Flow Testing Set, AirFlow Developments Ltd., Mississauga, Ontario). This manometer permitted the differential pressure to be read to $\pm$ 0.25 mm water column. The actual calculation of the mass flow rate was done using a PAMI developed computer program.

The mass flow rate computed by the PAMI developed program was compared to the mass flow rate measured by a pitot tube traverse. The comparison was done at a single operating point. The traverse was done using the same round tube used to verify the venturi. The tube was connected to the exhaust duct work at Section C in Figure 5.1. The traverse consisted of 20 readings taken along two diameters at centers of equal area and was performed 8.6 diameters from the pipe entrance and 7.4 diameters from the pipe exit. Since the nozzle station was upstream of the heat exchanger and the traverse was done downstream of the exchanger the effects of leakage could not be avoided. However, since the exhaust ductwork was shorter than, and sealed in the same way as, the supply ductwork it was expected to have the same leakage properties as the supply air ductwork. No leakage was detected in the supply air ductwork so none was expected in the exhaust air ductwork. The mass flow rate calculated from the nozzle data by the PAMI program was 0.542 kg/s. The pitot tube traverse indicated a mass flow of 0.514 $\pm$ 0.011 kg/s. Since, the mass flow rate from the nozzle data was not within the experimental error of the pitot-static traverse a multiplier correction of 0.948 was applied to all mass flows measured by the nozzle apparatus.

5.2.3 Temperature Measurement

5.2.3.1 Air Temperature Measurement

The air temperatures at the inlet and outlet on both sides of the heat exchanger were measured in the heat exchanger tests. The temperature sensor used in these tests (AD590KF, Analog Devices, Norwood, Mass.) was a two terminal integrated circuit temperature transducer which produced an output current proportional to absolute temperature. The sensor had good linearity and could be operated over a wide power supply voltage range. The sensors were prepared for use in a damp environment by sealing the sensors and their leads with a thermally conductive epoxy (Delta Cast 153, B4 Hardener, Wakefield Engineering, Wakefield, Mass.). All the sensors were calibrated prior to use (see Appendix B). The sensors were calibrated to an accuracy of between $\pm$ 0.88°C and $\pm$0.97°C at the 98 percent confidence level (see Appendix B, Table B.2).

ASHRAE (1975) indicated that when the air stream temperature and velocity are reasonably uniform the duct can be divided into equal areas and the temperature can be measured at the center of each area. The arithmetic average of the temperatures will represent the temperature at the section. The ducts used in this experiment were rectangular of dimensions 578 mm by 228 mm. The duct was divided into eight equal areas. Each area was 144 mm by 114 mm. At the center of each area a temperature sensor was placed. In order to verify the uniformity of the air velocity an 18 point equal area pitot tube traverse was performed very close to the four temperature measurement sections (see Figure 5.1). The average velocity and the standard deviation of the velocity were computed at each section. The results are shown in Table 5.3.

TABLE 5.3

VELOCITY DISTRIBUTION

TRAVERSE	TYPICAL TEMP. STD. DEV. (°C)	MEAN VELOCITY (m/s)	VELOCITY STD. DEV. (m/s)	VELOCITY MEASUREMENT ERROR (m/s)	TRAVERSE MASS FLOW (kg/s)	MEASURED MASS FLOW (kg/s)
OUTSIDE AIR*	0.25	4.196	0.829	±0.923		
SUPPLY AIR	2.67	3.463	0.308	±0.062	0.551 ±0.052	0.430 ±0.011
RETURN AIR	0.21	2.746	1.197	±0.069		
EXHAUST AIR	1.11	2.367	0.174	±0.092	0.360 ±0.063	0.303 ±0.011

* Flow was very unsteady.

Table 5.3 also gives the typical standard deviation of the individual temperature measurements at each section found during the tests. Table 5.3 shows that the air velocity was most nonuniform at the entrance to the heat exchanger but this was the location where the temperature was most uniform. Thus an arithmetic average of the temperature sensors would be representative of the temperature at those sections. The outlet sections were shown to have nonuniform temperature. However, the temperatures measured by the eight sensors at each of these sections consistently gave a distribution such that the four middle temperatures agreed with each other and the section average temperature while the four outside temperatures varied equally from the section average. The two temperatures on one side of the section were noticeably above the average and the two temperatures on the opposite side of the section were noticeably below the average. The velocity distribution was

uniform across the center of the section and decreased close to the duct walls. The nature of the temperature and velocity distributions indicated that an arithmetic average of the eight temperatures across the outlet sections was representative of the bulk air temperature. Thus, at the four temperature measurement sections given in Figure 5.1 the air stream bulk temperature was computed as the arithmetic average of the eight measurements at the section.

5.2.3.2 Core Temperature Measurement

Two sets of measurements of the heat exchanger core temperature were made. One set of measurements was used as input to the control algorithm. Another set of measurements was made to get an estimate of the heat exchanger core temperature distribution.

Six AD590KF sensors were used by the controller. The sensors were calibrated as described in Appendix B. The sensors were mounted in the heat exchanger by cementing them to the core with a thermally conductive adhesive (Loctite Corp., Newingon, CT.). To ensure that the sensors remained in place, a 25 mm square piece of aluminum tape was placed over each sensor. The placement of the sensors is shown in Figure 5.3. (The location of section A-A is shown in Figure 2.1). Three of the sensors were placed in the exhaust air passages near the exhaust outlet and the remaining three sensors were placed in the supply air passages near the supply inlet.

The average temperature measured by the three sensors in the supply passages was used by the controller as the core temperature. The average temperature measured by the three sensors in the exhaust passages was recorded for later comparison but was not used by the controller.

ALL THERMOCOUPLES ARE ON THE SUPPLY AIR SIDE

O - THERMOCOUPLE

X - AD590KF

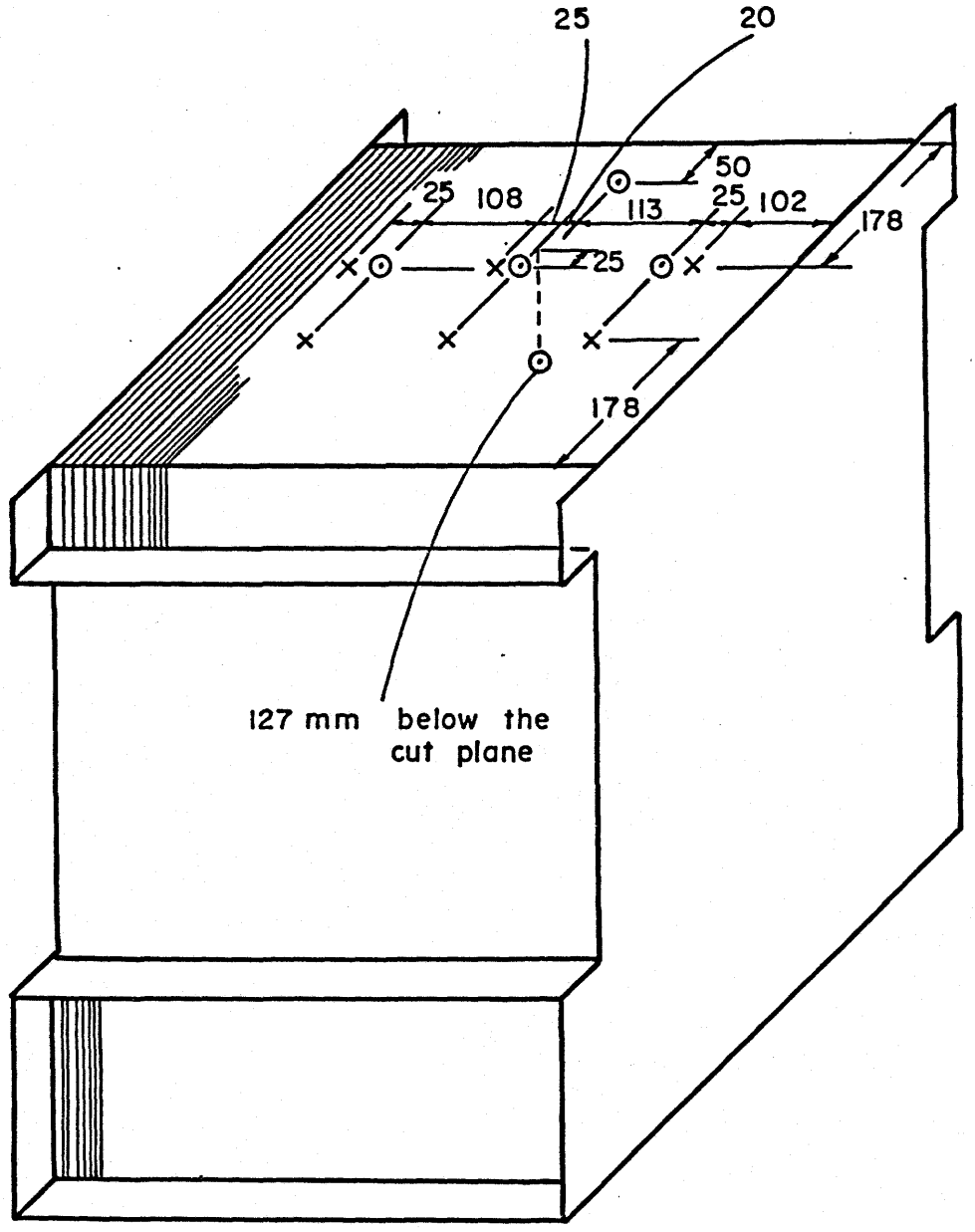

SECTION A-A

FIGURE 5.3

Core Temperature Sensors

The second set of core temperature sensors were used to get a better understanding of the core temperature distribution. Five Type T thermocouples were installed in the same manner as the AD590KF core sensors. All five sensors were mounted in the supply side passages (see Figure 5.3). The thermocouples were read with a hand held Type T Thermocouple Thermometer (Model 8110-25, Cole Panmer Instr. Corp., Chicago, Ill.). The thermometer display precision was $\pm$ 0.5°C but the accuracy was expected to be $\pm$ 2.0°C.

5.2.3.3 PAMI Temperature Measurement

The wet and dry bulb temperatures of the return air stream and the exhaust air stream were measured with the PAMI temperature measurement equipment. The wet and dry bulb temperatures were measured using two psychrometric boxes. The boxes were identical to the kind described in ASHRAE (1975). Before the return air stream wet and dry bulb temperatures were measured the return air passed through a mixing device. A sample of the mixed air was drawn through a psychrometric box where the wet and dry bulb temperatures were measured. The air velocity in the psychrometric box was 5.1 m/s. A second psychrometric box was used to measure the wet and dry bulb temperatures of the exhaust air stream. The air was drawn from the air stream through a sampling device. An attempt was made to measure the air velocity in this box but the velocity was so low it could not be measured. Thus the wet bulb reading of the exhaust air stream could have been in considerable error.

The sensors used by PAMI were Type T thermocouples. Before being used in this experiment, the four thermocouples in the psychrometric boxes were calibrated against the glass stick thermometer discussed in Appendix B. The thermocouples were bundled together around the thermometer and the bundle was submerged in a pail of room temperature water for five hours. At the end of the five hours, the reading on the glass thermometer was 17.5°C. The thermocouple monitor was adjusted such that all four thermocouple readings indicated 17.5°C $\pm$ 0.1°C. This calibration procedure ensured matched thermocouples.

5.2.4 Bypass Damper System Calibration

Dampers often do not give a change in flow proportional to the change in position. The nonlinear operation of the damper can dramatically affect a control strategy which relies on the adjustment of a damper to control flow. Since the control strategy tested in this experiment utilized a modulated bypass, it was necessary to calibrate the damper system.

The damper system consisted of two dampers connected through a 3:1 gear reduction to a stepper motor. The stepper motor and dampers are shown in Figure 5.1. The range of operation of the damper system was 280 steps. The results of the damper calibration are shown in Figure 5.4. The damper position adjustment in the range from 170 steps to 240 steps was of no value in controlling the flow since a change in position did not change the flow rate. For RUN 1, the controller selected damper positions throughout the entire damper position range and passed through steps 170 to 240 quickly.

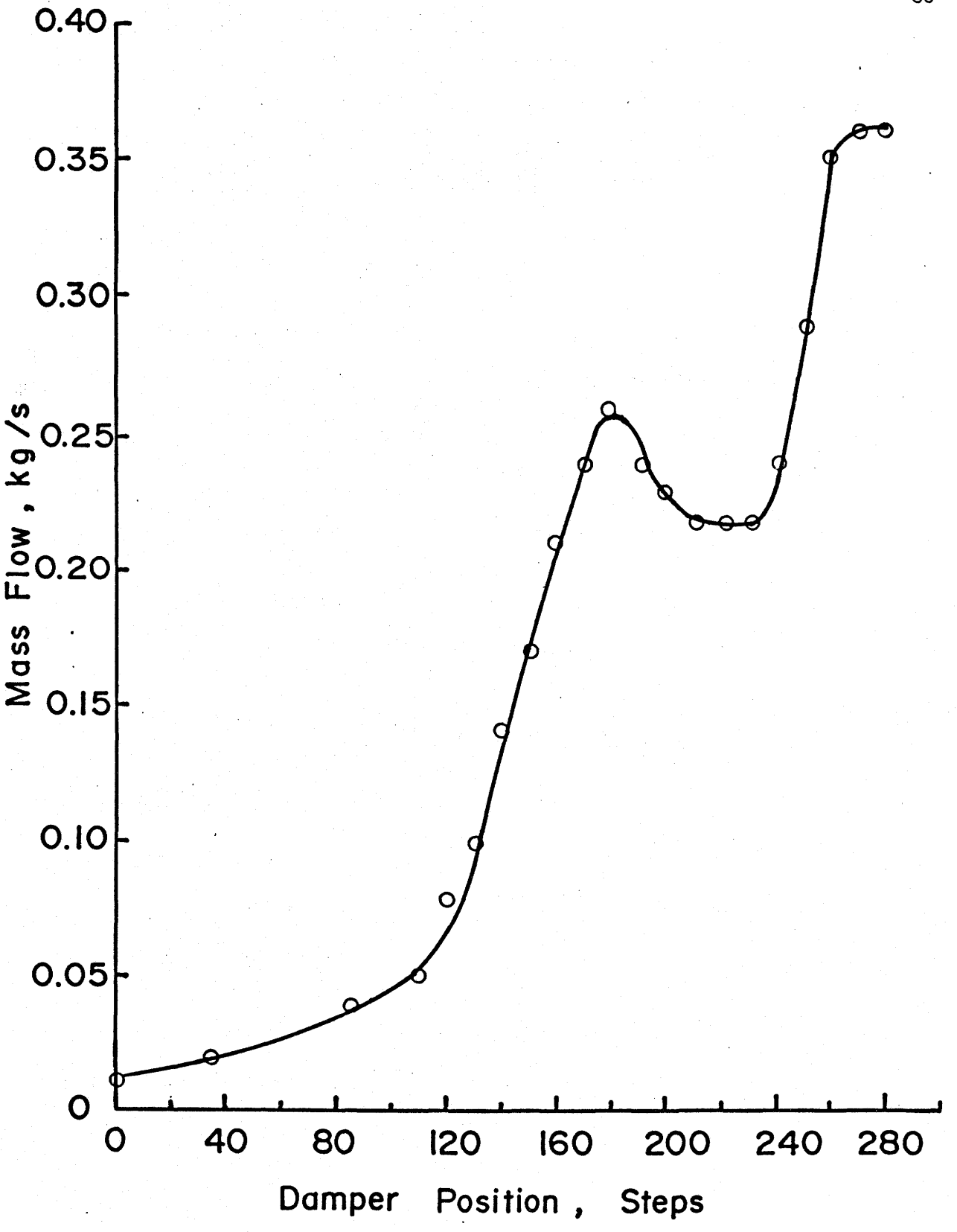

FIGURE 5.4

Damper System Calibration

The controller made no attempt to carefully control the flow between damper positions 170 steps and 240 steps but only passed through this range. For RUN 2, RUN 3 and RUN 4, the controller attempted to reach an operating state between damper positions 170 steps and 240 steps. Since the damper system gave very nonlinear flow control in this damper position range the control software was altered for RUN 2, RUN 3 and RUN 4 so that the damper was moved from step 170 to step 241 as if a single step had occurred. This change meant that the damper range was reduced from 280 steps to 209 steps. The change in the damper system range did not affect the comparison of the results of RUN 1 with the results of RUN 2, RUN 3 and RUN 4 because of changes made to the controller gain.

5.2.5 Condensate Measurement

Cooling of the return air stream in the heat exchanger caused condensation to form. Condensate from the heat exchanger was collected so that an energy balance could be calculated for the heat exchanger.

The heat exchanger was fitted with a drain on the exhaust side of the core. The condensate flowing from the drain was collected in a pail and weighed every 30 minutes on an electronic scale (Type 1404, Sartorius, West Germany). Condensate measurements were made for all runs except RUN 1 when the scale failed shortly after the test started.

5.2.6 Duct Insulation

The heat exchanger test setup was insulated to prevent heat leaks. Twenty-five millimeter thick fiberglass insulation with foil backing was used. Figure 5.1 shows the areas of the test setup which were insulated.

The section of duct from the venturi to the nearest temperature measurement section was double insulated. This was done to ensure that

the air temperature used in the computation of the outside air mass flow rate was as close to the air temperature in the venturi as possible. The error in mass flow rate measurement due to heat leakage was calculated to be 0.2 percent at most.

The ductwork between the heat exchanger outlets and the nearest temperature measurement sections were single insulated. The temperature measurements made on the exhaust side of the heat exchanger were consistently 0.3°C above the air temperature at the exchanger outlet. On the supply side of the heat exchanger the temperature measurement was between 0.1°C and 0.6°C above the outlet air temperature. The smallest error was in RUN 1 and the largest error was in RUN 4. All the temperature error estimates were calculated using methods described by ASHRAE (1985).

5.2.7 Measurement of Pressure Drop Across the Core

The pressure drop across the heat exchanger core on the exhaust side was measured because it was indicative of the amount of frost accumulated.

Two pressure taps were placed in the return air duct (Figure 5.1). Both taps were placed 178 mm from the heat exchanger. One was on top of the duct in the middle and the other was on the bottom of the duct in the middle.

In the same manner two more pressure taps were placed in the exhaust air duct. Both taps were placed 476 mm from the heat exchanger. One tap was on top of the duct in the middle and the other was on the bottom of the duct in the middle.

Each pair of pressure taps were manifolded and connected to opposite sides of a manometer (Type 4 and Type 5 Air Flow Testing Set, AirFlow Developments Ltd., Mississauga, Ontario).

5.2.8 Control and Data Acquisition System

The control and data acquisition system consisted of a computer controller board, an A/D convertor board, and a terminal.

The computer controller (BCC52, Micromint Inc., Cedarhurst, N.Y.) was a stand alone single board microcomputer which was programmable in Basic. This board permitted a reasonably complicated control and data acquisition algorithm to be implemented without the large development effort required for most digital control and data acquisition systems.

The signals from the temperature sensors and the pressure transducer were received by a 12-bit A/D convertor (BCC30, Micromint Inc., Cedarhurst, N.Y.) which was bus compatible with the computer controller. The A/D convertor had 16 channels available but only two were used. One channel was connected to the temperature sensor multiplexer and a second channel was connected to the pressure transducer demodulator.

The large number of AD590KF temperature sensors and the limited number of A/D channels required that the signals from the temperature sensors be multiplexed. The signals were multiplexed to a single A/D channel. The multiplexer was constructed similar to the matrix multiplexer suggested by Analog Devices in their AD590 product literature.

A terminal (Model 100, Radio Shack, Barrie, Ont.) was required to program the computer controller. The terminal and the computer controller were connected through RS232C ports. The terminal permitted programs to be uploaded to the computer controller and for data to be downloaded to the terminal.

Data were transferred from the terminal to a floppy disk after each test and then, via a modem, to a mainframe computer (VAX 11/780, College of Engineering).

5.3 Experimental Test Procedure

The steps followed in performing the tests are given in Appendix C. The data were recorded during each test in the following manner:

Starting when the test commenced and every 30 minutes thereafter the following manual readings were taken and recorded:

(a) time of measurement (local time)

(b) return air dry bulb temperature (°C)

(c) return air wet bulb temperature (°C)

(d) exhaust air dry bulb temperature (°C)

(e) exhaust air wet bulb temperature (°C)

(f) exhaust air mass flow rate (g/s)

(g) core pressure drop on the exhaust side (in w.c.)

(h) weight of condensate collected since the last reading (g)

(i) core thermocouple temperature sensors (°C)

(j) cold room temperature (°C)

(k) control error [RUN 2, RUN 3 and RUN 4](°C)

Starting when the test commenced and every six minutes thereafter the following readings were made by the controller:

(a) all of the temperature sensors

(b) pressure transducer.

The data were processed and the following results recorded:

(a) time (hrs) from start of test

(b) average outside air temperature (°C)

(c) average supply air temperature (°C)

(d) average return air temperature (°C)

(e) average exhaust air temperature (°C)

(f) mass flow rate of supply air (g/s)

(g) heat transfer rate (kW)[computed following Equation 4.1]

(h) average supply side core temperature (°C)

(i) average exhaust side core temperature (°C)

(j) damper position (counts)

(k) control signal (°C)

(l) pressure transducer output (counts/10)

(m) one-fifth of the raw temperature data. (Eight channels of the forty available were recorded. The eight channels corresponded to either all the temperature measurements from one of the temperature measurement sections or six core temperature measurements, the pressure transducer output and a blank channel. Memory limitations did not permit more data to be recorded).

6. RESULTS, COMPARISONS AND DISCUSSION

6.1 Results of Optimizing Controller Operation

The theory (see Section 4.2) and the simulation work demonstrated that an optimizing controller could not be developed. In order to verify that an optimizing controller would not function a test run was done at one particular set of input conditions (see Table 4.1). The control strategy used was identical to the one described in Section 4.2 and the controller parameters used were the best combination of controller parameters (see Table 4.2) determined with the earlier version of the heat exchanger model. The test began by closing the bypass damper completely and forcing all of the available outside air through the heat exchanger. At the next control time all the temperature sensors and the pressure transducer were read. This reading was a baseline measurement and corresponds to the sharp spike shown in all the results. After the baseline measurement, the test proceeded by first defrosting the heat exchanger core and then slowly increasing the outside air mass flow rate. Figures 6.1 and 6.2 show the outside air mass flow rate and the heat transfer rate measured in the test. The figures show that the outside air mass flow rate had reached a plateau at which either increasing or decreasing the outside air mass flow rate did not stop the degradation of the heat transfer rate. The other indications of uncontrolled frost accumulation were that the core pressure drop had increased from 107 Pa to 927 Pa and that the return air stream mass flow rate had decreased from 0.33 kg/s to 0.19 kg/s. These test results indicated that a stable state at which the heat exchanger could be operated continuously could not be found using the optimizing controller tested.

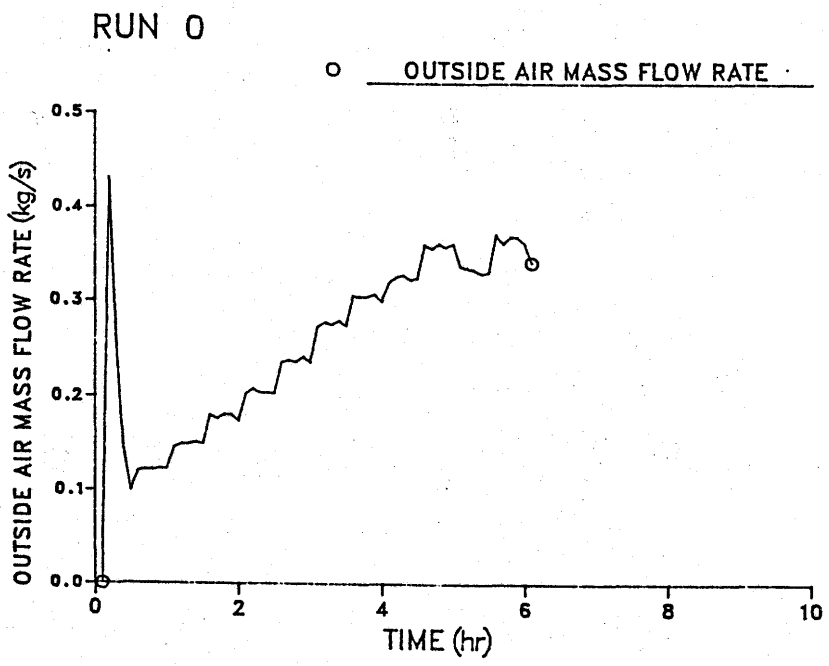

FIGURE 6.1

Optimizing Controller: Measured Outside Air Mass Flow Rate

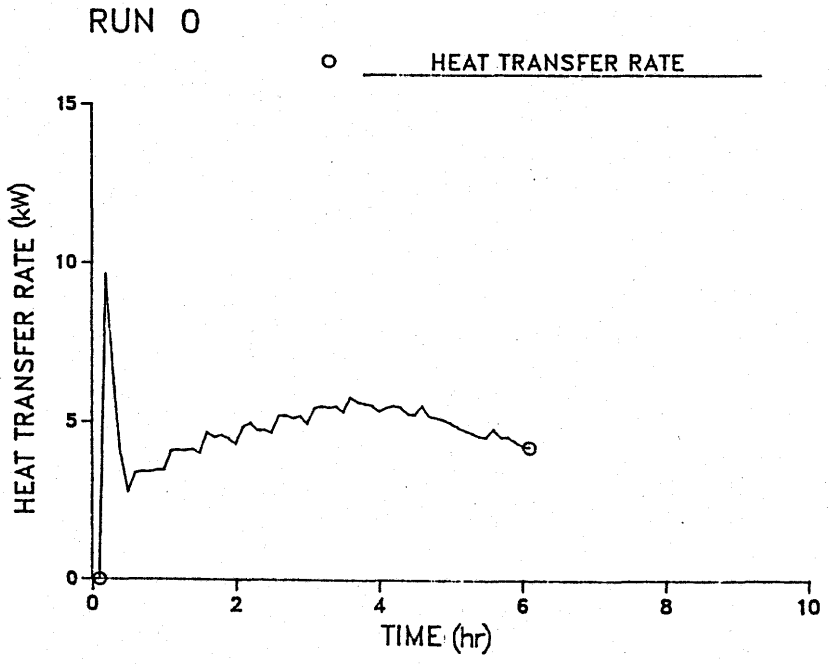

FIGURE 6.2

Optimizing Controller: Measured Heat Transfer Rate

6.2 Results of Defrost Controller Operation

The defrost controller operated by continuously following a series of three phases: defrost, exhaust air temperature set and heat transfer rate monitoring. The defrost involved bypassing more and more outside air until the core temperature exceeded 0°C. Once the heat exchanger was defrosted then the flow of outside air through the heat exchanger was increased. The mass flow rate of outside air was increased until the exhaust air temperature was within 1.0°C of 2.5°C (exhaust air setpoint temperature). The last phase of the controller operation was monitoring the heat transfer rate. Since during this phase the outside air mass flow rate was constant, the temperature change of the cold air stream was a direct measure of the heat transfer rate. Once the change in the temperature of the cold air stream had reduced by 2.5°C (control error for the cold air stream temperature change) a defrost was initiated and the control cycle repeated. The opening of the bypass damper for defrost and the closing of the bypass damper for exhaust air temperature set were both controlled using proportional control. The defrost controller was tested at four different sets of input conditions. The results showed that for the four conditions tested the controller could operate indefinitely and maintain a constant average rate of heat recovery (see Figures 6.3 to 6.6).

The frost controller was not only to maintain a constant time averaged rate of heat transfer but the rate of heat transfer achieved was to approach the maximum thermodynamic potential of the heat exchanger. At the beginning of each run the maximum thermodynamic potential of the heat exchanger was measured by closing the bypass and measuring the rate of heat transfer at the maximum outside air mass flow

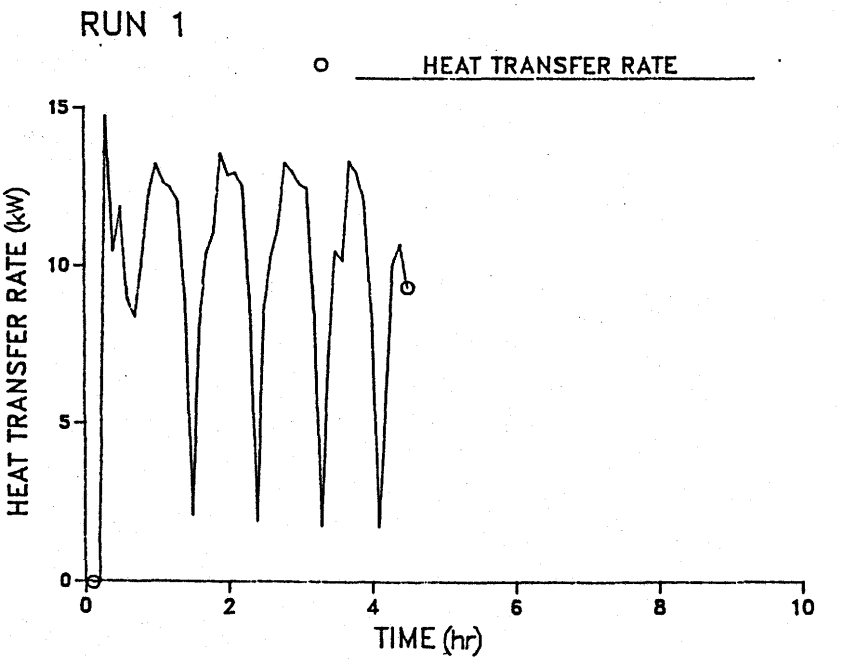

FIGURE 6.3

RUN 1: Measured Heat Transfer Rate

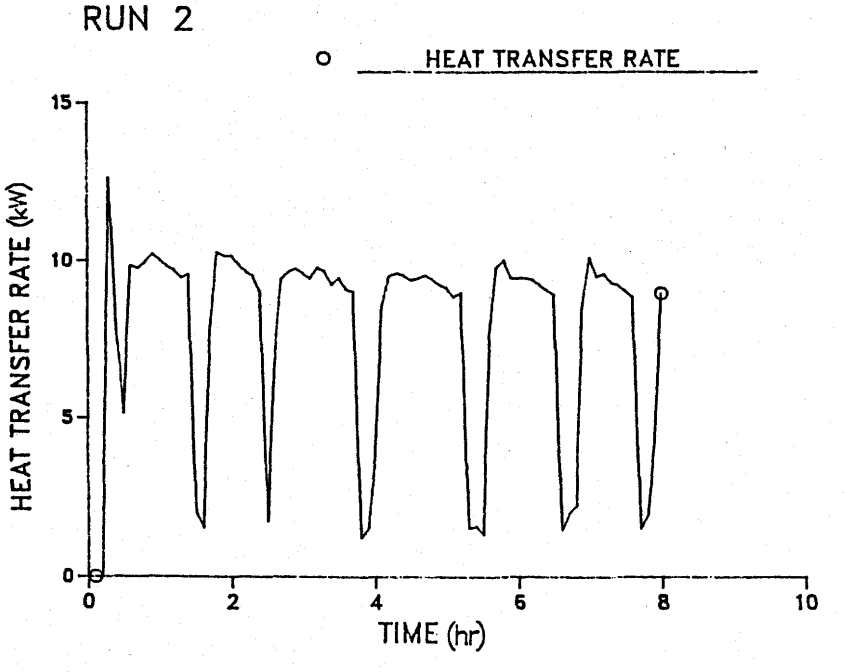

FIGURE 6.4

RUN 2: Measured Heat Transfer Rate

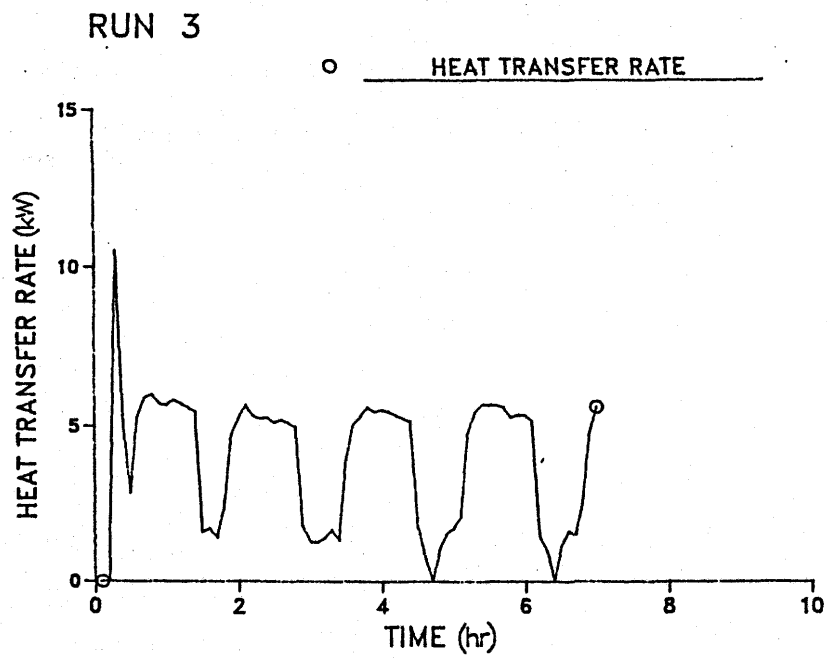

FIGURE 6.5

RUN 3: Measured Heat Transfer Rate

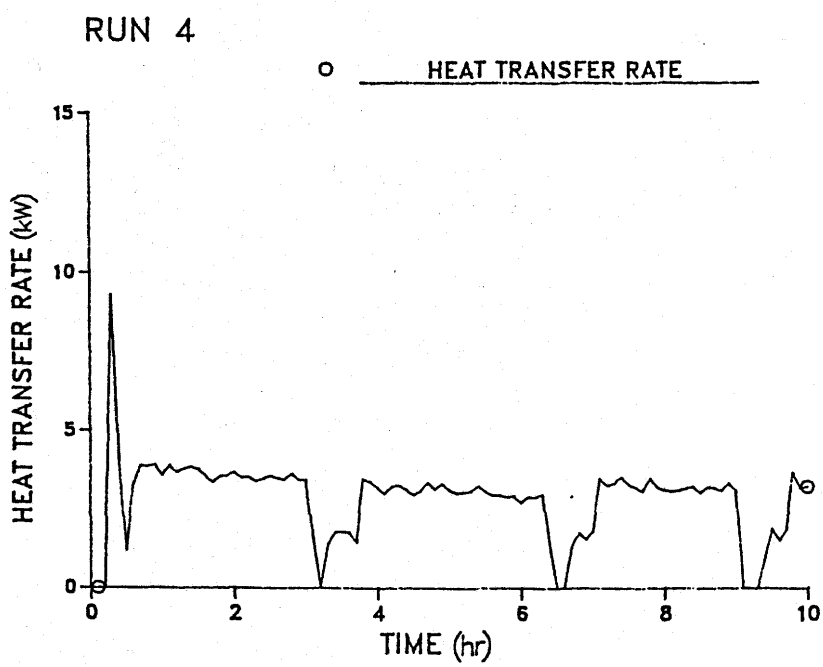

FIGURE 6.6

RUN 4: Measured Heat Transfer Rate

TABLE 6.1

Heat Exchanger Thermodynamic Potential

RUN	Heat Transfer Rate: Baseline Measurement (kW) A	Heat Transfer Rate: Beginning of Heat Transfer Rate Monitoring Phase (kW) B	$\frac{A}{B} * 100$ (%)
1	14.7	13.4	91
2	12.7	10.0	79
3	10.6	5.7	54
4	9.3	3.7	40

rate. Since this measurement (baseline measurement) was done at the beginning of each run the heat exchanger was virtually frost free. Comparing the baseline measurement with the heat transfer rate at the beginning of the heat transfer monitoring phase of the controller cycle indicated how close the heat exchanger was operated to its maximum thermodynamic potential. Table 6.1 shows the results of this comparison.

In RUN 1 the outside air mass flow rate was the maximum available but for the other three runs it was not. The controller did not select a larger outside air mass flow rate for RUNS 2, 3 and 4 because the exhaust air setpoint temperature (2.5°C) had been reached before the maximum outside air mass flow rate available was achieved. Selecting a lower exhaust air setpoint temperature would increase the outside air mass flow rate and increase the percentages (given in Column 3, Table 6.1) for RUNS 2, 3 and 4. But, selecting a lower exhaust air setpoint temperature increases the rate of frost accumulation.

The closeness of agreement between the two heat transfer rates given in Table 6.1 also depends on how quickly the outside air mass flow rate is increased from the low flow rate during defrost to the maximum flow rate during the heat transfer monitoring phase of the control cycle. The slower the change in outside air mass flow rate the more frost accumulates before the maximum mass flow rate of outside air is achieved. The accumulated frost causes the heat transfer to be degraded and thus the maximum heat transfer rate for an unfrosted heat exchanger cannot be achieved.

Table 6.1 only compares instantaneous rates of heat transfer but to completely evaluate the controller performance the time average rate of heat transfer must be considered. The third stage of the controller cycle was the heat transfer rate monitoring stage. During this stage the mass flow rate of outside air was constant and the largest that occurred during the controller cycle. Also, the heat transfer rate was the maximum that occurred during the controller cycle. The percentage of the total control cycle the controller operated with the heat exchanger at a constant outside air mass flow rate was calculated. The results are shown in Table 6.2.

TABLE 6.2

Controller Operating Fraction

RUN	Percentage of Controller Cycle at Constant Outside Air Mass Flow Rate (%)
1	35
2	56
3	43
4	74

The percentage of the controller cycle at a constant outside air mass flow rate represents the fraction of the controller cycle when significant heat transfer is occurring. Increasing the control error for the cold air stream temperature change will increase the percentage of the controller cycle at constant outside air mass flow rate, but the control error cannot be increased indefinitely because at some point more frequent defrosting actually would increase the time average rate of heat transfer.

The effect of changing the exhaust air setpoint temperature and the control error for the cold air stream temperature change can be seen by considering Figure 6.7. Decreasing the exhaust air setpoint temperature causes h to approach the maximum thermodynamic potential of the heat exchanger. But as h increases, the rate of frost accumulation also increases and the slope a/b decreases further. If the control error for the cold air stream temperature change is increased then the time between defrosts increases (i.e., l becomes larger). As l increases however the length of defrost becomes longer (i.e., m becomes larger). Figure 6.8 shows the heat transfer rate for an optimized defrost controller. Since h and l are both larger, the time average rate of heat transfer is increased when compared with the time average rate of heat transfer shown in Figure 6.7.

The overall effectiveness of the controller developed was evaluated by comparing the maximum possible heat transfer rate measured with the baseline measurement to the average heat transfer rate achieved. Table 6.3 compares the two heat transfer rates.

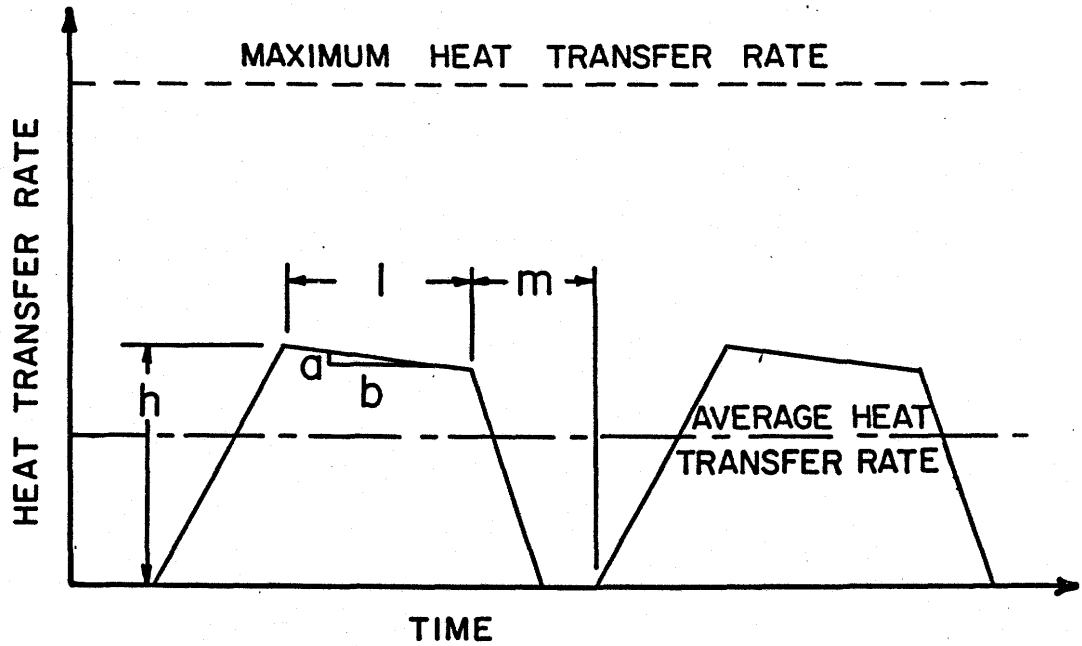

FIGURE 6.7

Heat Transfer Rate with Nonoptimized Defrost Controller

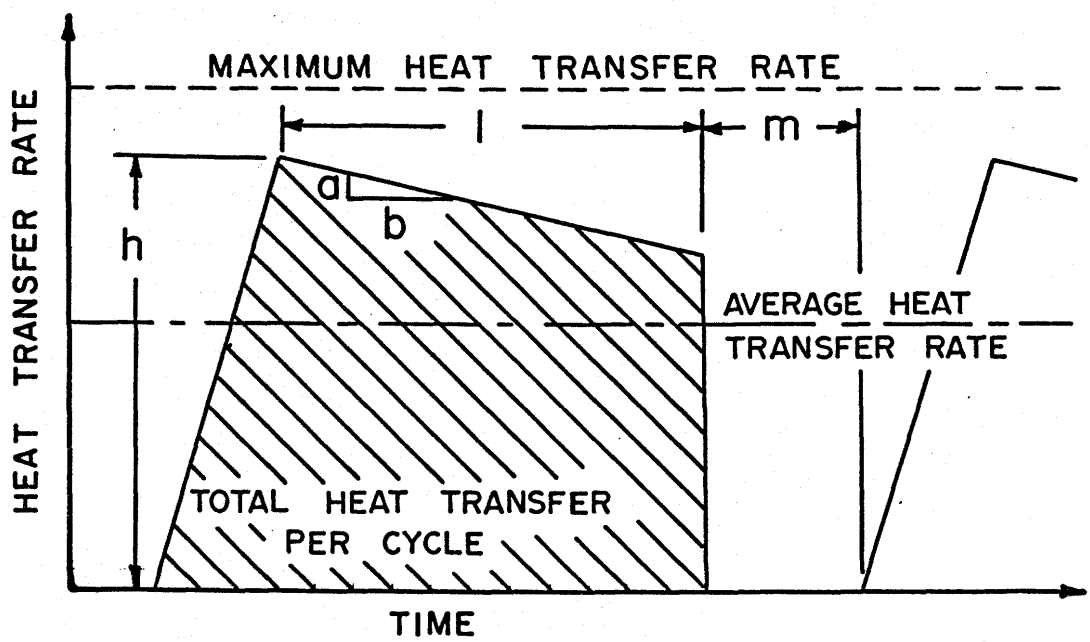

FIGURE 6.8

Heat Transfer Rate with Optimized Defrost Controller

TABLE 6.3

Comparison of Maximum and Average Heat Transfer Rates

RUN	Maximum Possible Heat Transfer Rate (kW) A	Average Heat Transfer Rate Achieved (kW) B	$\frac{B}{A} * 100$ (%)
1	14.7	8.6	59
2	12.7	6.4	50
3	10.6	3.7	35
4	9.3	2.8	30

It is expected, based on the comparison of Figure 6.7 and Figure 6.8, that the percentage of maximum heat transfer rate achieved could be increased by permitting more frost to accumulate before defrost (i.e., increasing the control error for the cold air stream temperature change) and by permitting a higher heat transfer rate during the heat transfer rate monitoring state of the controller cycle (i.e., a lower exhaust air setpoint temperature).

6.3 Comparison of Simulation Results and Experimental Results

The heat exchanger model was calibrated based on the experimental test results. The model calibration involved selecting the frost thermal conductivity and the return air fan pressure.

The frost thermal conductivity significantly affected the results of the simulation because the frost thermal conductivity affected both

the length of time the controller operated in the heat transfer monitoring state and the outside air mass flow rate during the heat transfer monitoring state. The frost thermal conductivity used in Equation 3.25 was 0.01 W/m K. This frost thermal conductivity was selected because it gave the best agreement between the model predictions and the experimental results of the length of time the controller operated in the heat transfer monitoring state and of the outside air mass flow rate during the heat transfer monitoring state. The available literature (Section 3.1.3.4) suggested that the frost thermal conductivity was significantly greater. For example, Yonko and Sepsy's (1967) equation (Equation 3.14), which was representative of the available literature, indicated a minimum frost thermal conductivity of 0.024 W/m K, 2.4 times greater. Also, since frost is an air ice mixture it was expected that the frost thermal conductivity should be less than the conductivity of ice (2.34 W/m K at -10°C) but greater than the conductivity of air (0.023 W/m K at -10°C).

Examination of the fan curve and the fact that the return air mass flow rate never decreased more than 10 percent from the mass flow rate with no frost accumulation, it was assumed that the fan operated at a constant pressure. The fan pressure selected from the fan curve was 2815 Pa. It was found that the equations used to calculate the return air mass flow rate only significantly affected the pressure drop across the hot side of the heat exchanger core and they did not affect the heat exchanger thermal performance.

The first hypothesis in Section 2 stated that a computer model could be developed that would simulate the thermal performance of a heat exchanger operating under frost forming conditions and which was operated with frost control. This hypothesis will be tested by comparing different thermal performance parameters predicted by the simulation with those measured in the tests. The detailed simulation results are presented in Appendix D. The graphs in Appendix D show the outside air mass flow rate, the heat transfer rate, the exhaust air stream temperature, the supply air stream temperature and the heat exchanger core temperature near the outside air stream inlet all as a function of time for the four RUNS. Appendix E shows the detailed experimental test results. The results are presented so that direct comparison can be made to the results in Appendix D. In Appendix E two core temperatures are given, one was the core temperature measured on the hot side of the heat exchanger core and the other was the core temperature measured on the cold side of the heat exchanger core.

Comparison of the heat exchanger thermal performance calculated by the simulation and measured in the tests was complicated by the controller action. Direct comparison of the time between defrosts, the heat transfer rate, the air stream outlet temperatures and the core temperature was difficult because the outside air mass flow rate through the heat exchanger was not the same between the simulation results and the test results for all the RUNS. Equation 4.1 indicates how mass flow rate would affect the outlet temperature. Table 6.4 compares the outside air mass flow rate selected by the simulation controller and the outside air mass flow rate selected by the experimental controller.

TABLE 6.4

Outside Air Mass Flow Rate During the Heat Transfer Monitoring State

RUN	Simulation Results (kg/s) A	Experimental Results (kg/s) B	$\frac{A}{B}$
1	0.43	0.43	1.00
2	0.44	0.34	1.29
3	0.16	0.19	0.84
4	0.10	0.12	0.83

The mass flow rates in Table 6.4 were the mass flow rates which occurred during the heat transfer monitoring phases of the controller cycle. Only in RUN 1 was the outside air mass flow rate selected by both controllers the same. The two mass flow rates were the same in this RUN because both the simulation controller and the experiment controller reached the maximum outside air mass flow rate before the exhaust air temperature setpoint was reached.

The average time of the heat transfer monitoring phase of the control cycle was compared between the simulation results and the test results. During the heat transfer monitoring phase the outside air mass flow rate was constant and frost accumulated at its maximum rate. The average time operated in the heat transfer monitoring state (line 1, Figure 6.7) between the simulation results and the test results is compared in Table 6.5.

TABLE 6.5

Time Controller Operated in the Heat Transfer Monitoring State*

RUN	Simulation Results (hr) A	Experimental Results (hr) B	$\frac{A}{B}$
1	0.90	0.31	2.90
2	1.17	0.62	1.89
3	1.41	0.72	1.96
4	2.55	2.21	1.15

* (Line 1, Figure 6.7)

Table 6.5 shows that for all RUNS the predicted time was greater than the measured time and that the best agreement occurred for RUN 4.

It was found that the outside air mass flow rate during the heat transfer monitoring phase of the controller cycle and the length of the heat transfer monitoring phase were closely tied to the heat exchanger heat transfer model. The heat transfer model depended critically on the frost thermal conductivity selected. The frost thermal conductivity that was selected gave the best overall agreement between the outside air mass flow rate during the heat transfer monitoring phase of the controller cycle and the time of the heat transfer monitoring phase between the simulation results and the test results for all four RUNS. It was found that decreasing the frost thermal conductivity decreased the outside air mass flow rate but increased the time of the heat transfer monitoring phase and vice versa. Tables 6.4 and 6.5 show that even though the best frost thermal conductivity was selected poor agreement between the simulation results and the test results were found.

Thus a computer model was not developed which would simulate the thermal performance of a heat exchanger operating under frost forming conditions and which was operated with frost control (i.e., Hypothesis One in Section 2 was rejected). RUN 4 displayed the best agreement. Figures 6.9 to 6.16 compare respectively the outside air mass flow rate, the heat transfer rate, the outlet air stream temperatures and the heat exchanger core temperature between the simulation results and the test results for RUN 4. Figure 6.13 and Figure 6.14 show the exhaust air temperature plotted with the supply air temperature. The superposition of the two curves does not imply any direct relationship between the two temperatures. Figure 6.15 was the core temperature calculated using Equation 3.24. Figure 6.16 compares the core temperature measured by the sensors mounted on the cold side of the heat exchanger core with the core temperature measured by the sensors mounted on the hot side of the heat exchanger core. The difference between the two temperatures was a measure of the influence of the convective heat transfer on the side of the sensor which was not in contact with the heat exchanger core. The average of the two core temperatures in Figure 6.16 can be compared with the core temperature in Figure 6.15.

Several aspects of the heat exchanger simulation were expected to have contributed to the less than perfect agreement between the simulation predictions and the experimental results.

The frost growth equation used in the simulation was Equation 3.12 developed by O'Neal and Tree (1984). This equation was developed for frost growth in a parallel plate heat exchanger with a plate spacing of 12.7 mm, a typical wall temperature variation of $\pm$0.5°C and flow Reynolds numbers between 4400 and 15900. But the heat exchanger tested had a plate spacing of 5.4 mm, a typical plate temperature variation greater than 10°C and flow Reynolds numbers less than 2300. These

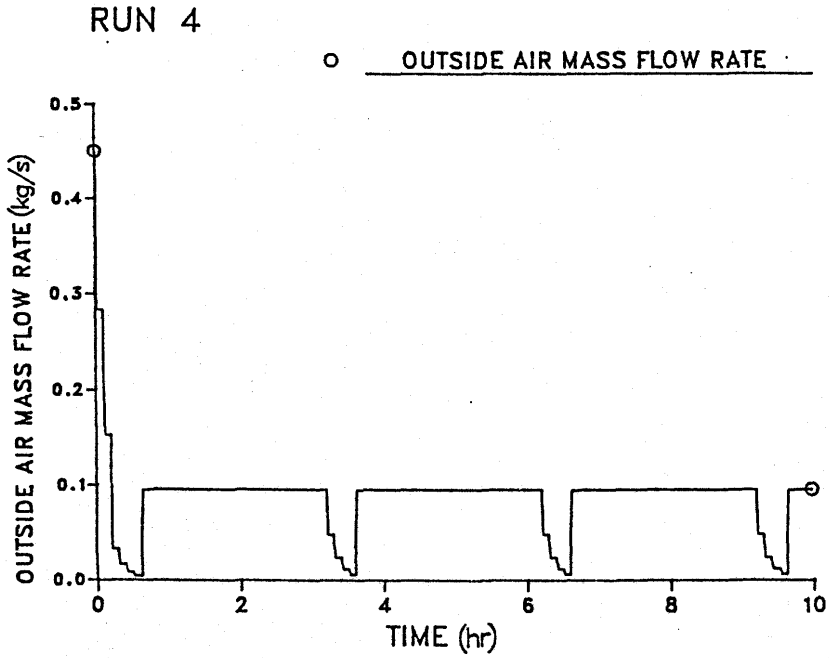

FIGURE 6.9

RUN 4: Predicted Outside Air Mass Flow Rate

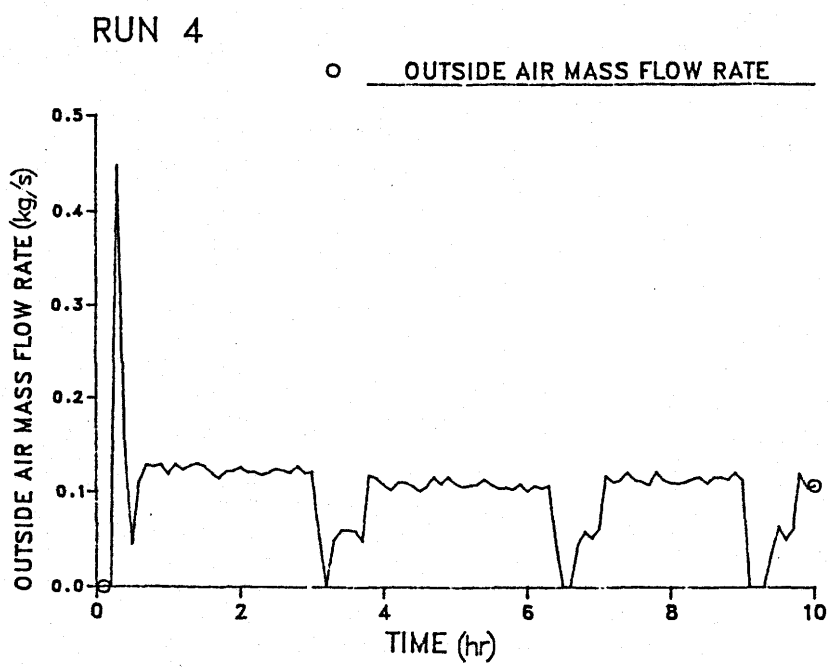

FIGURE 6.10

RUN 4: Measured Outside Air Mass Flow Rate

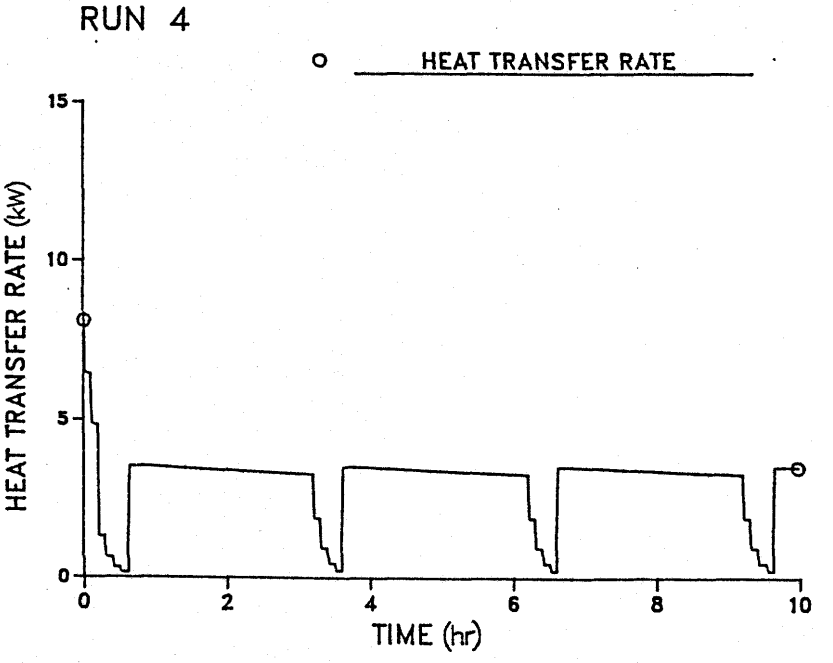

FIGURE 6.11

RUN 4: Predicted Heat Transfer Rate

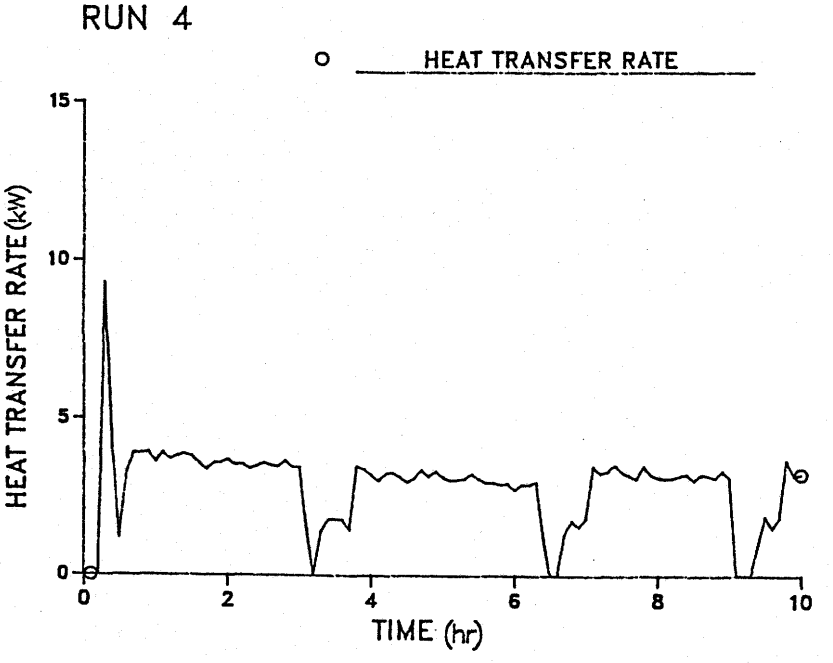

FIGURE 6.12

RUN 4: Measured Heat Transfer Rate

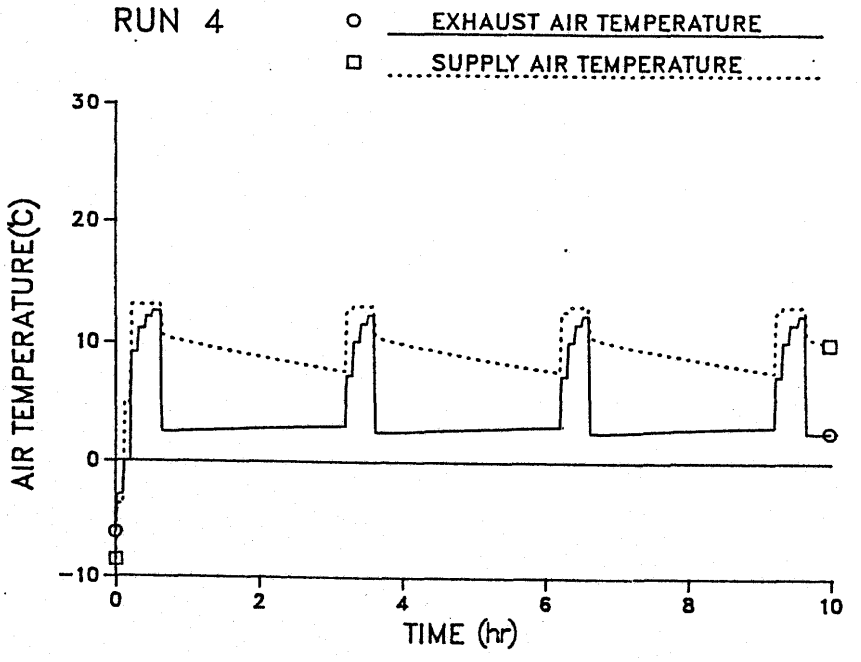

FIGURE 6.13

RUN 4: Predicted Outlet Air Stream Temperatures

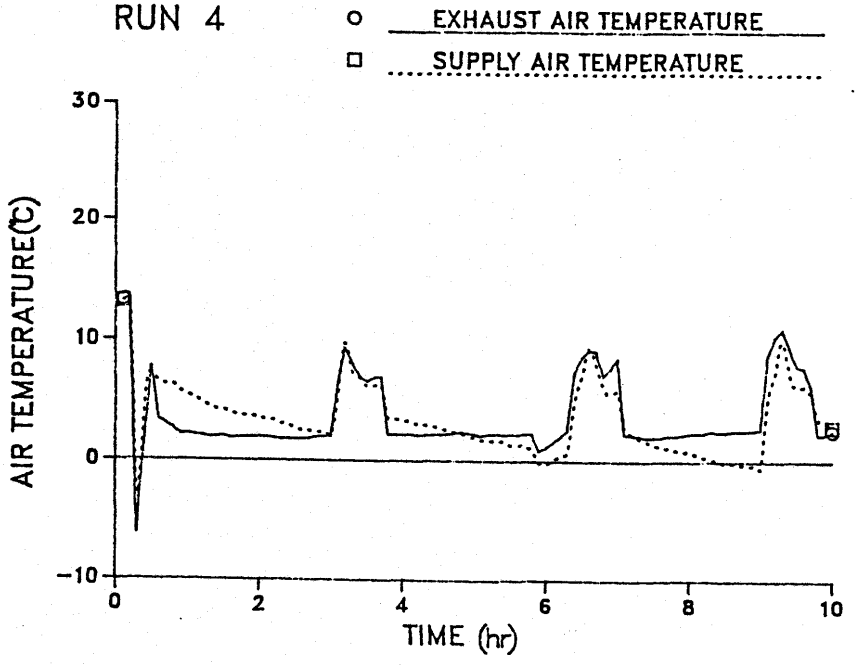

FIGURE 6.14

RUN 4: Measured Outlet Air Stream Temperatures

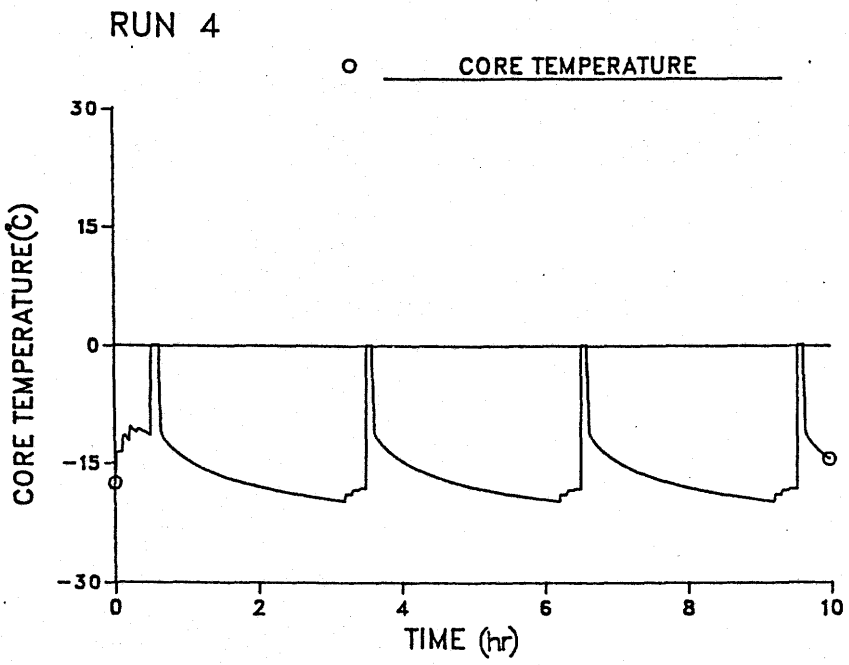

FIGURE 6.15

RUN 4: Predicted Core Temperature

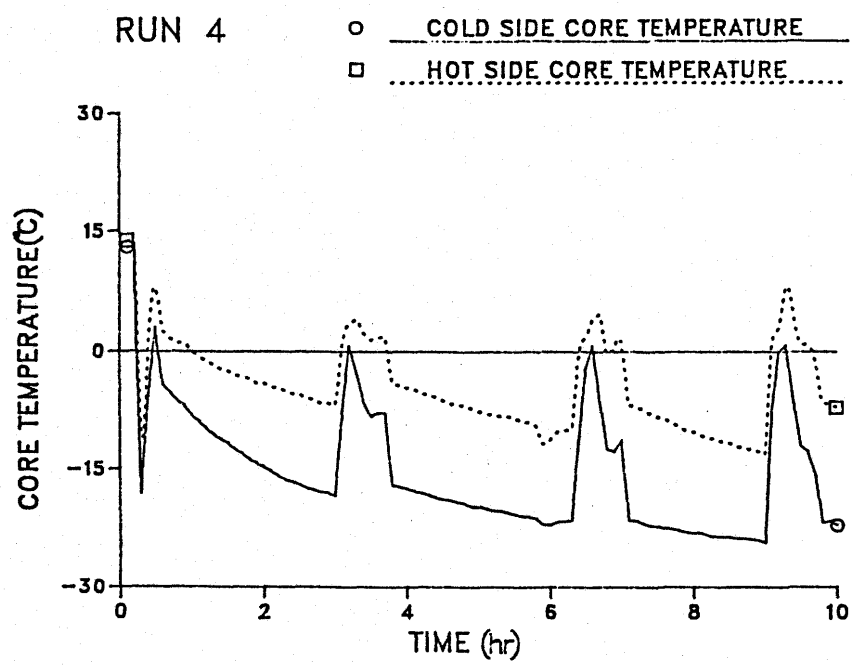

FIGURE 6.16

RUN 4: Measured Core Temperatures

differences may have significantly contributed to the disagreement found.

The sensible heat transfer in the wet region was calculated using the dry convection heat transfer coefficient. But Guillory and McQuiston (1973) as well as others had pointed out that the presence of condensate may significantly affect the convection heat transfer coefficient. The mass transfer coefficient was computed based on the convection heat transfer coefficient (see Equation 3.23) but no experimental data was found that confirmed that this equation was valid for flow in a thin passage. The uncertainty in the heat and mass transfer coefficients may also have contributed to the disagreement.

The heat and mass transfer processes in the heat exchanger were modelled using temperature potential but Kreid et al. (1978) pointed out that enthalpy potential may be a more appropriate way to model heat transfer in a heat exchanger which has both wet and dry passages.

The heat exchanger was modelled by dividing the heat exchanger into a wet region and a dry region. The frosting process was modelled by dividing the heat exchanger into 42 locations. These two models were blended together by representing the frost as a simple conduction resistance in the overall heat transfer equation (Equation 3.26). But the frost layer participated intimately in the heat and mass transfer processes which occurred in the hot air stream passages. A superior approach would probably have been to break the heat exchanger into many small control volumes as Kettleborough and Hsieh (1983) did and then apply one of the more sophisticated frost models [Jones and Parker (1975)] discussed in Section 3.1.3.2.

The frost accumulation in the heat exchanger was assumed to be one

dimensional but since the air entered orthogonal to the length of the heat exchanger, exitted orthogonal to the length of the heat exchanger and since the height of the entrance and exit planes were a significant part of the heat exchanger length the flow was two dimensional. The two dimensional nature of the flow would cause frost to accumulate much more quickly than was predicted by the model in certain areas of the heat exchanger (near the outside air entrance). The two dimensional accumulation of frost would cause the flow pattern inside the heat exchanger to be altered. The important aspect of the flow pattern alteration would be that less and less of the warm moist air would pass through the coldest part of the heat exchanger as frost accumulated. Since the model developed was a one dimensional model, alteration of the flow patterns in the heat exchanger could not be predicted and this effect was subsequently not accounted for. Thus the heat transfer rate degradation with frost accumulation could have resulted from the combined effect of the increased thermal resistance due to frost accumulation and the shift of the warm moist air flow pattern, the later effect being possibly the most significant.

Despite the lack of good agreement between the simulation results and the test results the heat exchanger simulation was essential in developing the frost controller because the simulation was able to predict the thermal performance trends of the heat exchanger. The trends predicted caused the viability of the optimizing controller to be questioned and the value of the defrost control to be studied. The simulation also aided in the selection of the defrost controller setpoints and gains.

The comparison between the simulation results and the test results was completed by comparing the heat transfer rate, the outlet air stream temperatures, the core temperature, the minimum return air stream mass

flow rate and the maximum pressure drop across the hot side of the heat exchanger core for the four runs.

Table 6.6 compares the average heat transfer rate during the heat transfer rate monitoring phase of the controller cycle between the simulation predictions and the experimental results.

TABLE 6.6

Average Heat Transfer Rate Comparison

RUN	Model Predictions (kW)	Experimental Results (kW)
1	11.4	12.7
2	8.8	9.5
3	5.0	5.4
4	3.5	3.3

Table 6.7 compares the exhaust air temperature and the supply air temperature between the simulation predictions and the experimental results. The comparison was made just prior to defrost.

TABLE 6.7

Outlet Air Stream Temperature Comparison

	Exhaust Air Stream Temperature		Supply Air Stream Temperature	
RUN	Simulation Prediction (°C)	Experimental Results (°C)	Simulation Prediction (°C)	Experimental Results (°C)
1	9.5	7.7	1.2	4.1
2	6.4	4.1	-6.6	1.2
3	3.9	3.7	2.9	0.8
4	2.9	2.5	7.7	0.8

The difference between the outlet temperatures predicted by the simulation and those measured in the experiment can be explained by the differences in the heat transfer rate and the outside air mass flow rate.

The heat exchanger core temperatures were measured near the outside air inlet and the exhaust air outlet. Table 6.8 compares the measured core temperatures with the predicted core temperature just prior to defrost. The difference in the core temperature measured on the hot side and the core temperature measured on the cold side was due to the influence of the convection heat transfer from the bulk air stream to the temperature sensor.

TABLE 6.8

Core Temperature Comparison

RUN	Core Temperature Predicted (°C)	Core Temperature Measured on the Hot Side (°C)	Core Temperature Measured on the Cold Side (°C)
1	-17.2	-8.8	-18.8
2	-19.7	-13.4	-21.6
3	-20.6	-6.6	-18.1
4	-19.7	-9.1	-21.6

The return air stream mass flow rate and the pressure drop across the hot side of the heat exchanger core were calculated by the simulation and measured in the tests. The minimum flow rates and maximum pressure drops are given in Table 6.9. Since the mass flow rate and the pressure drop were measured every 30 minutes in the tests the minimums and maximums given in Table 6.9 for the measured minimum mass flow rate and the measured maximum pressure drop may not correspond to the most extreme conditions.

TABLE 6.9

Minimum Return Air Stream Mass Flow Rate and Maximum Pressure Drop Across the Hot Side of the Heat Exchanger

RUN	Predicted Minimum Mass Flow Rate (kg/s)	Predicted Maximum Pressure Drop (Pa)	Measured Minimum Mass Flow Rate (kg/s)	Measured Maximum Pressure Drop (Pa)
1	0.307	115	0.298	199
2	0.314	162	0.288	289
3	0.324	153	0.319	224
4	0.324	165	0.317	197

The pressure drop calculated was consistently below the pressure drop measured. Correspondingly the minimum mass flow rate calculated was consistenty above the minimum mass flow measured. Closer agreement between the pressure drops and the mass flows could have been achieved by slightly altering the calculation of the exchanger minimum free-flow area (Equation 3.28). This was not done because neither the pressure drop nor the return air mass flow rate were found to significantly affect the heat exchanger thermal performance when compared with the effect of the frost thermal conductivity.

6.4 Additional Experimental Results

6.4.1 Core Temperature Distribution

In order to gain an insight into the temperature distribution five thermocouples were placed on the heat exchanger core. The distribution of the thermocouples was shown in Figure 5.3. The temperature of the three thermocouples mounted in a row were generally within 1°C of their average temperature. This indicated that the core temperature was

probably quite uniform across the width of the core. The temperature of the thermocouple placed closest to the outside air inlet was always within a few degrees of the outside air stream temperature except during defrost. The temperature of the thermocouple placed closest to the center of the core varied between 1°C and 4°C from the average temperature of the three in line thermocouples. The most variation among the thermocouple temperatures generally occurred just after defrost and the least variation generally occurred just prior to defrost.

6.4.2 Condensate Accumulation

For RUN 1, condensate continuously flowed from the heat exchanger with the greatest release occurring during the defrost period. For RUN 2, RUN 3 and RUN 4 condensate flowed from the heat exchanger only during the defrost periods. Table 6.10 shows the average amount of condensate released during the defrost periods for RUN 2, RUN 3 and RUN 4. RUN 1 is not shown in Table 6.10 because the weigh scale failed during the test and no condensate measurements were made.

TABLE 6.10

Average Condensate Release

RUN	Average Condensate Release (kg/defrost)
2	2.471
3	2.386
4	0.462

6.4.3 Heat Transfer Rate Balance

The heat released by the hot air stream should equal the heat absorbed by the cold air stream if no heat is lost to the environment.

An energy balance was done for RUN 1, RUN 2, RUN 3 and RUN 4. For each run an energy balance was performed at two different times. The times were selected as much as possible close to midway between successive defrosts so that the cold air stream mass flow rate had been constant for some time.

The rate of heat absorption by the cold air stream was computed by the control and data acquisition system (CDAS). Equation 6.1 was used for the calculation.

$$Q_c = m_c C_p (T_s - T_o) \qquad 6.1$$

where

Q_c = rate of heat absorption by the cold air stream (kW)

m_c = mass flow rate of the cold air stream (kg/s)

C_p = specific heat at constant pressure of dry air (1.006 kJ/kg)

T_s = supply air stream temperature (°C)

T_o = outside air stream temperature (°C)

Hand calculations verified that the CDAS correctly computed the rate of heat absorption. Due to duct heat gains the supply air stream temperature measured was slightly greater than the supply air stream temperature at the heat exchanger exit. To obtain the true rate of heat absorption a correction was applied. Table 6.11 shows the heat absorption rate measured by the CDAS, the heat absorption rate corrected for the supply air stream temperature error and the expected errors of the measurements.

TABLE 6.11

Heat Transfer Rate Balance

RUN	Time (hr)	Q_{Cold} (kW)	Q_{Cold} Corrected (kW)	Q_{Hot} (kW)	Q_{Hot} Corrected (kW)	Difference (kW)
1	2.0	12.839	12.791 ±0.329	13.913	14.074	1.283
	3.0	12.595	12.547 ±0.329	11.861	12.022	0.525
2	2.1	9.867	9.780 ±0.316	9.932	10.093	0.313
	5.0	9.154	9.067 ±0.316	9.289	9.450	0.383
3	2.4	5.282	5.198 ±0.345	5.461	5.622	0.424
	6.0	5.339	5.255 ±0.345	5.226	5.387	0.132
4	1.4	3.861	3.798 ±0.397	3.990	4.151	0.353
	8.1	3.108	3.045 ±0.397	3.856	4.017	0.972

The rate of heat release from the hot air stream was calculated using Equation 6.2.

$$Q_h = m_h (h_{in} - h_{out}) - h_F \, dm \qquad 6.2$$

where

Q_h = rate of heat release by the hot air stream (kW)

m_h = return air stream mass flow rate (kg dry air/s)

h_{in} = enthalpy of the return air stream (kJ/kg dry air)

h_{out} = enthalpy of the exhaust air stream (kJ/kg dry air)

h_F = enthalpy of frost (-341.78 kJ/kg)

dm = rate of accumulation of frost (kg/s)

A term to represent the volume flow rate of liquid water was not included in Equation 6.2 because the enthalpy of liquid water was nearly 0 kJ/kg.

The return air enthalpy was calculated using the wet and dry bulb air temperatures measured by the PAMI Temperature Measurement Equipment (PTME) and the dry bulb air temperature measured by the CDAS. The two measurement systems were used because the return air stream experienced a temperature increase between the PTME and the CDAS. The temperature rise was due to a large pressure drop between the two measurement points. The wet and dry bulb temperatures measured by the PTME were used to calculate the return air stream humidity ratio. The humidity ratio and the dry bulb temperature measured by the CDAS were together used to calculate the return air stream enthalpy.

The exhaust air stream enthalpy was calculated differently for RUN 4 compared to the other three Runs. For RUN 1, RUN 2 and RUN 3 the exhaust air stream was observed to be foggy. The fog indicated that the air stream relative humidity was 100 percent. The wet and dry bulb temperatures measured by the PTME indicated that the relative humidity was between 80 and 90 percent. The discrepancy was due to the poor

resolution of the dry bulb temperature. The dry bulb temperature had poor resolution because the thermocouple sensor failed shortly after the start of RUN 1 and was replaced with the glass stick thermometer described in Appendix B. The glass stick thermometer could only be read to $\pm$ 0.5°C. Assuming 100 percent relative humidity and using the dry bulb temperature measured by the CDAS the exhaust air stream enthalpies were calculated for RUN 1, RUN 2 and RUN 3. For RUN 4 the exhaust air stream relative humidity was less than 100 percent since no fog was observed. The PTME wet and dry bulb temperatures were used to calculate the exhaust air stream enthalpy. But it was observed that a 1.6°C difference existed between the dry bulb temperature measured by the PTME and the dry bulb temperature measured by the CDAS. For RUN 2 and RUN 3 the difference was 0.4°C and for RUN 1 even less. Water accumulation on the CDAS temperature sensors may have caused the differences between the two dry bulb temperatures.

Due to heat gains in the exhaust air stream duct the heat release rate calculated using Equation 6.2 had to be corrected to account for the heat gain. Table 6.11 shows the calculated heat release rate and the heat release rate corrected for the exhaust duct heat loss.

Table 6.11 shows the difference between the heat release rate from the hot air stream and the heat absorption rate to the cold air stream. The large difference in heat transfer rates at 2.0 hours in RUN 1 was attributed to the rapidly changing conditions. Since the manual measurements could not all be made at the same instant and since the RUN was very near defrost the difference resulted. In RUN 4 the large error was probably linked to the dry bulb temperature discrepancy mentioned earlier. The heat transfer rate balances done at the other six times showed good agreement. The good agreement lends confidence to the experimental results.

7. CONCLUSIONS AND RECOMMENDATIONS

The main objective of this study was to investigate the frost formation process in a heat exchanger and to design and test a suitable frost control strategy that would maximize the overall rate of heat transfer in a heat exchanger. To meet this objective two hypothesis were tested.

The first hypothesis was:

> An existing computer model developed by Besant and Bugg (1981), with modification, will simulate the thermal performance of a heat exchanger operating under frost forming conditions and under frost control.

A computer model of a frosting and condensing heat exchanger was developed. Comparison of the test results with the simulation predictions showed considerable agreement in spite of many simplifying assumptions. The most significant differences were that the model predicted longer times between defrosts and different outside air mass flow rates during the frost accumulation periods. Although the trends of behavior were predicted, a computer model was not developed which would simulate the thermal performance of a heat exchanger operating under frosting conditions and under frost control (i.e., Hypothesis One was rejected). The expected reasons for the lack of agreement were:

(1) the frost growth equation used was not developed for the conditions under which it was applied,

(2) the heat and mass transfer coefficients used in the condensing region of the heat exchanger were developed theoretically and not verified experimentally,

(3) the heat and mass transfer processes were modelled using temperature potential while possibly enthalpy potential may have been used more appropriately,

(4) the heat exchanger was modelled as two regions and the frosting process was superimposed on the condensing heat exchanger model while a model which broke the exchanger into many small control volumes with an integrated frost model may have given better results,

(5) the assumption of one dimensional frost growth may have significantly contributed to the disagreement.

The second hypothesis tested was:

> A controller can be designed and implemented on a plate type commercial heat exchanger operating under frosting conditions that will find and continuously maintain a constant rate of heat transfer. The constant rate of heat transfer achieved will approach the maximum thermodynamic potential of the heat exchanger and will increase the efficiency of the heat exchanger compared to commonly used frost control strategies.

The second hypothesis was rejected because it was shown that a constant rate of heat transfer approaching the maximum thermodynamic potential of the heat exchanger could not be achieved continuously if the heat exchanger was operated under frosting conditions. The experimental tests performed demonstrated that a viable frost controller had been designed and that the control strategy developed has the ability to maintain from the heat exchanger a constant time average rate of heat transfer approaching the maximum thermodynamic potential of a heat exchanger. The tests did show however that the controller was not optimized. The factors identified as being important in developing an optimum controller were:

(1) The Exhaust Air Setpoint Temperature

The lower the exhaust air setpoint temperature the greater the maximum outside air mass flow rate, the greater the rate of heat transfer but also the greater the rate of frost accumulation.

(2) The Control Error for the Cold Air Stream Temperature Change

The larger this control error the longer the time between defrosts but correspondingly the longer the defrost.

(3) The Gains Used in the Proportional Control Phases of the Control Cycle

Increasing the proportional control gains and the addition of integral control could be used to increase the rate at which the controller moves to and moves from the defrosting phases of the controller cycle.

All three factors are interconnected and how all three would be changed to achieve the optimum controller is yet to be attempted.

Two summary conclusions have emerged from the present work:

(1) The heat exchanger model developed has prepared the foundation and pointed out the key parameters in developing a condensing and frosting heat exchanger model but much work is still required before such a model would be developed. Future work on the development of the heat exchanger model would proceed by evaluating the importance of the five simplified assumptions identified in this section.

(2) The frost control strategy tested is superior to all other agricultural frost control strategies and can be aplied to any heat exchanger irrespective of flow configuration. But further heat exchanger modelling and testing will be required to develop a controller which optimizes the overall rate of heat transfer. The three controller parameters identified in this section would need to be adjusted simultaneously in order to obtain the optimum controller. The effect of varying inlet temperatures (the validity of Equation 4.4) would also need to be investigated. The development of an off-the-shelf controller which could be used on any heat exchanger is possible but the hardware development and packaging are yet to be done.

REFERENCES

American Society of Heating, Refrigerating and Air-Conditioning Engineers, Inc. 1985. ASHRAE Handbook - 1985 Fundamentals. ASHRAE, Atlanta, GA.

American Society of Heating, Refrigerating and Air-Conditioning Engineers, Inc. 1979. ASHRAE Handbook and Product Directory - 1979 Equipment. ASHRAE, Atlanta, GA.

American Society of Heating, Refrigerating and Air-Conditioning Engineers, Inc. 1976. ASHRAE Standard 41.5-75. Standard measurement guide engineering analysis of experimental data. ASHRAE, Atlanta, GA.

American Society of Heating, Refrigerating and Air-Conditioning Engineers, Inc. 1975. ASHRAE Standard 41.1-74. Standard measurements guide: section on temperature measurements. ASHRAE, Atlanta, GA.

Anonymous (Northern Research and Engineering Corp.). 1965. Computer programs for the prediction of thermal transients in compact heat exchangers: Volume I - Development of Theory and Solution Procedures. NASA-CR-128708:1-82.

Bean, H. S. (Ed.). 1971. Fluid meters, their theory and application. 6th edition. The American Society of Mechanical Engineers, New York, N. Y.

Beatty Jr., K. O., E. B. Finch, and E. M. Schoenborn. 1951. Heat transfer from humid air to metal under frosting conditions. Refrig. Eng. 59:1203-1207.

Begin, J. C. and G. E. Frehlich. 1982. Testing agricultural air-to-air heat exchangers. ASAE paper 83-4510. Am. Soc. Agric. Eng., St. Joseph, Mich.

Besant, R. W. and J. D. Bugg. 1981. The performance of a counterflow air-to-air heat exchanger with water vapor condensation and frosting. 1981 International Seminar Advancements in Heat Exchangers, Dubrovnik, Yugoslavia.

Biguria, G. and L. A. Wenzel. 1970. Measurement and correlation of water frost thermal conductivity and density. Ind. Eng. Chem. Fundam. 9(1):129-138.

Brian, P. L. T., R. C. Reid, and Y. T. Shah. 1970. Frost deposition on cold surfaces. Ind. Eng. Chem. Fundam. 9(3):375-380.

Brian, P. L. T., R. C. Reid, and I. Brazinsky. 1969. Cryogenic frost properties. Cryogenic Technology 5:205-212.

Burmeister, L. C. 1983. Convection heat transfer. John Wiley and Sons, New York, N. Y.

Chan, C. Y. L. 1973. Performance tests of model plate heat exchangers with wetted plates. Internal Report No. 120. CSIRO Division of Mechanical Engineering, Highett, Victoria, Australia.

Demetri, E. P. and R. D. Siegel. 1970. Development of a computerized analytical technique for the design and optimization of wet gas heat exchangers: Volume I - Development of Theory and Design Procedures. NASA-CR-108621:1-252.

Denny, V. E., A. F. Mills, and V. J. Jusionis. 1971. Laminar film condensation from a steam-air mixture undergoing forced flow down a vertical surface. ASME Journal of Heat Transfer 93: 297-304.

Draper, C. S. and Y. T. Li. 1951. Principles of optimalizing control systems and an application to the internal combustion engine. The American Society of Mechanical Engineers Publication, New York, N. Y.

Duleba, G. S. and A. J. P. Lloyd. 1977. Modelling heat exchangers as part of a large system simulation. ASME publication 77-ENAs-9. Am. Soc. Mech. Eng., New York, N. Y.

Gatchilov, T. S. and V. S. Ivanova. 1979. Characteristics of the frost formed on the surface of the finned air coolers. Report presented by B1 Commission at V International Congress of Refrigeration, Venice.

Gates, R. R., C. F. Sepsy, and G. D. Huffman. 1967. Heat transfer and pressure loss in extended surface heat exchangers operating under frosting conditions, part 1: literature survey, test apparatus and preliminary results. ASHRAE Transactions 73(2):I.2.1-I.2.13.

Giese, H. and T. E. Bond. 1952. Design of a plate-type heat exchanger. Agric. Eng. 33(10):617-622.

Giese, H. and G. G. E. Downing. 1950. Application of heat exchanger to dairy barn ventilation. Agric. Eng. 31(4):167-174.

Giese, H. and A. A. Ibrahim. 1950. Ventilation of animal shelters by the use of heat exchangers. Agric. Eng. 31(7):329-333.

Guillory, J. L. and F. C. McQuiston. 1973. An experimental investigation of air dehumidification in a parallel plate exchanger. ASHRAE Transactions 29:146-151.

Haar, L., J. S. Gallagher, and G. S. Kell. 1984. NBS/NRC steam tables - thermodynamic and transport properties and computer programs for vapor and liquid states of water in SI units. McGraw-Hill International Book Company, Toronto, Ont.

Hayashi, Y., K. Aoki, and H. Yuhara. 1977. Study of frost formation based on a theoretical model of the frost layer. Heat Transfer in Japanese Research 6:79-94.

Hodgkinson, D. G. and D. Small. 1984. Field evaluation of a single-plate air-to-air heat exchanger for livestock buildings. CSAE paper 84-403. Can. Soc. Agric. Eng., Ottawa, Ont.

Hosoda, T. and H. Uzuhashi. 1967. Effects of frost on the heat transfer coefficient. Hitachi Review 16(6):254-259.

Huffman, G. D. and C. F. Sepsy. 1967. Heat transfer and pressure loss in extended surface heat exchangers operating under frosting conditions, part II: data analysis and correlation. ASHRAE Transactions 73(2):I.3.1-I.3.16.

Jones, B. W. and J. D. Parker. 1975. Frost formation with varying environmental parameters. ASME Journal of Heat Transfer 97:255-259.

Karlekar, B. V. and R. M. Desmond. 1977. Engineering heat transfer. West Publishing Company, St. Paul, Minn.

Kays, W. M. and A. L. London. 1984. Compact heat exchangers, 3rd edition. McGraw-Hill Book Company, New York, N. Y.

Kays, W. M. and E. Y. Leung. 1963. Heat transfer in annular passages - hydrodynamically developed turbulent flow with arbitrarily prescribed heat flux. Int. J. Heat Mass Transfer 6:537-557.

Kettleborough, C. F. and C. S. Hsieh. 1983. The thermal performance of the wet surface plastic plate heat exchanger used as an indirect evaporative cooler. ASME Journal of Heat Transfer 105:366-373.

Kreid, D. K., B. M. Johnson, and D. W. Faletti. 1978. Approximate analysis of heat transfer from the surface of a wet finned heat exchanger. ASME publication 78-HT-26. Am. Soc. Mech. Eng., New York, N. Y.

Lampman, W. P. and E. B. Moysey. 1984. A regenerative heat exchanger for livestock buildings. Trans ASAE 27(5):1505-1510.

Larkin, B. S. and J. E. Turnbull. 1979. The economics of heat recovery systems for animal shelters. Can. Agric. Eng. 21(1):53-59.

Larkin, B. S. and J. E. Turnbull. 1977. Effects of poultry dust on performance of a thermosiphon heat recovery system. Can. Agric. Eng. 19(1):37-39.

Larkin, B. S., J. E. Turnbull, and R. S. Gowe. 1975. Thermosiphon heat exchanger for use in animal shelters. Can. Agric. Eng. 17(2):85-89.

Li, Y. T. 1952. Optimalizing system for process control. Instruments 25(1,2,3):72-77, 190-193, 228, 324-327, 350, 352.

Maclaine-cross, I. L. and P. J. Banks. 1981. A general theory of wet surface heat exchangers and its application to regenerative evaporative cooling. ASME Journal of Heat Transfer 103:579-585.

Marinyuk, B. T. 1980. Heat and mass transfer under frosting conditions. Revue Internationale du Froid 3(6):366-368.

McGinnis, D. S. 1984. Computer model of an air-to-air, shell-and-tube heat exchanger. Can. Agric. Eng. 26(2):151-161.

McGinnis, D. S., J. R. Ogilvie, D. R. Pattie, K. W. Blenkhorn, and J. E. Turnbull. 1983. Shell-and-tube heat exchanger for swine buildings. Can. Agric. Eng. 25(1):69-74.

McQuiston, F. C. 1978b. Correlation of heat, mass and momentum transport coefficients for plate-fin-tube heat transfer surfaces with staggered tubes. ASHRAE Transactions 84(1): 294-309.

McQuiston, F. C. 1978a. Heat, mass and momentum transfer data for five plate-fin-tube heat transfer surfaces. ASHRAE Transactions 84(1):266-293.

McQuiston, F. C. 1976. Heat, mass and momentum transfer in a parallel plate dehumidifying exchanger. ASHRAE Transactions 82(2): 87-106.

Merte, H. 1973. Condensation heat transfer. Adv. Heat Transfer 9:181-272.

Meyer, D. J., H. B. Manbeck, and P. N. Walker. 1983. Performance of a polytube heat exchanger in a farrowing-nursery building. ASAE paper 83-4563. Am. Soc. Agric. Eng., St. Joseph, Mich.

O'Neal, D. L. and D. R. Tree. 1984. Measurement of frost growth and density in a parallel plate geometry. ASHRAE Transactions 90(2A):278-290.

Parish, H. C. and C. F. Sepsy. 1972. A numerical analysis of frost formation under forced convection. ASHRAE Transactions 78(1): 236-251.

Pescod, D. 1968. Unit air cooler using plastic plate heat exchanger with evaporatively cooled plates. Australian Refrigeration Air Conditioning and Heating. 22:22-26.

Petukhov, B. S. and V. N. Popov. 1963. Theoretical calculation of heat exchange and frictional resistance in turbulent flow in tubes of an incompressible fluid with variable physical properties. Trans. in High Temperature 1(1):69-83.

Rohsenow, W. M. and J. P. Hartnett. 1973. Handbook of heat transfer. McGraw-Hill Book Company, New York, N. Y.

Saskatchewan Agriculture. 1983. Livestock ventilation heat recovery systems. Saskatchewan Agriculture, Regina, Saskatchewan.

Schneider, H. W. 1978. Equation of the growth rate of frost forming on cooled surfaces. Int. J. Heat Mass Transfer 21:1019-1024.

Schulte, D. W. and R. H. Howell. 1982. The effect of air turbulence on the rate of frost growth on a horizontal flat plate. ASHRAE Transactions 88(2):201-216.

Shah, R. K. and A. L. London. 1978. Supplement 1 - laminar flow forced convection in ducts, in Advances in Heat Transfer, T. F. Irvine and J. P. Hartnett, Eds. Academic Press, New York, N. Y.

Shah, R. K. and A. L. London. 1974. Thermal boundary conditions and some solutions for laminar duct flow forced convection. ASME Journal of Heat Transfer 96:159-165.

Shibani, A. A. and M. N. Ozisik. 1977. A solution to heat transfer in turbulent flow between parallel plates. Int. J. Heat Mass Transfer 20:565-573.

Sokhansanj, S., K. A. Jordon, L. A. Jacobson, and G. L. Messer. 1980. Economic feasibility of using heat exchangers in ventilation of animal buildings. Trans. ASAE 23(6):1525-1528.

Stoecker, W. F. 1960. Frost formation on refrigeration coils. ASHRAE Transaction 66:91-103.

Stoecker, W. F. 1957. How frost formation on coils affects refrigeration systems. Refrig. Eng. 65(2):42-46.

Swift, W. R., J. E. Turnbull, and J. A. Munroe. 1981. Dairy barn exhaust heat reclaimer heats calf barn. ASAE paper 81-205. Am. Soc. Agric. Eng., St. Joseph, Mich.

Thornton, E. 1983. Heat exchangers: field experiences in Alberta. ASAE paper PNR83-303. Am. Soc. Agric. Eng., St. Joseph, Mich.

Threlkeld, J. L. 1970. Thermal environmental engineering - 2nd ed. Prentice-Hall Inc., Englewood Cliffs, New Jersey.

Tokura, I., H. Saito, and K. Kishinami. 1983. Study on properties and growth rate of frost layers on cold surfaces. ASME Journal of Heat Transfer 105:895-901.

Tree, D. R. and W. A. Helmer. 1976. Experimental heat and mass transfer data for condensing flow in a parallel plate heat exchanger. ASHRAE Transactions 82(1):289-299.

Van Lambalgen, H., A. Beresh, and K. Eberle. 1986. Design and field testing of a frost controller for an air-to-air heat exchanger in a dairy barn. Mechanical Engineering Design Project, Department of Mechanical Engineering, University of Saskatchewan, Saskatoon, Saskatchewan.

White, J. E. and C. J. Cremers. 1981. Prediction of growth parameters of frost deposits in forced convection. ASME Journal of Heat Transfer 103:3-6.

Wilhelm, L. R. 1976. Numerical calculation of psychrometric properties in SI units. Trans. ASAE 19(2): 310-321, 325.

Witz, R. L., G. L. Pratt, and M. L. Buchanan. 1976. Livestock ventilation with heat exchange. Trans. ASAE 19(6):1187-1192.

Yamakawa, N. and S. Ohtani. 1972. Heat and mass transfer in the frost layer. Heat Transfer - Japanese Research 1(3):75-82.

Yamakawa, N., N. Takahashi, and S. Ohtani. 1972. Forced convection heat and mass transfer under frost conditions. Heat Transfer - Japanese Research 1(2):1-10.

Yonko, J. D. and C. F. Sepsy. 1967. An investigation of the thermal conductivity of frost while forming on a flat horizontal plate. ASHRAE Transactions 73(2): I.1.1 - I.1.11.

APPENDIX A

Simulation Flow Charts

Main Simulation Flow Chart

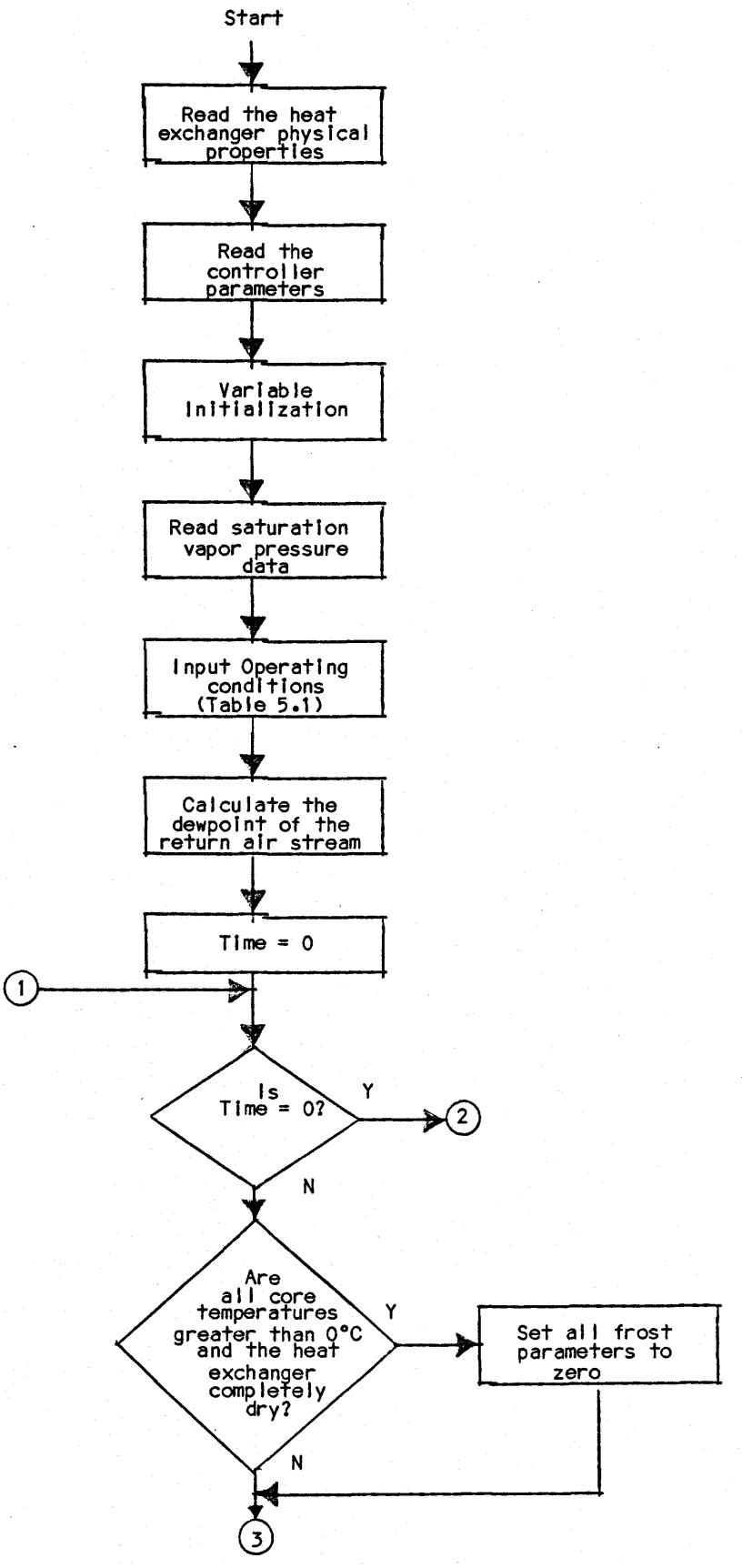

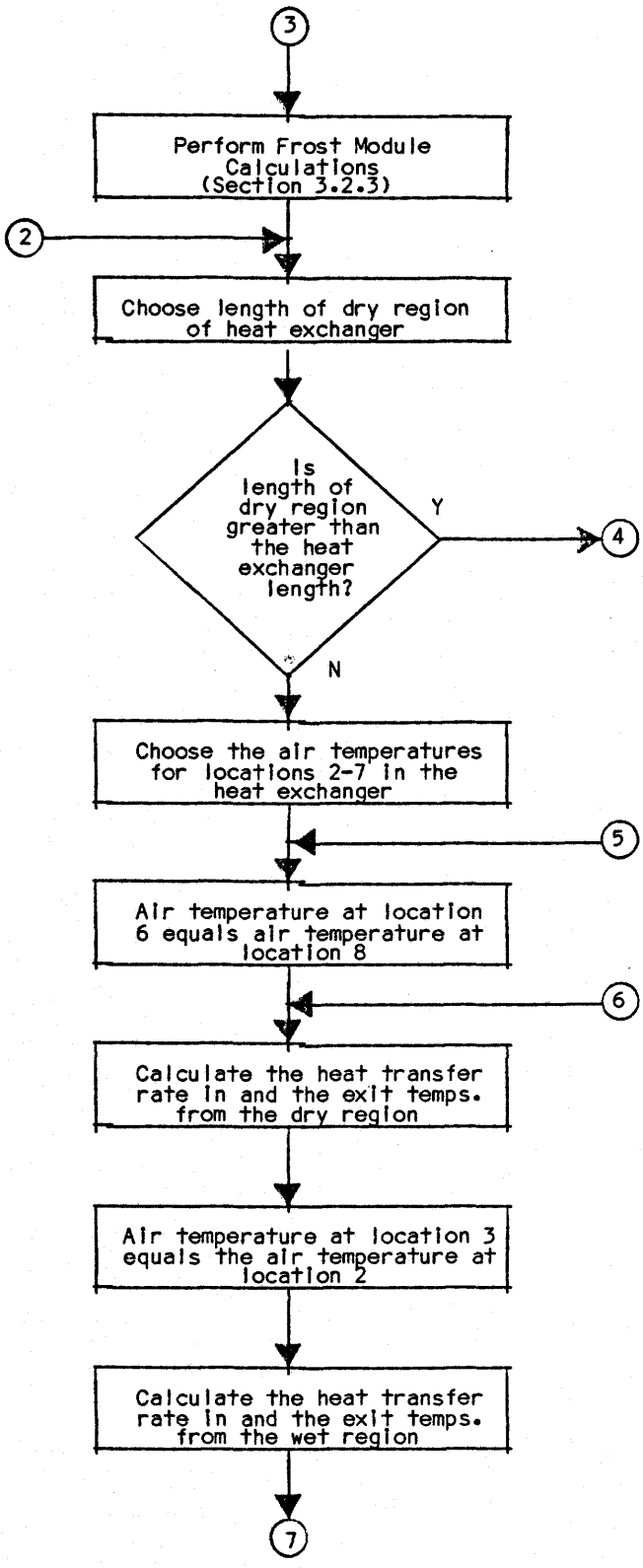
3
Perform Frost Module Calculations (Section 3.2.3)
2
Choose length of dry region of heat exchanger
Is length of dry region greater than the heat exchanger length?
Y
4
N
Choose the air temperatures for locations 2-7 in the heat exchanger
5
Air temperature at location 6 equals air temperature at location 8
6
Calculate the heat transfer rate in and the exit temps. from the dry region
Air temperature at location 3 equals the air temperature at location 2
Calculate the heat transfer rate in and the exit temps. from the wet region
7

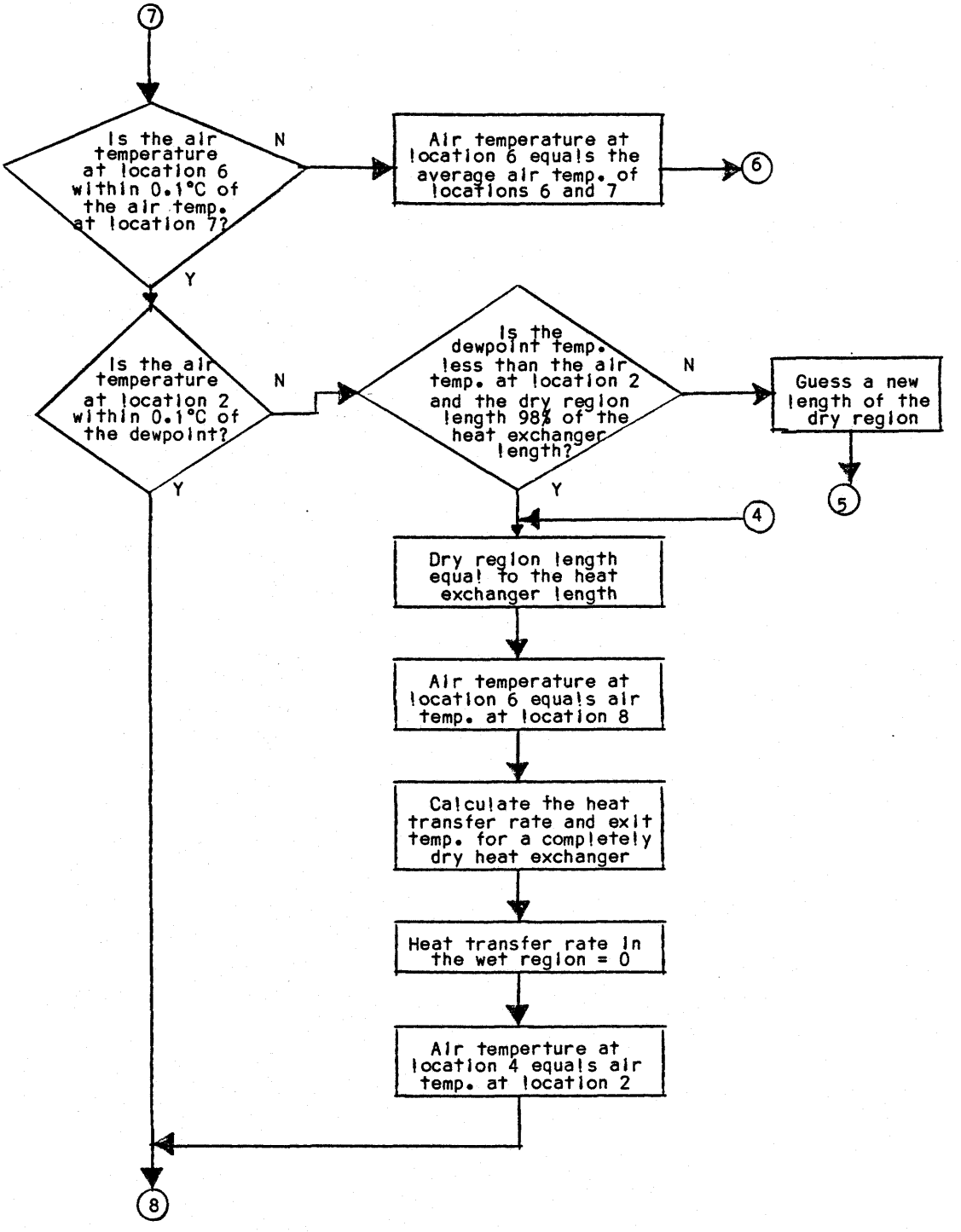
7
Is the air temperature at location 6 within 0.1°C of the air temp. at location 7?
N
Air temperature at location 6 equals the average air temp. of locations 6 and 7
6
Y
Is the air temperature at location 2 within 0.1°C of the dewpoint?
N
Is the dewpoint temp. less than the air temp. at location 2 and the dry region length 98% of the heat exchanger length?
N
Guess a new length of the dry region
5
Y
4
Y
Dry region length equal to the heat exchanger length
Air temperature at location 6 equals air temp. at location 8
Calculate the heat transfer rate and exit temp. for a completely dry heat exchanger
Heat transfer rate in the wet region = 0
Air temperture at location 4 equals air temp. at location 2
8

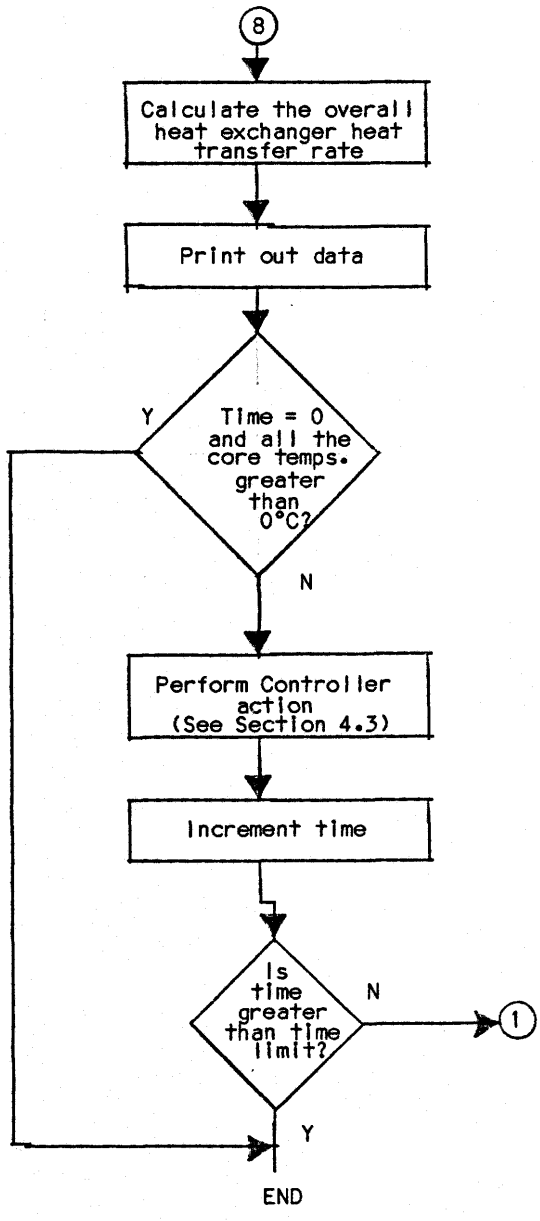
8
Calculate the overall heat exchanger heat transfer rate
Print out data
Y
Time = 0 and all the core temps. greater than 0°C?
N
Perform Controller action (See Section 4.3)
Increment time
Is time greater than time limit?
N
1
Y
END

Dry Exchange Flow Chart

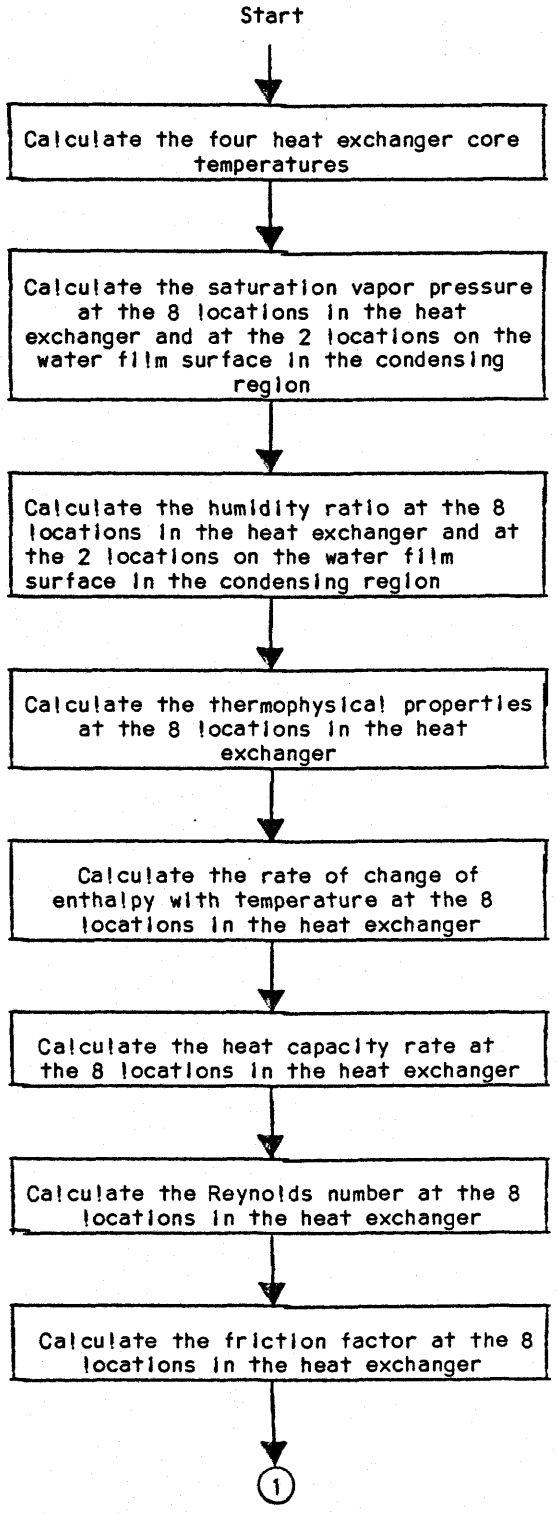

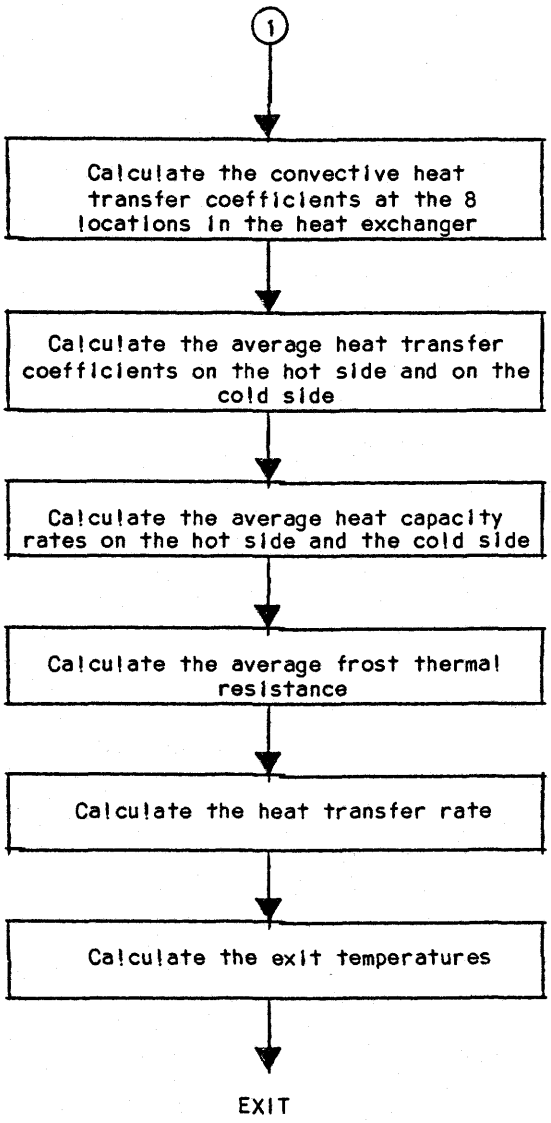
1
Calculate the convective heat transfer coefficients at the 8 locations in the heat exchanger
Calculate the average heat transfer coefficients on the hot side and on the cold side
Calculate the average heat capacity rates on the hot side and the cold side
Calculate the average frost thermal resistance
Calculate the heat transfer rate
Calculate the exit temperatures
EXIT

Wet Exchange Flow Chart

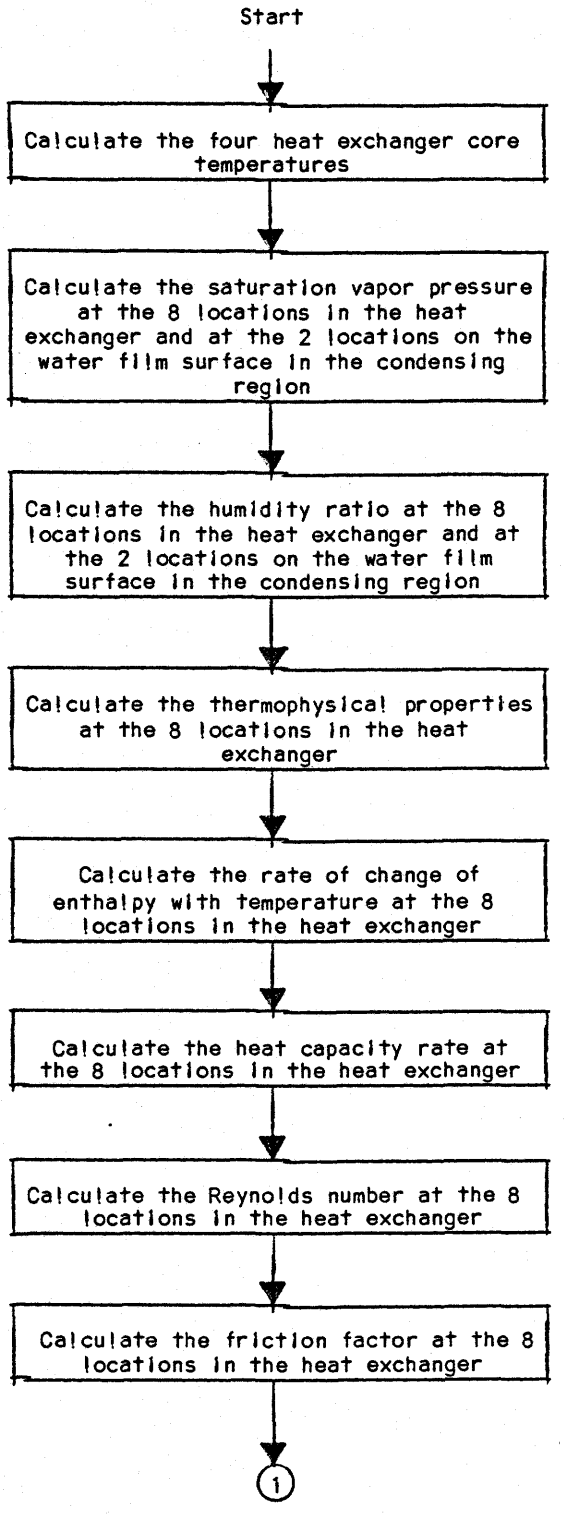

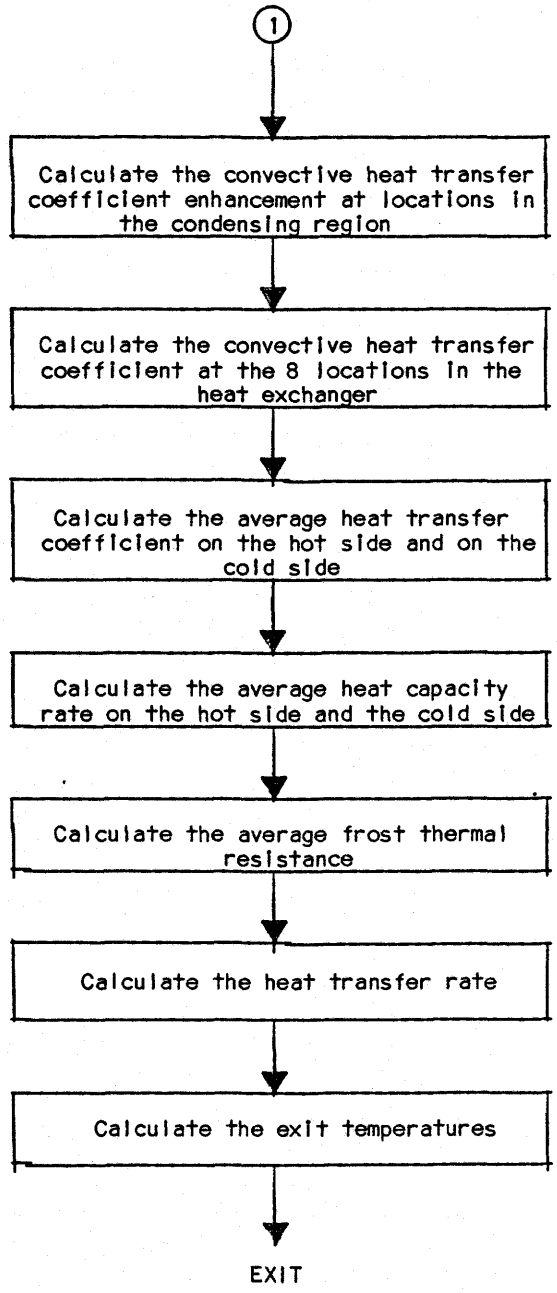
1
Calculate the convective heat transfer coefficient enhancement at locations in the condensing region
Calculate the convective heat transfer coefficient at the 8 locations in the heat exchanger
Calculate the average heat transfer coefficient on the hot side and on the cold side
Calculate the average heat capacity rate on the hot side and the cold side
Calculate the average frost thermal resistance
Calculate the heat transfer rate
Calculate the exit temperatures
EXIT

Frost Module Flow Chart

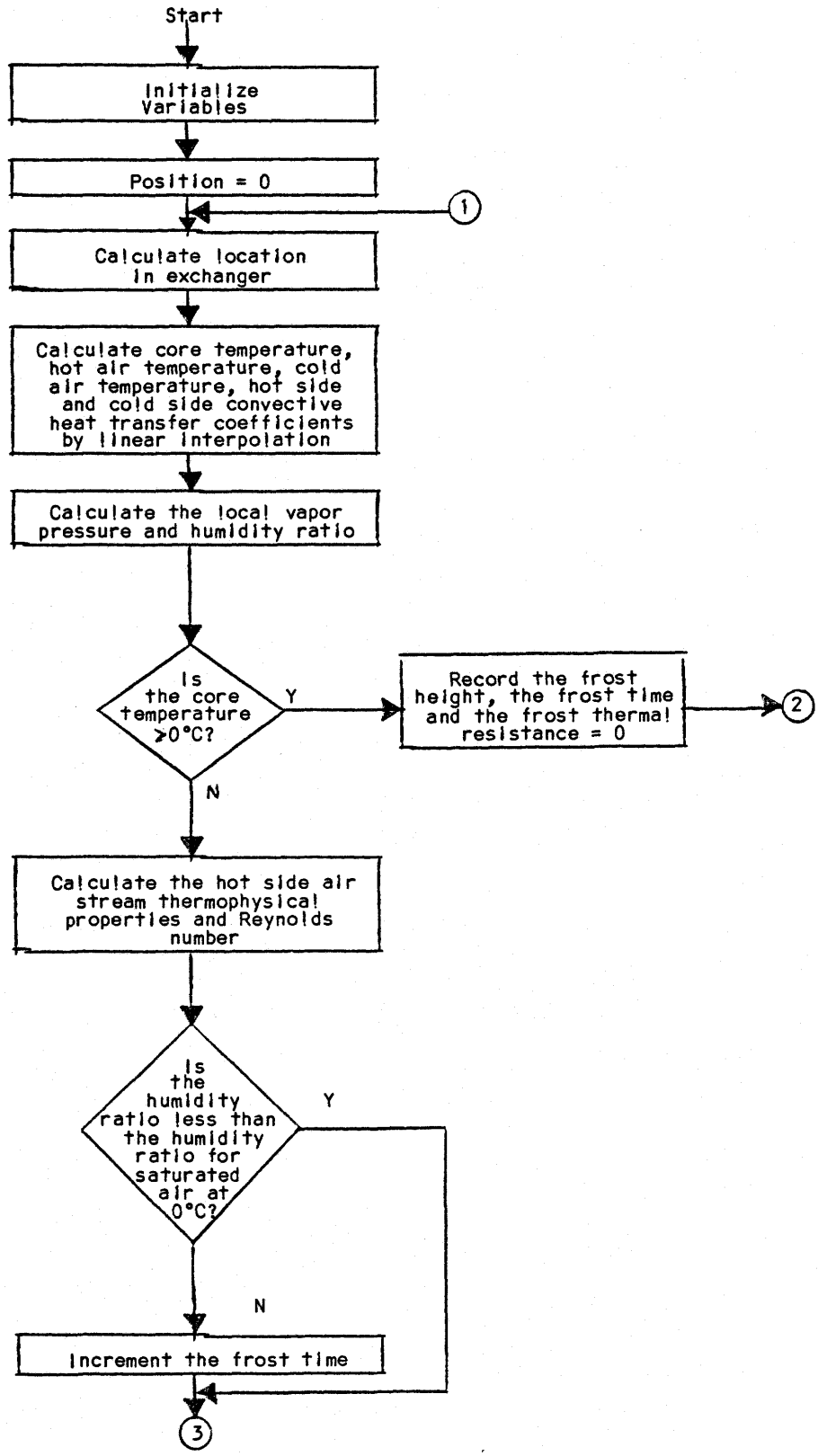

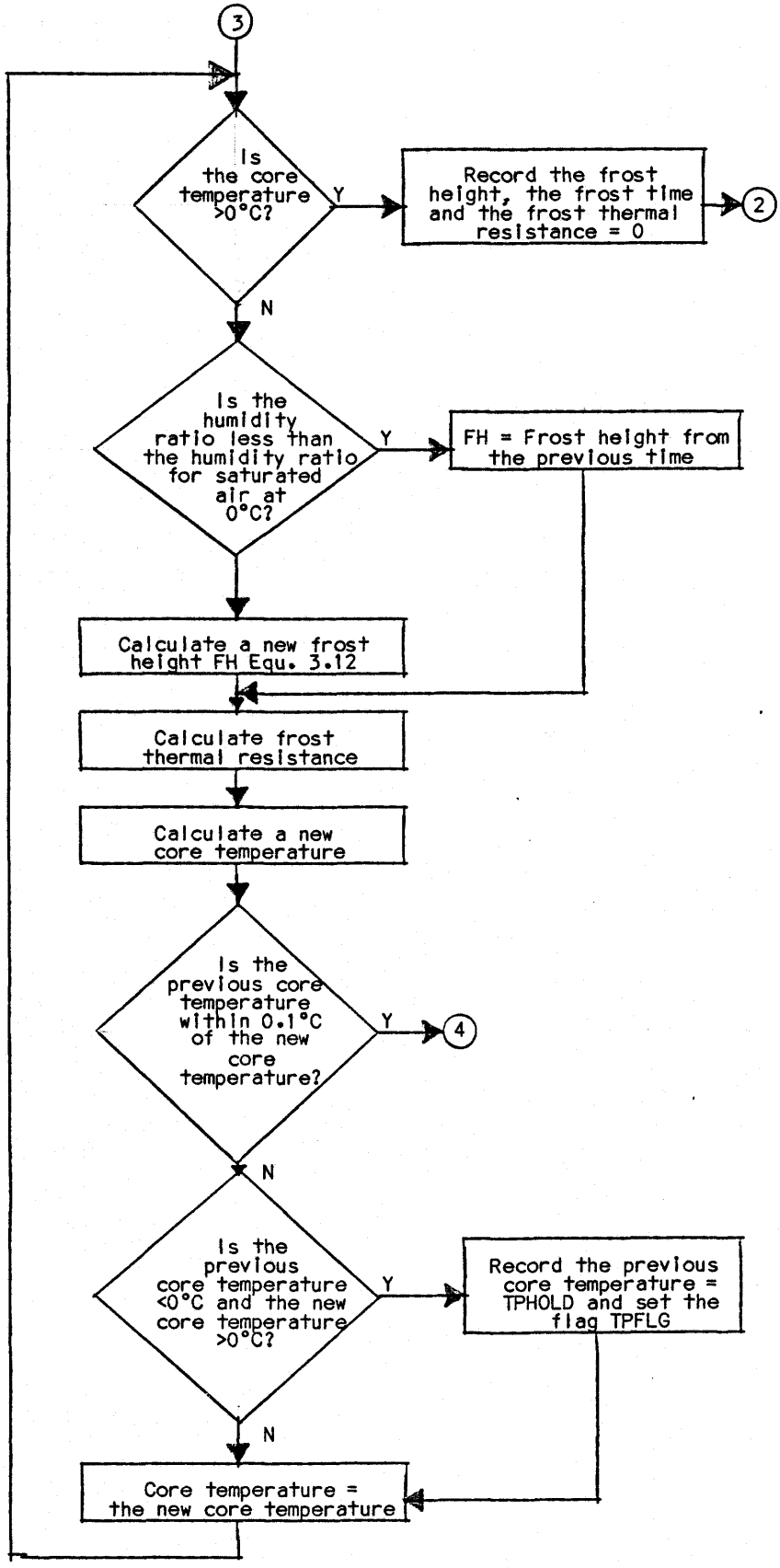
3
Is the core temperature >0°C?
Y
Record the frost height, the frost time and the frost thermal resistance = 0
2
N
Is the humidity ratio less than the humidity ratio for saturated air at 0°C?
Y
FH = Frost height from the previous time
Calculate a new frost height FH Equ. 3.12
Calculate frost thermal resistance
Calculate a new core temperature
Is the previous core temperature within 0.1°C of the new core temperature?
Y
4
N
Is the previous core temperature <0°C and the new core temperature >0°C?
Y
Record the previous core temperature = TPHOLD and set the flag TPFLG
N
Core temperature = the new core temperature

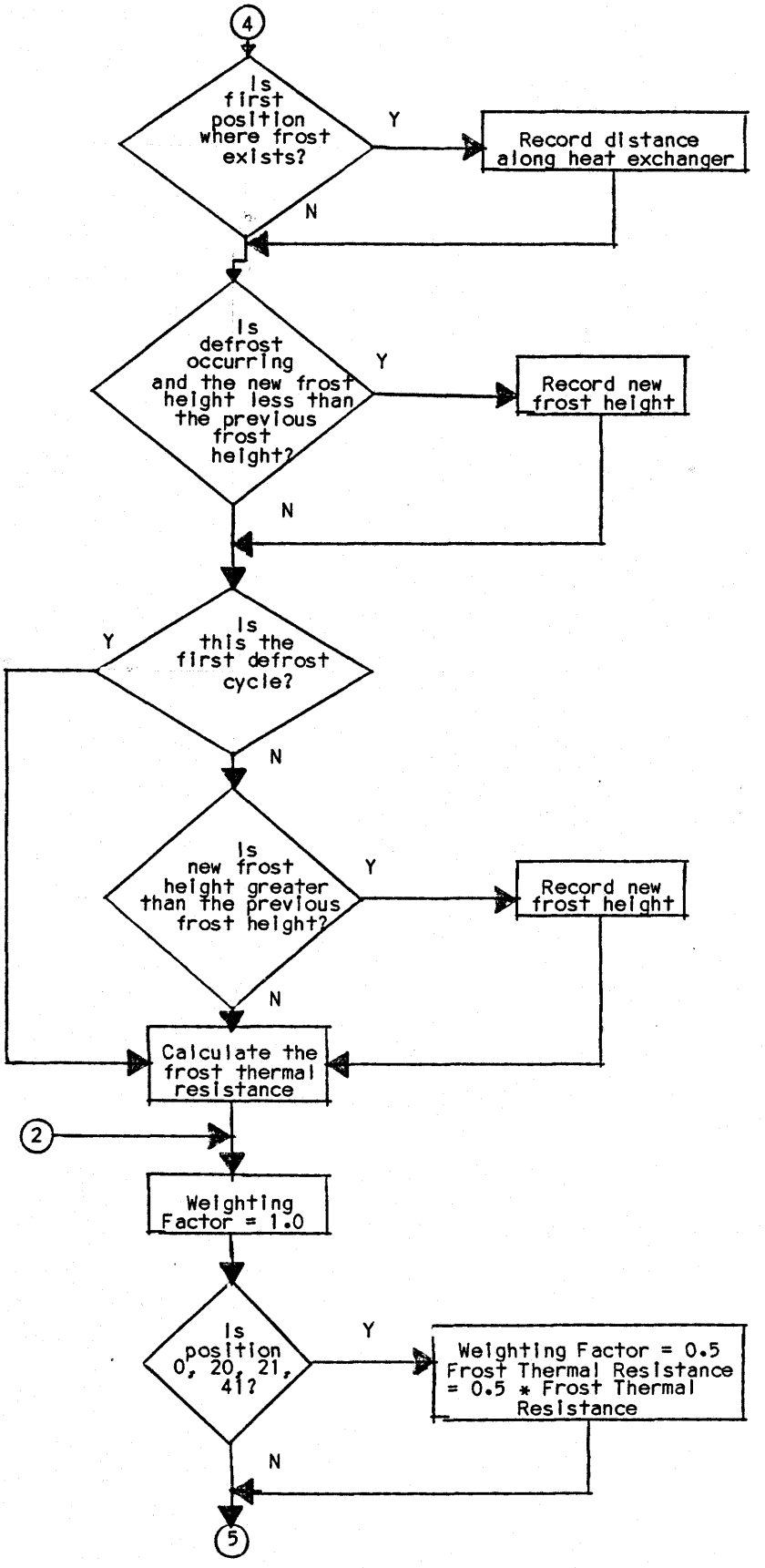
4
Is first position where frost exists?
Y
Record distance along heat exchanger
N
Is defrost occurring and the new frost height less than the previous frost height?
Y
Record new frost height
N
Is this the first defrost cycle?
Y
N
Is new frost height greater than the previous frost height?
Y
Record new frost height
N
Calculate the frost thermal resistance
2
Weighting Factor = 1.0
Is position 0, 20, 21, 41?
Y
Weighting Factor = 0.5
Frost Thermal Resistance = 0.5 * Frost Thermal Resistance
N
5

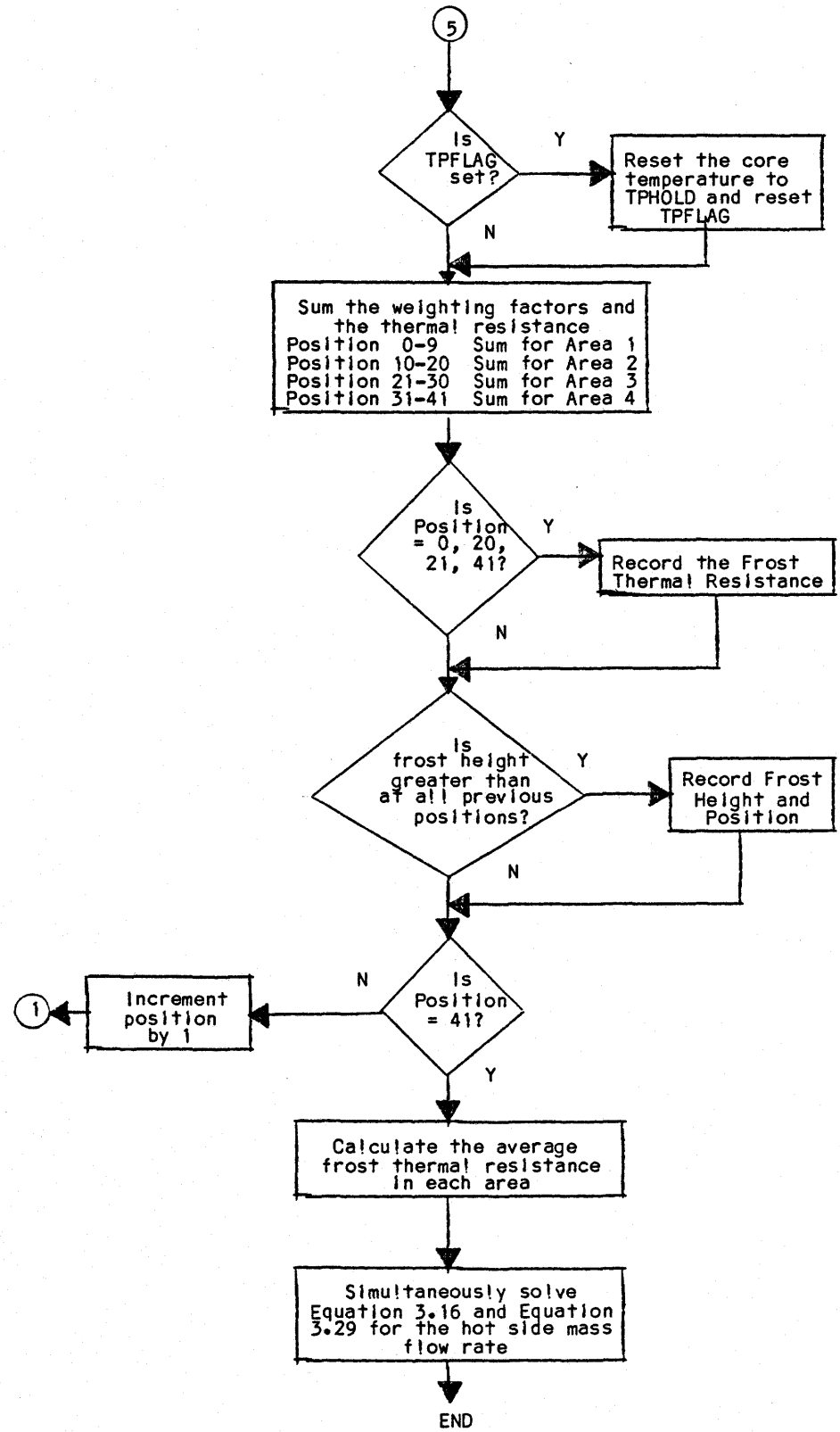
5
Is TPFLAG set?
Y
Reset the core temperature to TPHOLD and reset TPFLAG
N
Sum the weighting factors and the thermal resistance
Position 0-9 Sum for Area 1
Position 10-20 Sum for Area 2
Position 21-30 Sum for Area 3
Position 31-41 Sum for Area 4
Is Position = 0, 20, 21, 41?
Y
Record the Frost Thermal Resistance
N
Is frost height greater than at all previous positions?
Y
Record Frost Height and Position
N
Is Position = 41?
N
Increment position by 1
1
Y
Calculate the average frost thermal resistance in each area
Simultaneously solve Equation 3.16 and Equation 3.29 for the hot side mass flow rate
END

APPENDIX B

AD590KF Temperature Sensor Calibration

AD590KF Temperature Sensor Calibration

Calibration of the temperature sensors required the selection of a temperature standard. Since no standard with current calibration was available, three different thermometers were compared and one selected as a standard. The three thermometers compared were:

(1) Thermocouple Simulator/Calibrator (Model 1100, Ectron, San Diego, California)

(2) Glass Stick Thermometer (#15-030, Fisher Scientific Co.)

(3) Digital Thermometer (Model 2802A, Hewlett Packard).

The three thermometers were compared by suspending them in a temperature controlled, circulating glycol bath. The bath temperature was found to be very well controlled and uniform. The three thermometers were compared at three different temperatures. The results achieved are given in Table B.1. The results indicate very close agreement among the three thermometers. The Thermocouple Simulator/Calibrator was selected as the standard for calibration of the AD590KF's because of the ease of use.

The A/D board used was of the continuous convert type rather than the integrating type. As a result 60 Hz noise was present in the temperature measurements. The noise was eliminated by reading each sensor 256 times over a time period which was a multiple of the 60 Hz period.

During calibration it was observed that the temperature measurements would drift. The drift was linked to current leakage from the sensor leads. Since a current change of one microamp corresponded to a 0.1°C temperature change a small current leakage was significant. The current leakage was partially eliminated by suspending the sensors in a

high volume resistivity fluid. In the actual tests, the current leakage was taken to be small because each sensor was individually suspended in the air stream and air has a very high volume resistivity.

The temperature sensors were calibrated by wrapping them in a close bundle. A Type T thermocouple connected to the Thermocouple Simulator/Calibrator was placed in the center of the bundle. The bundle was placed in a plastic freezer bag. The bag was squeezed tight and the remaining air was forced out by filling the bag with white mineral oil. The bag of sensors was suspended in the glycol bath. The sensors were placed in a freezer bag filled with mineral oil rather than suspended directly in the glycol bath in order to reduce the effects of current leakage.

The sensors were calibrated at three different temperatures -24.15°C, +0.75°C and +25.25°C. The calibration at +0.75°C was done in two steps. An initial scan of all the temperature sensors was made followed 300 seconds later by four additional scans every 30 seconds. The calibration reading for each sensor was obtained by averaging the measurements made in the final four scans. The first scan measurements were compared with the average measurements of the final four scans to check for thermal stability. Calibration at +25.25°C and -24.15°C was done over 10 hour period. This was done in order to assess measurement drift. The maximum measurement and the minimum measurement made by each sensor during the 10 hour period was recorded. For each sensor, the average of the maximum measurement and the minimum measurement was the calibration reading. The range of the measurements made by each sensor was a measure of the sensor repeatability.

The factors affecting the accuracy of each sensor were calibration standard error, sensor nonlinearity between calibration points, sensor repeatability error and bath nonuniformity. The calibration standard error was the accuracy given in ASHRAE (1975) for a Type T thermocouple. The sensor nonlinearity was computed from an applications note (Analog Devices, Norwood, Mass.). The repeatability error was taken as the variation of the temperature measurements found for calibration at +25.25°C and -24.15°C. The bath nonuniformity error was the difference in temperature between the calibration standard and a thermometer suspended in the glycol bath. This error was only present at the lowest calibration temperature because the system mixing the glycol bath was much less efficient at this calibration temperature. The calibration errors found at the calibration extremes are given in Table B.2.

TABLE B.1

CALIBRATION STANDARDS

THERMOMETER	FIRST COMPARISON POINT (°C)	SECOND COMPARISON POINT (°C)	THIRD COMPARISON POINT (°C)
THERMOCOUPLE SIMULATOR/ CALIBRATOR	-25.6 ± 0.1	+0.5 ± 0.1	+25.5 ± 0.1
GLASS STICK THERMOMETER	-25.5 ± 0.5	+1.0 ± 0.5	+25.5 ± 0.5
DIGITAL THERMOMETER	-25.5 ± 0.1	+0.7 ± 0.1	+25.5 ± 0.1

TABLE B.2

CALIBRATION ERRORS

ERROR	CALIBRATION -24.15°C	CALIBRATION +25.25°C
CALIBRATION	±0.83	±0.83
NONLINEARITY	±0.20	±0.10
REPEATABILITY	±0.19	±0.50
BATH NONUNIFORMITY	±0.15	0.00
TOTAL	±0.88	±0.97

APPENDIX C

Test Procedure

Test Procedure

Prior to commencing tests:

(1) Assemble the ductwork following drawing 19850l. Seal all joints with silicon caulking.

(2) Install the motor and drive system. Ensure the dampers are properly synchronized. Record in the test log:

  (a) Number of steps from full closed to full open.
  (b) The backlash (in steps) of the drive system.

(3) Connect the code testers and make connection to the refrigeration system and the conditioner box.

(4) Red line drawing 19850l or record in the test log the dimensions and location of equipment.

(5) Install four pressure taps on the exhaust side, two on the entry and two on the exit. Record arrangement in test log.

(6) Insulate the ductwork and record on drawing 19850l the insulation provided.

(7) Take extensive photos of the test arrangement.

(8) Record the details of the PAMI refrigeration system, i.e., capacity, manufacturer.

(9) Record details of the PAMI conditioner box.

(10) Record details of the PAMI code testers.

  (a) Dry and Wet bulb accuracies.
  (b) Volume/mass flow accuracy.

(11) Record specification, accuracy and calibration information of the condensate weigh scale.

(12) Adjust the fixed bypass dampers to give flow for full heat exchange or full bypass.

(13) Adjust the supply fan to give maximum flow or 0.55 kg/s whichever is lesser. Set the exhaust fan to give balanced flow or maximum flow whichever is lesser. Do at ambient conditions.

For each individual test run:

(1) Assure pressure lines are free of blockage.

(2) Start the exhaust fan operating and the conditioner box. Let stabilize.

(3) Check and record the full scale setting of the pressure transducer.

(4) Read all temperature sensors once and record the ambient temperatures measured.

(5) Record run parameters.

(6) Record the controller parameters.

(7) Record atmospheric pressure.

(8) Delete memory files.

(9) Adjust the drive system to full bypass of supply air.

(10) Exhaust is running full exchange.

(11) Start supply side fan running and let run full bypass for few minutes.

(12) Balance and zero PAMI manometer. Start PAMI data acquisition system operating.

(13) Start the data acquisition system operating. Start making entries in the data sheets.

(14) Record time of test start.

(15) In test log, record frost that is observed forming in the core. Take photos where possible.

(16) Monitor the motor current and adjust to ensure no motor burn out.

(17) Record time of test end.

(18) After the test period, transfer data to the disk drive using the file name given in table.

(19) Record all file names used.

APPENDIX D

Simulation Results

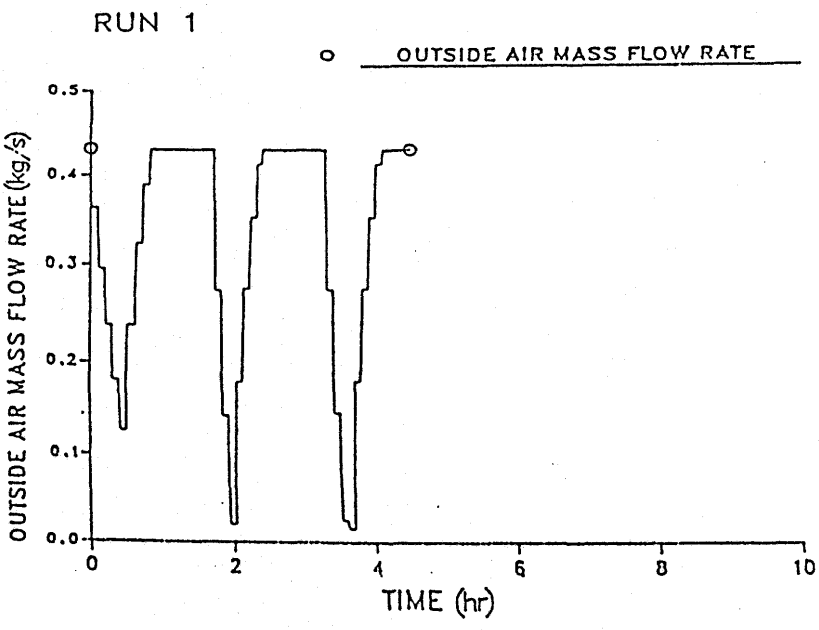

FIGURE D.1

RUN 1: Predicted Outside Air Mass Flow Rate

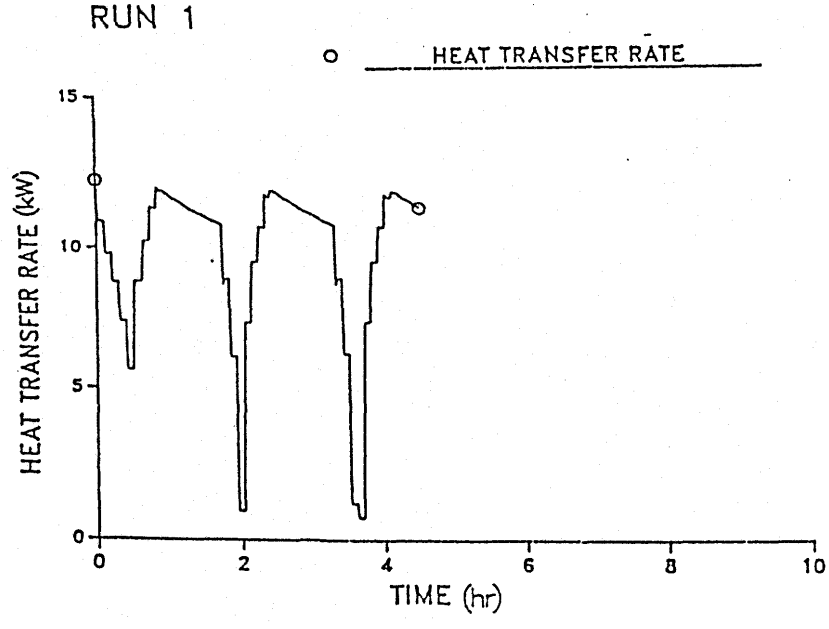

FIGURE D.2

RUN 1: Predicted Heat Transfer Rate

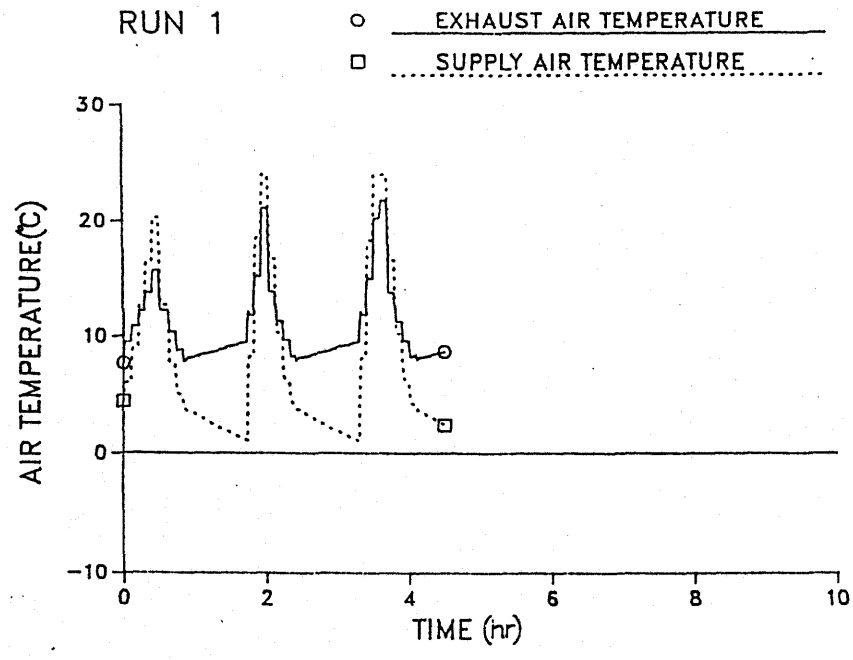

FIGURE D.3

RUN 1: Predicted Outlet Temperatures

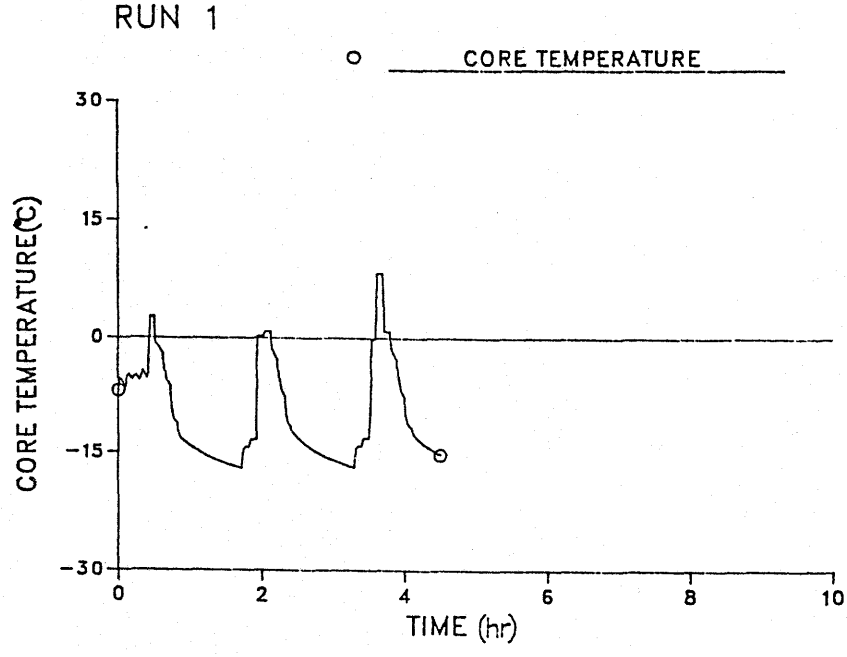

FIGURE D.4

RUN 1: Predicted Core Temperature

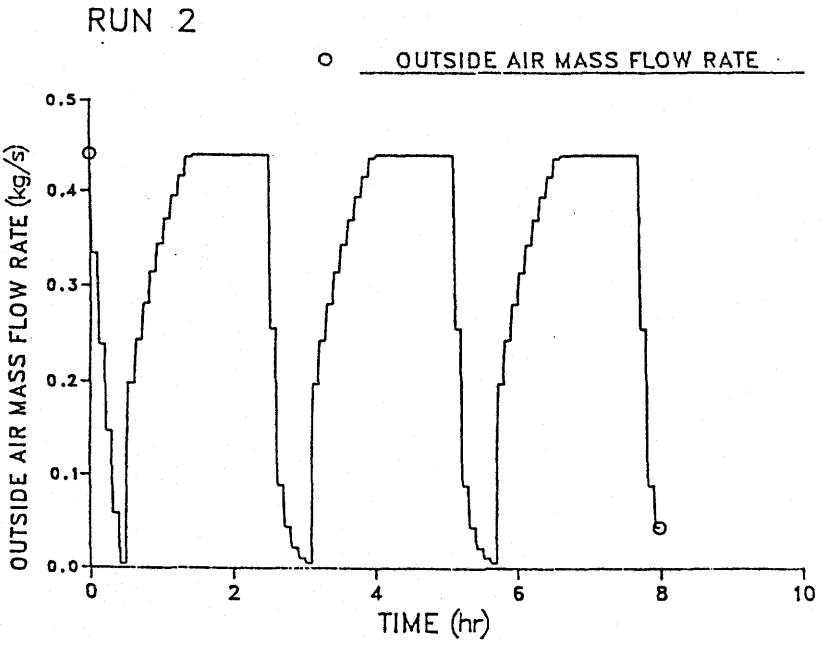

FIGURE D.5

RUN 2: Predicted Outside Air Mass Flow Rate

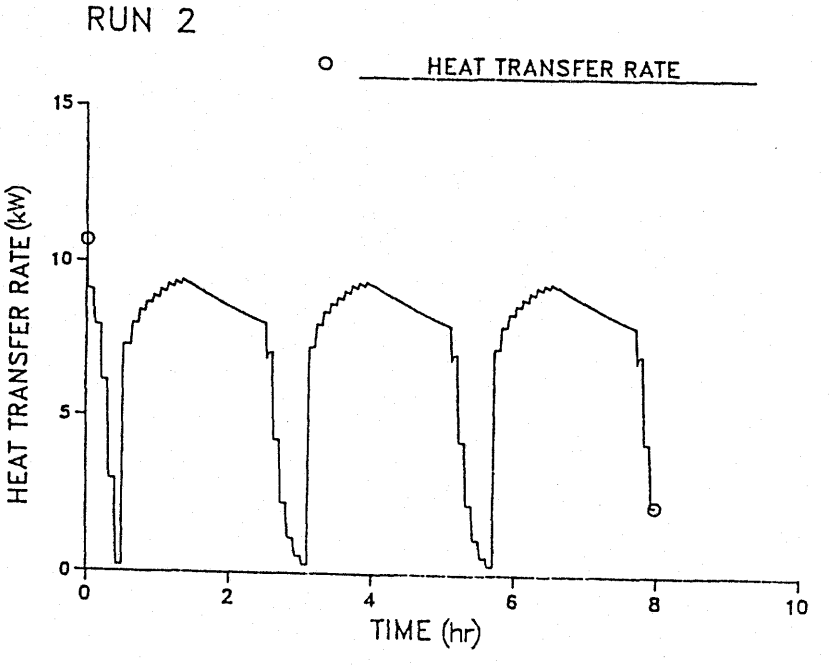

FIGURE D.6

RUN 2: Predicted Heat Transfer Rate

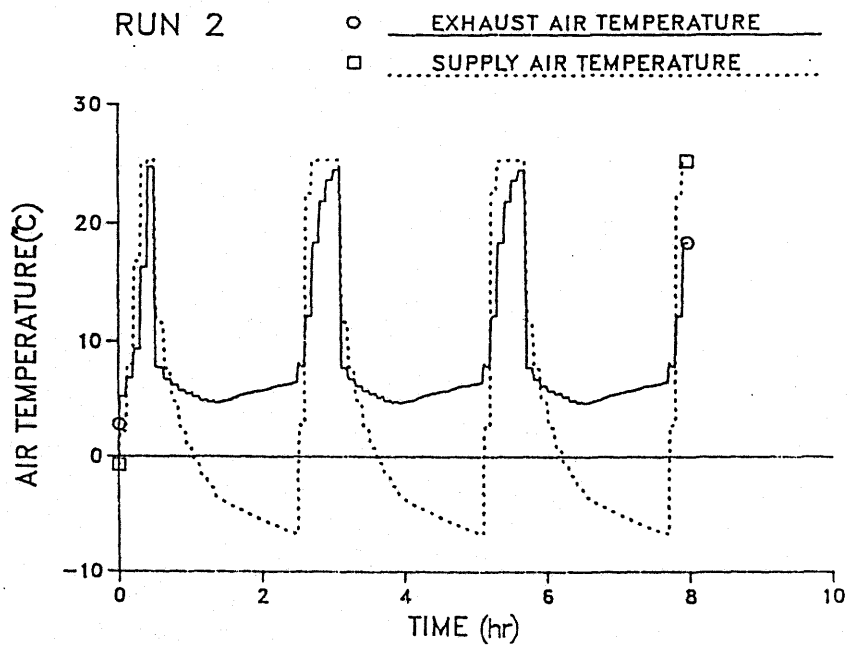

FIGURE D.7

RUN 2: Predicted Outlet Temperatures

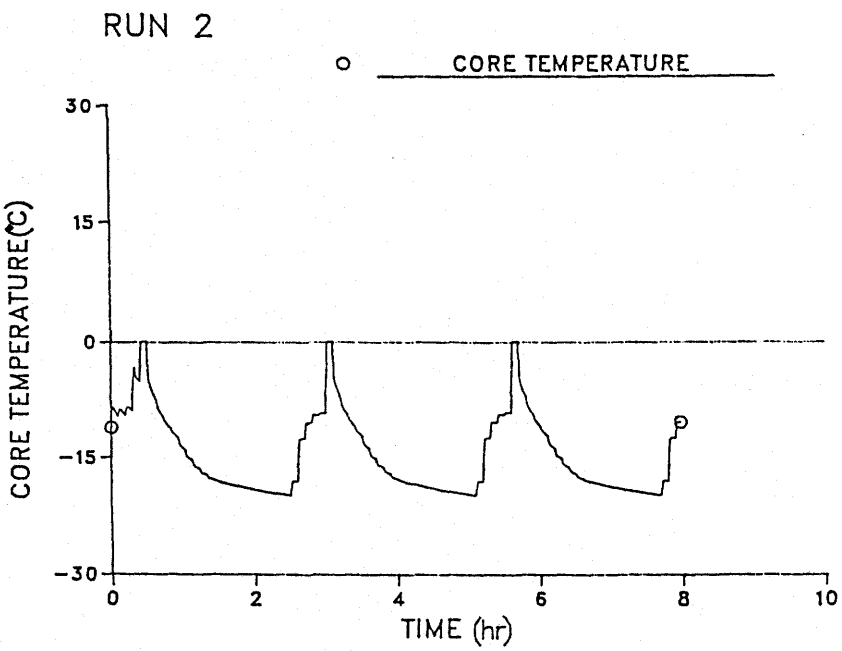

FIGURE D.8

RUN 2: Predicted Core Temperature

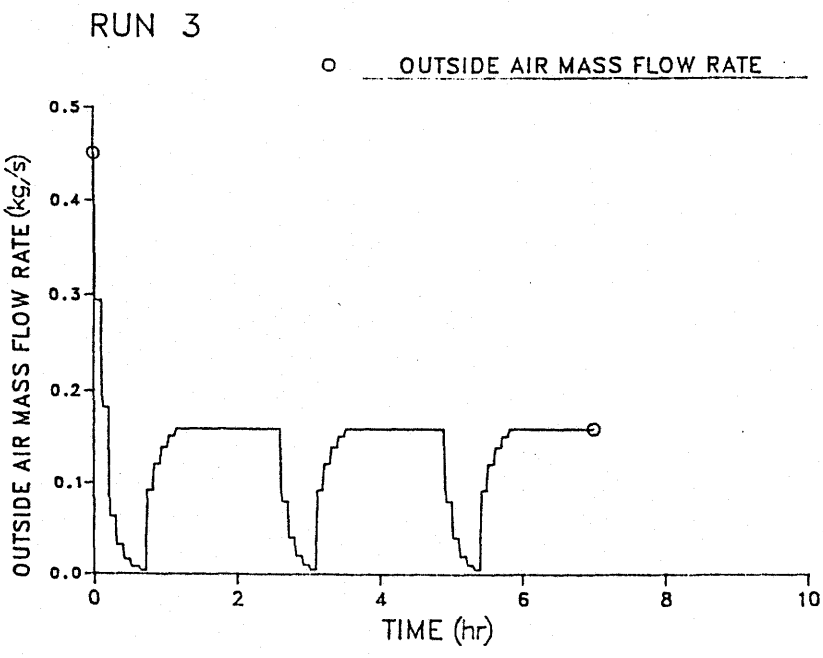

FIGURE D.9

RUN 3: Predicted Outside Air Mass Flow Rate

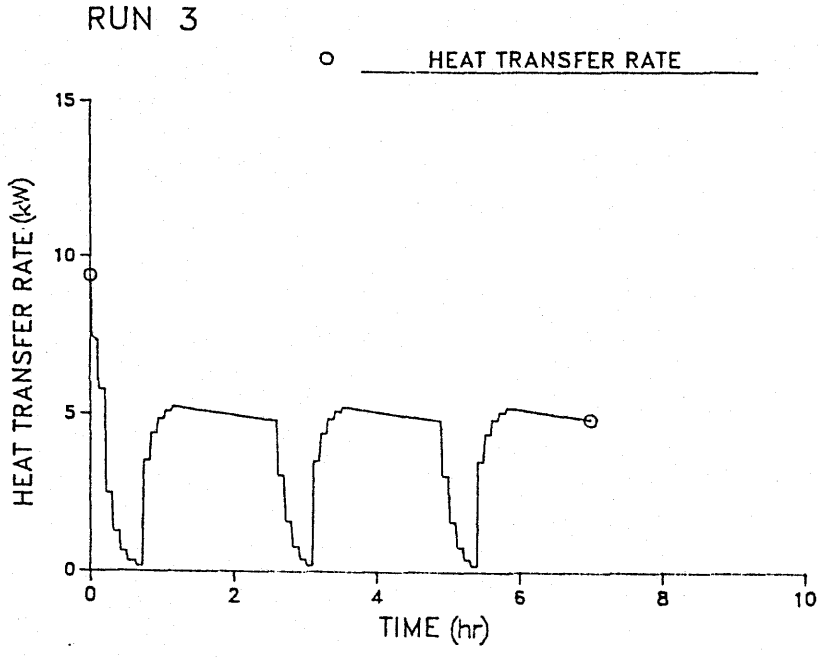

FIGURE D.10

RUN 3: Predicted Heat Transfer Rate

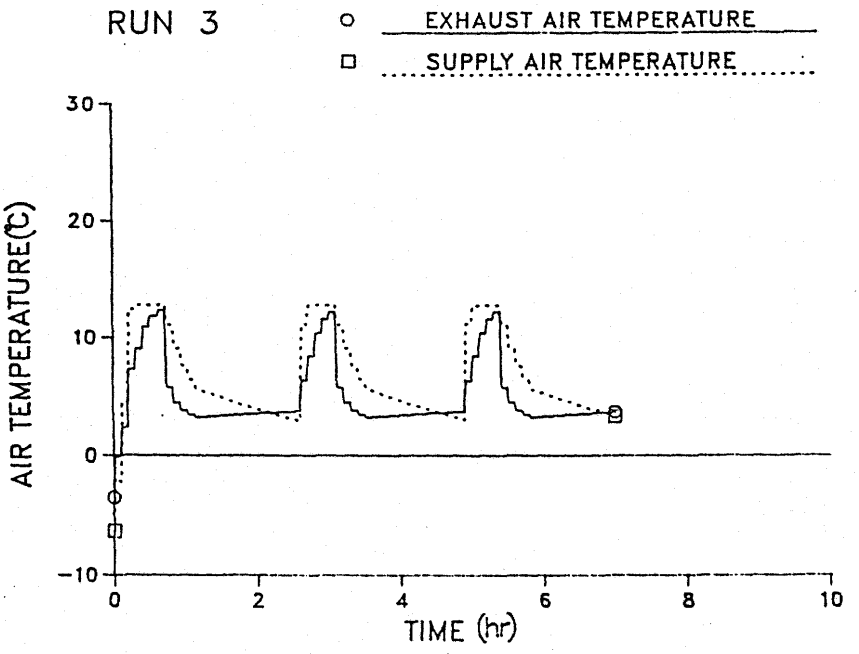

FIGURE D.11

RUN 3: Predicted Outlet Temperatures

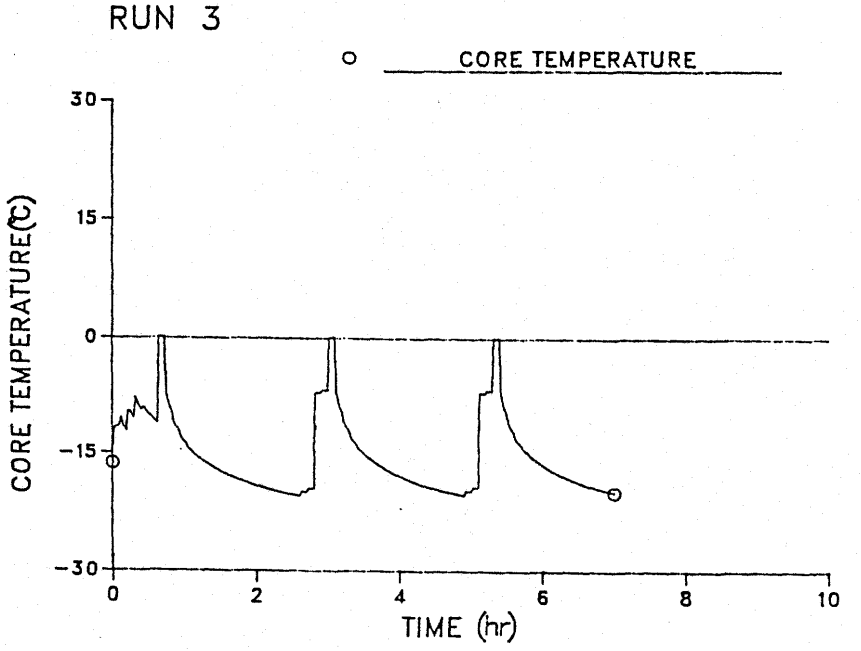

FIGURE D.12

RUN 3: Predicted Core Temperature

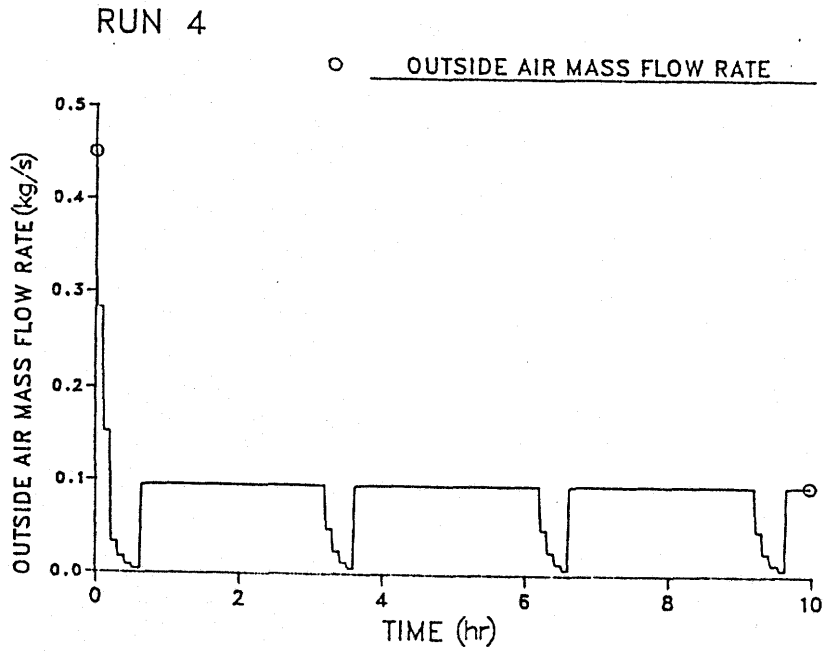

FIGURE D.13

RUN 4: Predicted Outside Air Mass Flow Rate

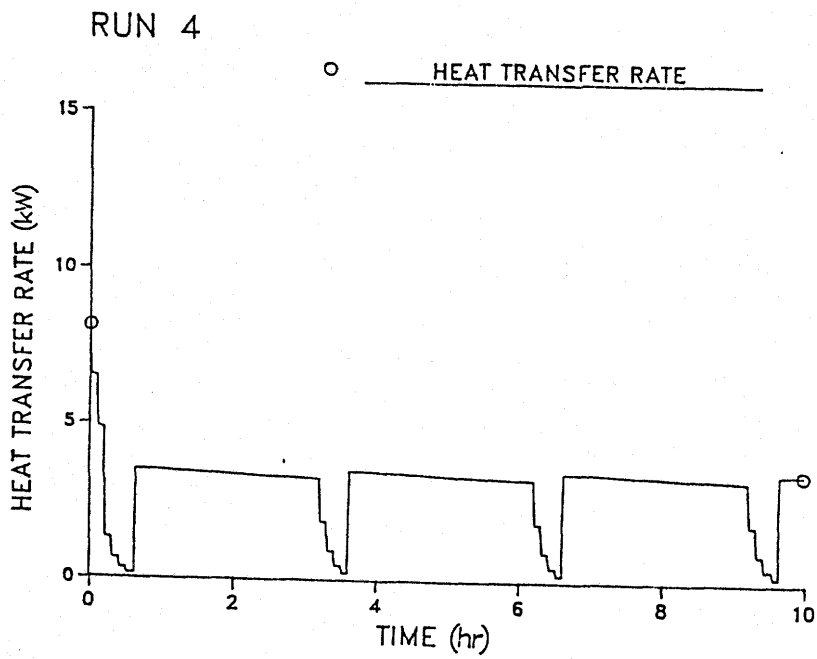

FIGURE D.14

RUN 4: Predicted Heat Transfer Rate

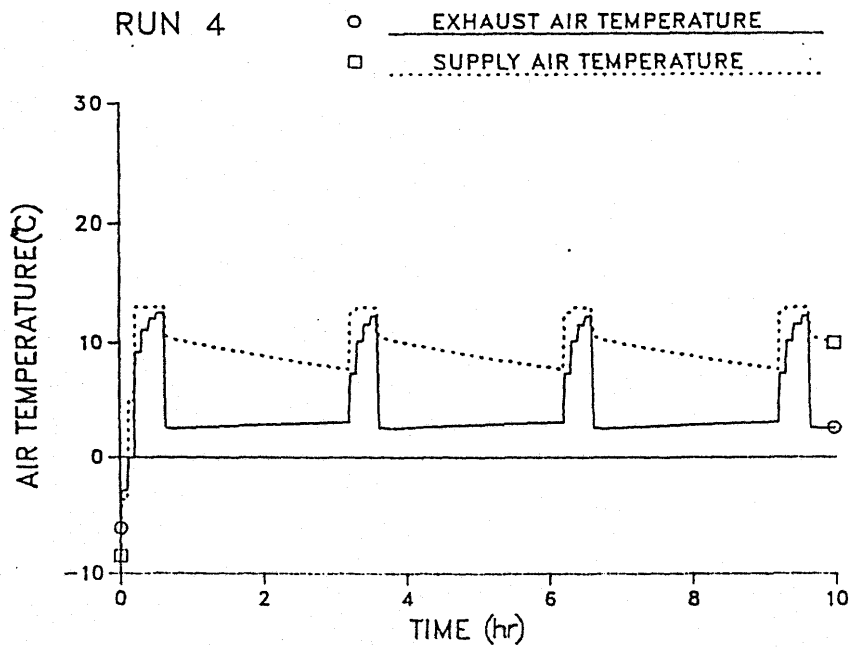

FIGURE D.15

RUN 4: Predicted Outlet Temperature

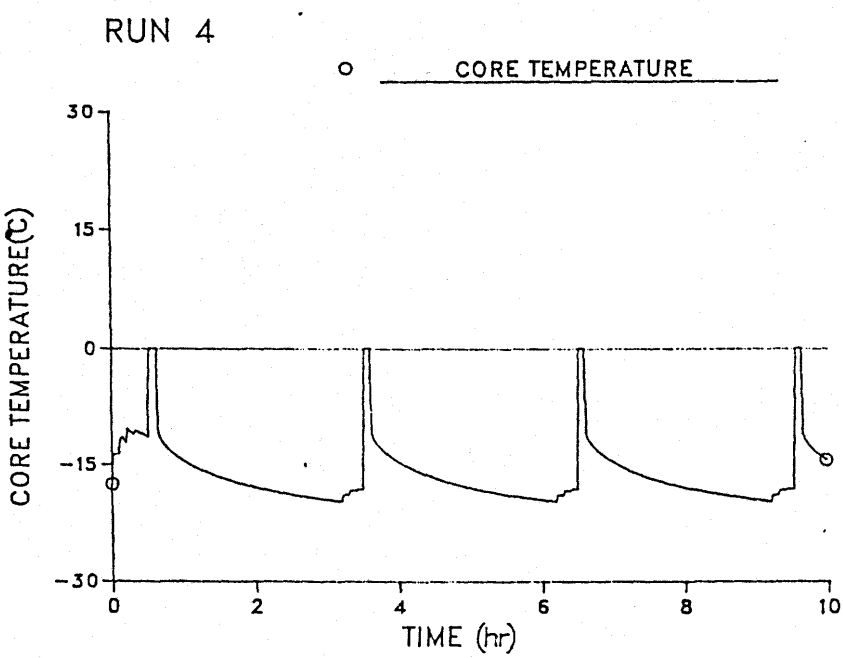

FIGURE D.16

RUN 4: Predicted Core Temperature

APPENDIX E

Experimental Results

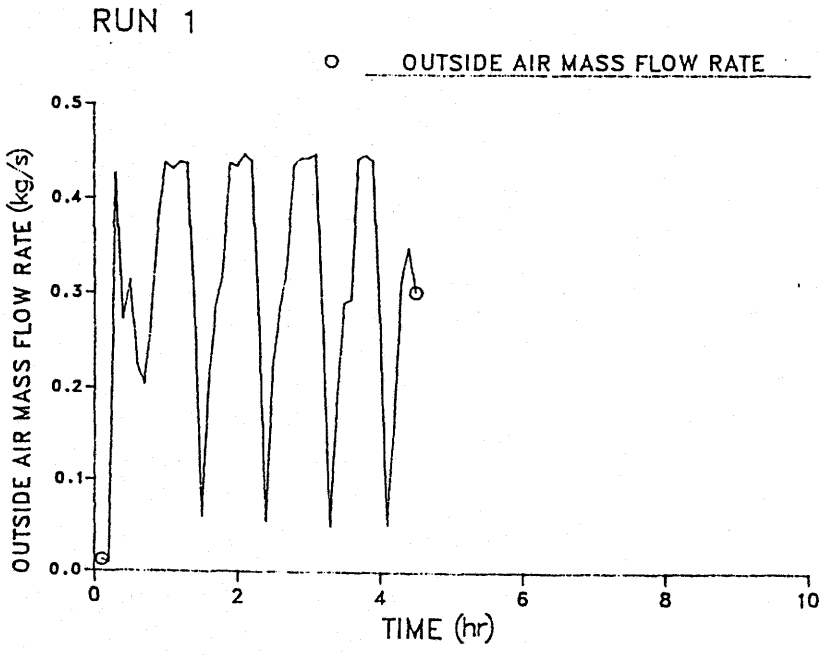

FIGURE E.1

RUN 1: Measured Outside Air Mass Flow Rate

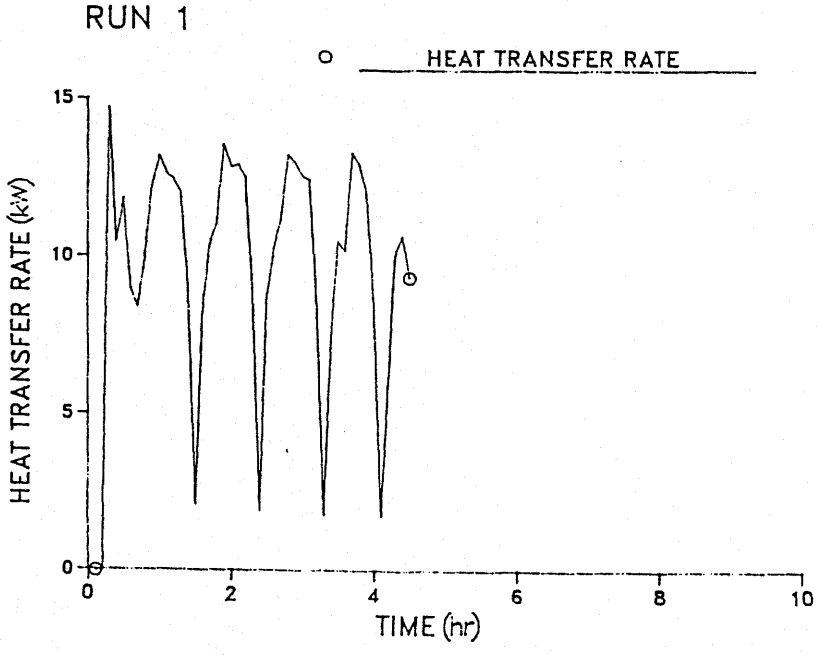

FIGURE E.2

RUN 1: Measured Heat Transfer Rate

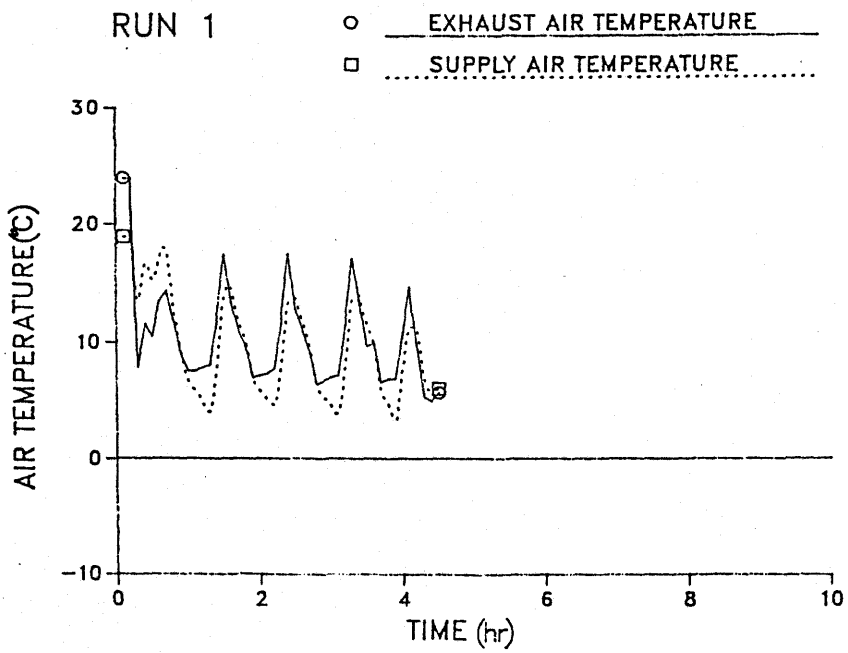

FIGURE E.3

RUN 1: Measured Outlet Temperatures

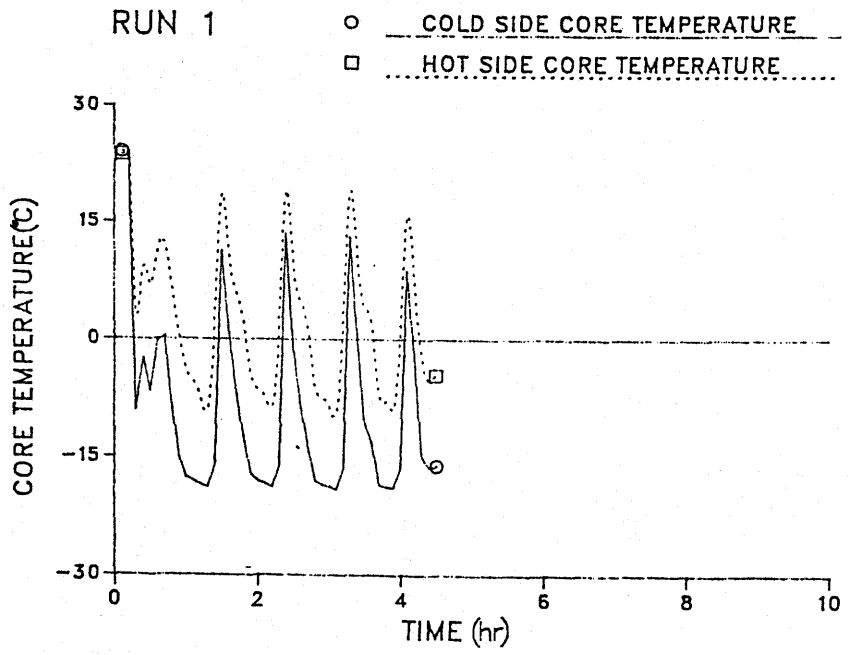

FIGURE E.4

RUN 1: Measured Core Temperatures

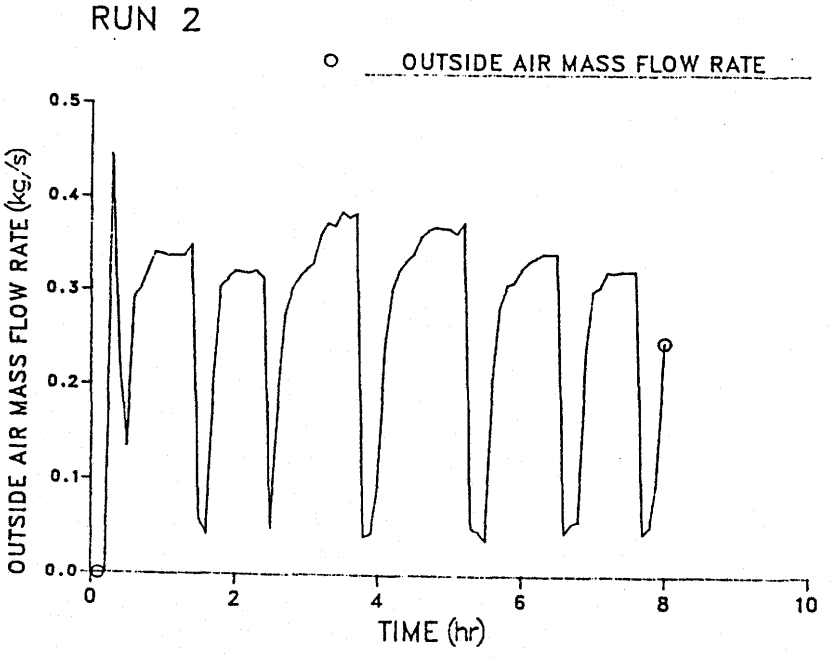

FIGURE E.5

RUN 2: Measured Outside Air Mass Flow Rate

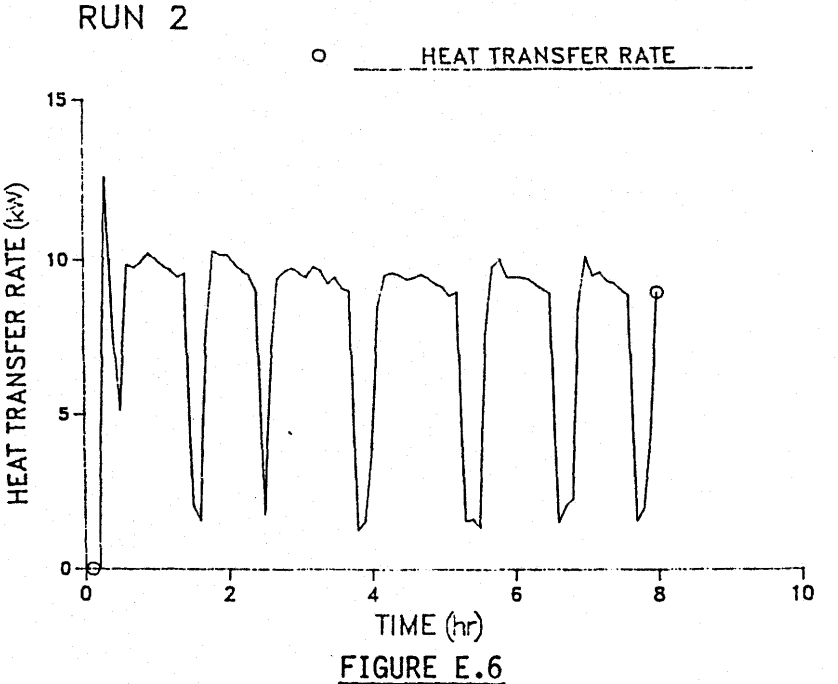

FIGURE E.6

RUN 2: Measured Heat Transfer Rate

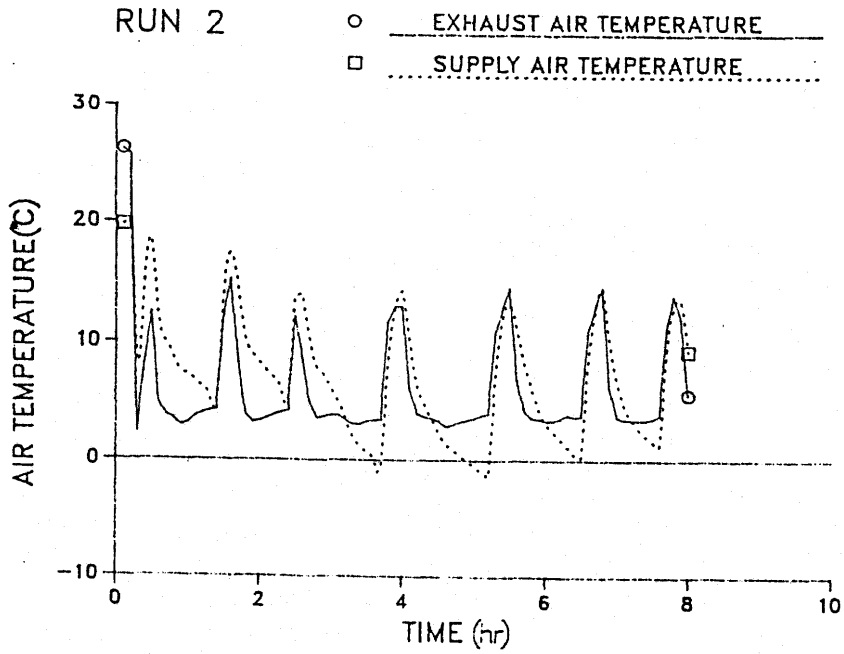

FIGURE E.7

RUN 2: Measured Outlet Temperatures

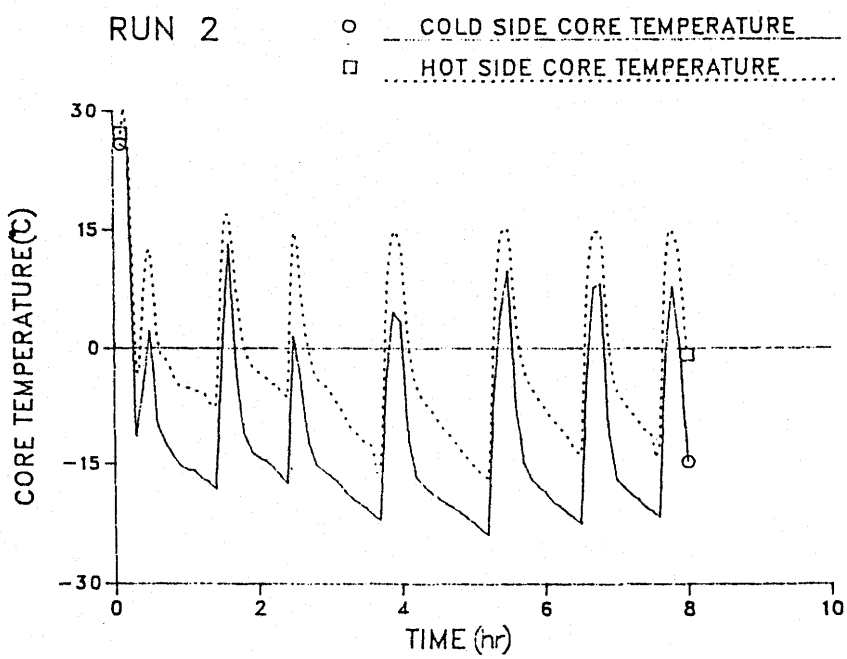

FIGURE E.8

RUN 2: Measured Core Temperatures

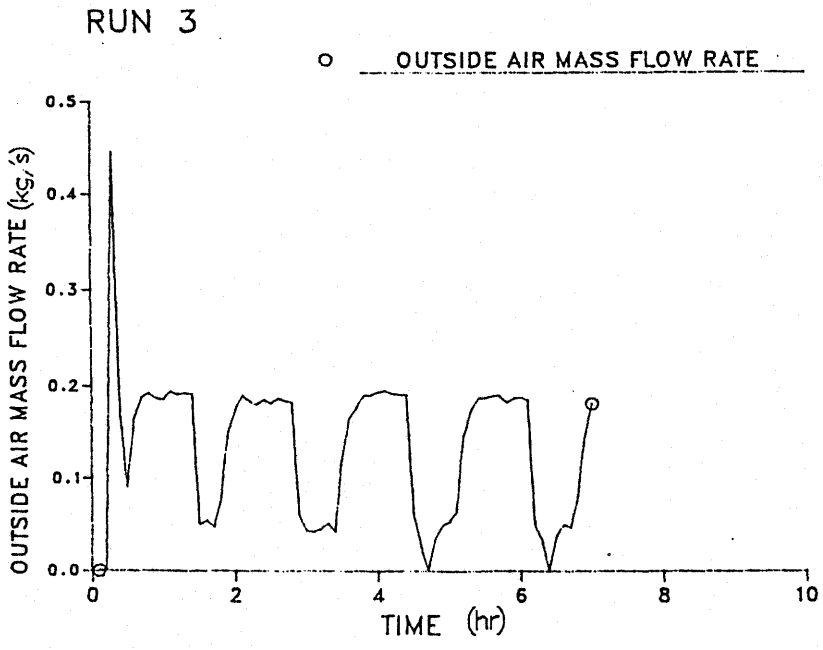

FIGURE E.9

RUN 3: Measured Outside Air Mass Flow Rate

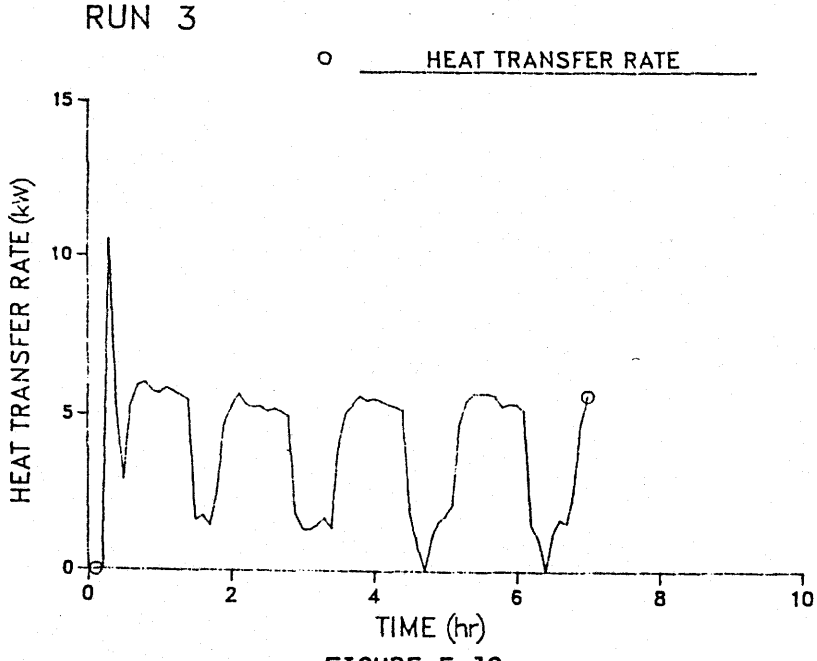

FIGURE E.10

RUN 3: Measured Heat Transfer Rate

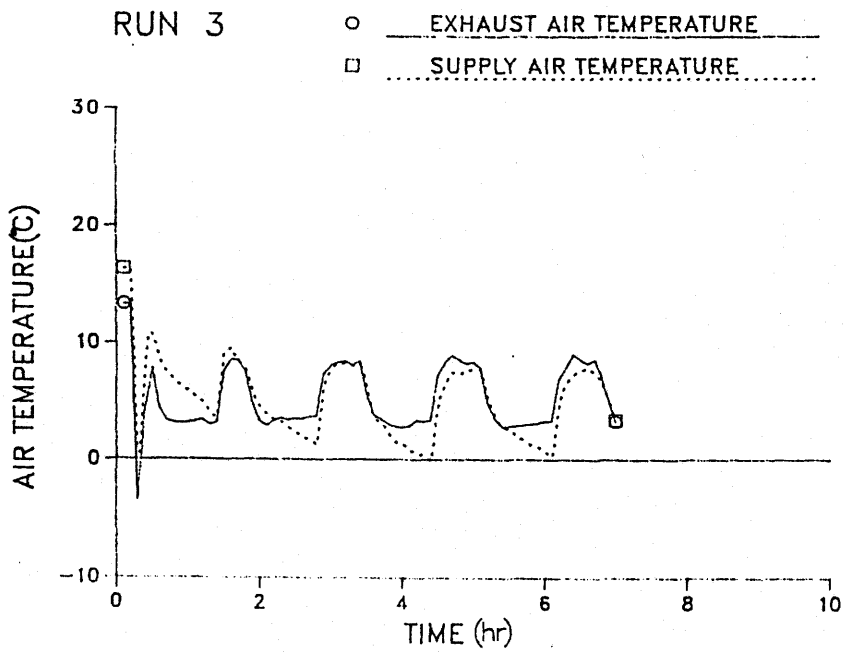

FIGURE E.11

RUN 3: Measured Outlet Temperatures

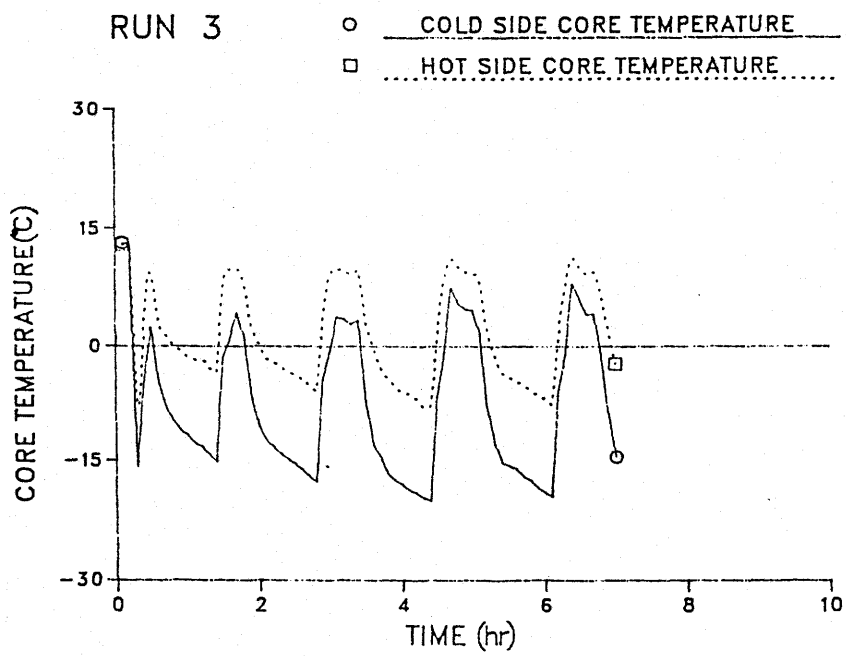

FIGURE E.12

RUN 3: Measured Core Temperature

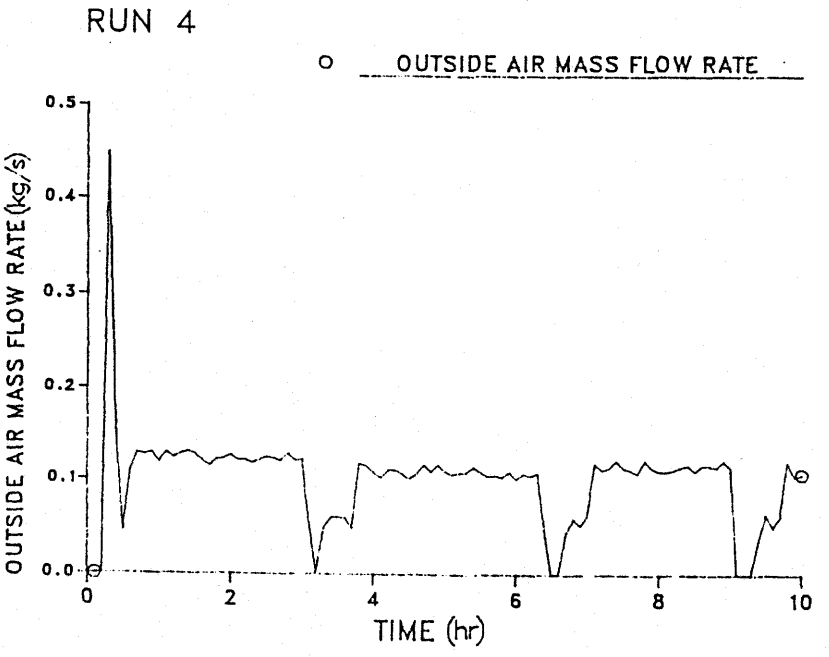

FIGURE E.13

RUN 4: Measured Outside Air Mass Flow Rate

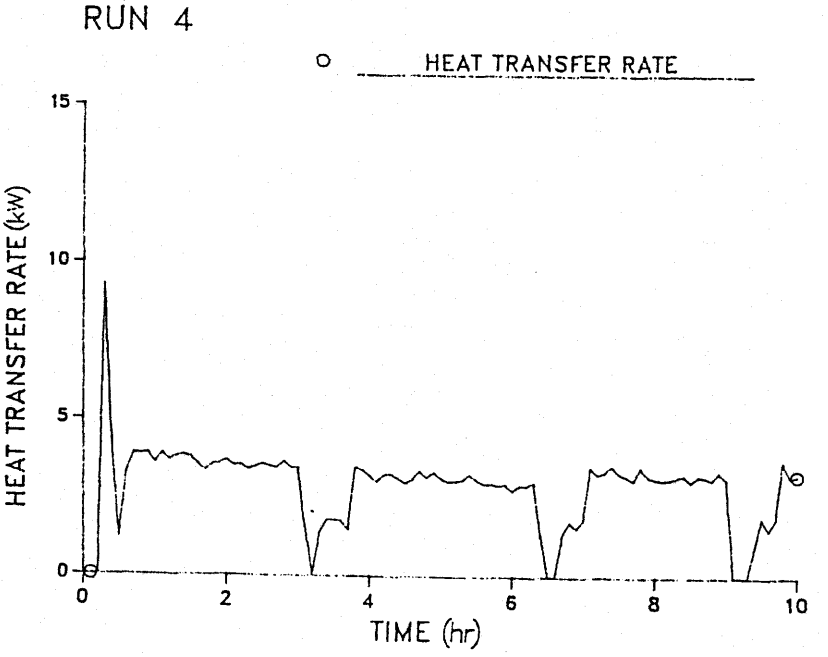

FIGURE E.14

RUN 4: Measured Heat Transfer Rate

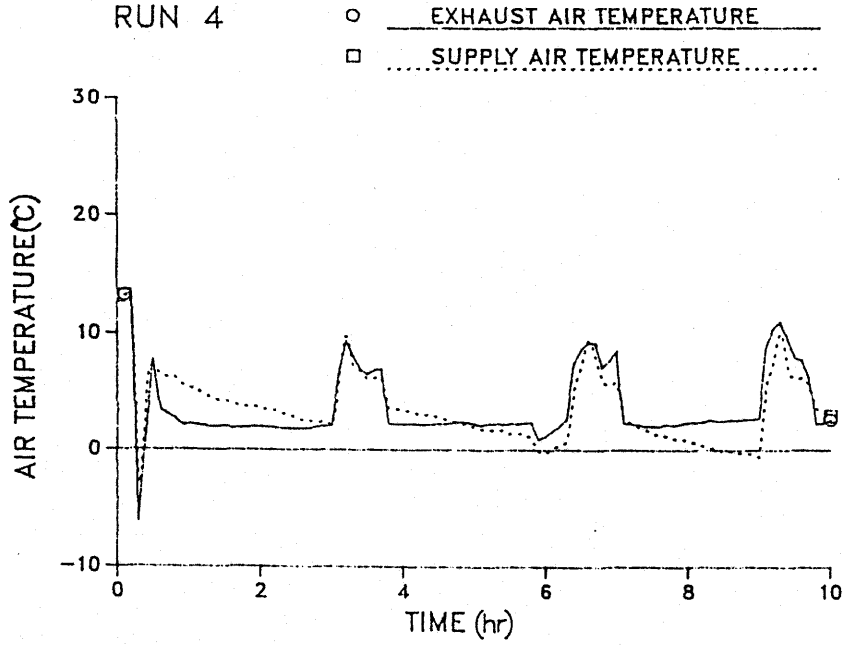

FIGURE E.15

RUN 4: Measured Outlet Temperatures

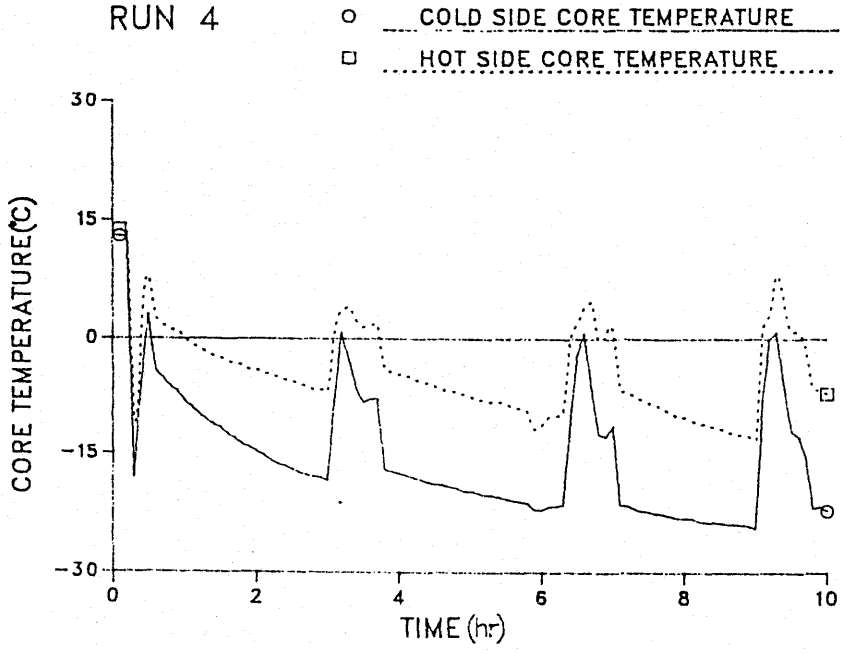

FIGURE E.16

RUN 4: Measured Core Temperatures

APPENDIX F

Simulation Listing

PROGRAM AMENDMENT

The turbulent friction factor (coefficient of frictional resistance) must be divided by 4 in order to calculate the heat exchanger pressure drop. The turbulent friction factor (coefficient of frictional resistance) is correct for calculation of the convective heat transfer coefficient.

```
************************************************************************
*                                                                      *
*       SIMULATION OF A CONDENSING AND FROSTING                        *
*                 AIR TO AIR HEAT                                      *
*                   EXCHANGER                                          *
*                                                                      *
************************************************************************
*                                                                      *
*                                                                      *
*--------------------DIMENSION MATRICES-------------------------------*
*                                                                      *
*       DIMENSION A(7,7),B(7)                                          *
        DIMENSION BO(7)
*                                                                      *
*--------------------SET UP COMMON BLOCKS-----------------------------*
*                                                                      *
        COMMON/CBLK1/T(8),PROP(5,8),PWS(8),PW(8),DPWSDT(8)
     #          ,DWDT(8),DENTDT(8),C(8),RE(8),H(8),F(8),SVAPP(61)
        COMMON/CBLK2/XX,XXLOW,XXHIGH
        COMMON/CBLK3/KTA,KTW,KVA,KVW,PRA,PRW,CPA,CPW
        COMMON/CBLK4/W(8),PATM,RLHMHI,RLHMCI
        COMMON/CBLK5/MFRH,MFRC,NH,NC,WDTH,S,OMFRH,OMFRC
        COMMON/CBLK6/DEWPT
        COMMON/CBLK7/NS,L,DW,KW,TEMPIN(4),TEMPSU(4)
        COMMON/CBLK8/RF,Q,DC,KC,NFLPRT
        COMMON/CBLK9/TIME,TISTEP,TIEND,CT,DLMASS,CONERR,PEAKQ,CONDIR,
     #          NSTFLG,CNTIME,CNTSTP,CGAIN,NS2FLG
        COMMON/CBLK10/FROSTH(0:41),FROSTT(0:41),DHC(4),PFAN,FSCOND,
     #          DHTC(0:41),DHCEND(4),FHMAX,XOMAX,FROSTP,DPO,TOTDP
        COMMON/CBLK11/UDRY,UWET,QDRY,QWET
        COMMON/CBLK12/ISTFLG
        COMMON/CBLK13/PWSW(4),PWW(4),WW(4),ENHH(4)
        REAL KW,L,MFRH,MFRC,KC,KTA,KTW,KVA,KVW,LMTD,NTU,ITFTMP
        INTEGER CT,FL
        CHARACTER*15 FNAME
*                                                                      *
************************************************************************
*                                                                      *
*                        MAIN PROGRAM                                  *
*                                                                      *
************************************************************************
*                                                                      *
*                                                                      *
*       REQUEST REVISION OF GEOMETRIC OR PHYSICAL DATA                 *
*       ---------------------------- ----------------                  *
*                                                                      *
        WRITE(5,100)
100     FORMAT( ' DO YOU WISH TO REVISE THE GEOMETRIC OR PHYSICAL ',
     #  'DATA? (1 OR 0)',$)
        READ(5,300) J
300     FORMAT(11)
```

```
      IF(J.EQ.1) CALL DESCRP
      OPEN(UNIT=22,FILE='XCHGR.DAT',STATUS='OLD')
      READ(22,*) S
      READ(22,*) RF
      READ(22,*) DW
      READ(22,*) KW
      READ(22,*) L
      READ(22,*) WDTH
      READ(22,*) NH
      READ(22,*) NC
      READ(22.*) NS
      CLOSE(UNIT=22)
*                                                                     *
*---------------READ TIME SERIES DATA-----------------------------  --*
*                                                                     *
      OPEN(UNIT=22,FILE='CONTRL.DAT',STATUS='OLD')
      READ(22,*) TISTEP
      READ(22,*) TIEND
      READ(22,*) CGAIN
      READ(22,*) DLMASS
      READ(22,*) CONERR
      READ(22,*) CNTSTP
      CLOSE(UNIT=22)
*                                                                     *
*---------------SET TIME TO ZERO-----------------  -----------------*
*                                                                     *
      TIME=0.0
*                                                                     *
*-----------SET FLAG : DETAILED PRINTOUT OR SHORT PRINTOUT-  -------*
*                                                                     *
      NFLPRT=1
*                                                                     *
*----------SET FROST MODULE TIME AND FROST HEIGHT TO ZERO----------*
*       ALSO SET THE HEAT TRANSFER COEF ENHANCEMENT TO ONE            *
*                                                                     *
      FRTOLD=0.0
      FRHOLD=0.0
      DO 11 I=1,4
      DHC(I)=0.0
      ENHH(I)=0.0
11    CONTINUE
      FROSTP=0.0
      FHMAX=0.0
      XOMAX=0.0
*                                                                     *
*----------INITIALIZE CONTROL MODULE PARAMETERS  -----------------*
*                                                                     *
      PEAKQ=0.0
      CONDIR=1.0
      NSTFLG=0
      CNTIME=0.0
```

```
*                                                                      *
*---------INITIALIZE THICKNESS OF CONDENSATE FILM------------ ----*
*                                                                      *
        DC=0.0002
        KC=0.5745
*                                                                      *
*------------INITIALIZE THE ENHANCEMENT MATRIX--------------------*
*                                                                      *
        ENHH(3)=1.0
        ENHH(4)=1.0
*                                                                      *
*---------LOAD SATURATION VAPOR PRESSURE MATRIX---------------- --*
*          FROM ASHRAE FUND SI 85                                      *
*                                                                      *
        OPEN(UNIT=22,FILE='SVAPP.DAT',STATUS='OLD')
        DO 59 I=1,60,4
        READ(22,*) SVAPP(I),SVAPP(I+1),SVAPP(I+2),SVAPP(I+3)
59      CONTINUE
        READ(22,*) SVAPP(61)
        CLOSE(UNIT=22)
*                                                                      *
*---------------INPUT OF OPERATIONAL DATA-------- ----------------*
*                                                                      *
        WRITE(5,2)
2       FORMAT(' NOW, INPUT THE OPERATIONAL DATA AS REQUESTED')
        WRITE(5,4)
4       FORMAT(10X,'COLD AIR:')
        WRITE(5,6)
6       FORMAT(14X,'MASS FLOWRATE (DRY) (KG/SEC)=',$)
        READ(5,*) MFRC
        OMFRC=MFRC
        WRITE(5,10)
10      FORMAT(14X,'INLET TEMPERATURE (DEGREES C)='$)
        READ(5,*) T(8)
        WRITE(5,14)
14      FORMAT(14X,'RELATIVE HUMIDITY (PERCENTAGE)='$)
        READ(5,*) RLHMCI
        WRITE(5,20)
20      FORMAT(/,10X,'HOT AIR:')
        WRITE(5,22)
22      FORMAT(14X,'MASS FLOWRATE (DRY) (KG/SEC)='$)
        READ(5,*) MFRH
        OMFRH=MFRH
        WRITE(5,26)
26      FORMAT(14X,'INLET TEMPERATURE (DEGREES C)='$)
        READ(5,*) T(1)
        WRITE(5,30)
30      FORMAT(14X,'RELATIVE HUMIDITY (PERCENTAGE)='$)
        READ(5,*) RLHMHI
        WRITE(5,33)
33      FORMAT(/,10X,'ATMOSPHERIC PRESSURE (KILOPASCALS)='$)
```

```
      READ(5,*) PATM
      WRITE(5,35)
35    FORMAT(/,10X,'FAN STATIC PRESSURE (PASCALS)='$)
      READ(5,*) PFAN
      WRITE(5,36)
36    FORMAT( 10X,'FROST CONDUCTIVITY (W/M C)='$)
      READ(5,*) FSCOND
      WRITE(5,34)
34    FORMAT(/,10X,'FILE TO OUTPUT DATA TO=',$)
      READ(5,*) FNAME
      OPEN(UNIT=22,STATUS='NEW',FILE=FNAME)
      WRITE(22,309)
309   FORMAT( 1X,'  TIME  ','TH OUT',2X,'TC OUT',2X,'  Q    ',2X,
     #         'TP IN',2X,'TP OUT',3X,'DRYFRA',1X,'MFRC',2X,'MFRH',
     #         1X,'FST POS',2X,'DP',3X,'FHMAX',/,/)
      T(1)=T(1)+273.16
      T(8)=T(8)+273.16
      RLHMHI=RLHMHI/100
      RLHMCI=RLHMCI/100
*                                                                    *
*-----------CHECK OF INPUTTED DATA-----------------------------------*
*                                                                    *
      IF(T(1)-T(8)) 110,130,130
110   WRITE(5,111)
111   FORMAT( /,/,'PLEASE CORRECT INPUT DATA',/,13X,'COLD INLET ',
     #  'CANNOT BE WARMER THAN HOT INLET!')
      GOTO 999
130   IF(RLHMCI.GT.1 .OR. RLHMHI.GT.1) GOTO 140
      GOTO 150
140   WRITE(5,141)
141   FORMAT( /,/,' PLEASE CORRECT INPUT DATA',/,13X,'RELATIVE ',
     #  'HUMIDITY CANNOT BE GREATER THAN 100%! ')
      GOTO 999
*                                                                    *
*-----CALCULATION OF THE DEWPOINT OF THE HOT ENTERING AIR------*
*                                                                    *
150   T(2)=T(1)
      T(3)=T(1)
      T(4)=T(1)
      T(5)=T(8)
      T(6)=T(8)
      T(7)=T(8)
      CALL SATVAP
      CALL HUMRAT
      IF(W(1)-.0038) 180,190,190
180   DEWPT=5.994+12.41*ALOG(PW(1))+.4273*(ALOG(PW(1)))**2
      GOTO 191
190   DEWPT=6.983+14.38*ALOG(PW(1))+1.079*(ALOG(PW(1)))**2
191   DEWPT=DEWPT+273.16
*                                                                    *
*-------INITIALIZE THE INTERFACE TEMPERATURE ON THE HOT----------*
```

```
*       SIDE EQUAL TO THE DEWPOINT                                      *
*                                                                       *
        ITFTMP=DEWPT
*                                                                       *
*-------INITIALIZE THE PLATE TEMPERATURES-----------------------------*
*                                                                       *
        TEMPSU(1)=(T(1)+T(5))/2.0-273.16
        TEMPSU(2)=(T(2)+T(6))/2.0-273.16
        TEMPSU(3)=(T(3)+T(7))/2.0-273.16
        TEMPSU(4)=(T(4)+T(8))/2.0-273.16
*                                                                       *
*-------DO LOOP FOR TIME SERIES----------------------------------------*
*                                                                       *
        DO 1000 TIME=0,TIEND,TISTEP
        IF(TIME.EQ.0) GOTO 151
        IF(TEMPIN(4).GE.0.0.AND.XX.EQ.L) CALL REINIT
        CALL FROST
*                                                                       *
*-----INITIALIZE THE DRY LENGTH XX LIMITS : SET INITIAL XX-------------*
*                                                                       *
151     XXLOW=0.0
        XXHIGH=L
        XX=L*(T(1)-DEWPT)/(T(1)-T(8))
        IF(XX.GT.L) GOTO 270
*                                                                       *
*-------INITIALIZE STABILITY FLAG--------------------------------------*
*                                                                       *
        ISTFLG=0
*                                                                       *
*-------INITIAL ASSUMPTION OF REQUIRED TEMPERATURE-------------- ---*
*                                                                       *
        T(2)=T(1)
        T(3)=T(1)
        T(4)=T(1)
        T(5)=T(8)
        T(6)=T(8)
        T(7)=T(8)
        GOTO 261
*                                                                       *
*--------INTERPOLATION TO FIND XX---------------------------------------*
*                                                                       *
260     ITFTMP=DEWPT
        IF(ABS(ITFTMP-T(2)).LT.0.1) GOTO 250
        XXHOLD=XX
        IF((ITFTMP-T(2)).GT.0.0) XX=(XX+XXLOW)/2.0
        IF((ITFTMP-T(2)).GT.0.0) XXHIGH=XXHOLD
        IF((ITFTMP-T(2)).LT.0.0.AND.(XX/L).GT.0.98) GOTO 270
        IF((ITFTMP-T(2)).LT.0.0) XX=(XX+XXHIGH)/2.0
        IF((ITFTMP-T(2)).LT.0.0) XXLOW=XXHOLD
*                                                                       *
*----------SCAN THE INTERFACE TEMPERATURE----------------------------*
```

```
*                                                                       *
261     T(6)=T(8)
        GOTO 262
170     T(6)=(T(6)+T(7))/2.0
        IF(T(6).GT.T(7)) ISTFLG=1
        IF(T(6).GT.T(7)) WRITE(6,891) T(6),T(7)
891     FORMAT( 1X,' STABILITY FLAG SET : T6= ',F8.2,' T7= ',F8.2)
262     CALL DRY
        T(3)=T(2)
        CALL WET
*                                                                       *
*----------CHECK IF THE INTERFACE TEMPERATURES MATCH-----------------*
*                                                                       *
        IF(ABS(T(6)-T(7)).LT.0.1) GOTO 260
        GOTO 170
*                                                                       *
*--------TO HANDLE COMPLETELY DRY HEAT EXCHANGER--------------------*
*                                                                       *
270     XX=L
        T(6)=T(8)
        CALL DRY
        QWET=0.0
        T(4)=T(2)
*                                                                       *
*---------CACULATE PERFORMANCE PARAMETERS---------------------------*
*                                                                       *
250     Q=QDRY+QWET
        CC=XX/L*((C(5)+C(6))/2)+(1-XX/L)*((C(7)+C(8))/2)
        EFF=Q/(CC*(T(1)-T(8)))
        UA=WDTH*NS*(UDRY*XX+UWET*(L-XX))
        IF((T(1)-T(5)).LE.0.0) GOTO 253
        LMTD=((T(1)-T(5))-(T(4)-T(8)))/(ALOG((T(1)-T(5))/(T(4)-T(8))))
        CF=Q/(UA*LMTD)
253     T(4)=T(4)-273.16
        T(5)=T(5)-273.16
        Q1F=QDRY/Q*100
        Q2F=QWET/Q*100
        DRYFRA=XX/L*100
        WETFRA=(L-XX)/L*100
        IF(C(1).GT.C(8)) GOTO 251
        CMIN=C(1)
        CMAX=C(8)
        GOTO 252
251     CMIN=C(8)
        CMAX=C(1)
252     R=CMIN/CMAX
        NTU=UA/CMIN
        IF(NFLPRT.EQ.1) GOTO 301
*                                                                       *
*------------OUTPUT OF RESULTS-------------------------------------*
*                                                                       *
```

```
      WRITE(5,21)
21    FORMAT( 34X,'STEADY STATE RUNNING CONDITIONS')
      WRITE(5,44)
44    FORMAT( 33X,'**********************************')
      WRITE(5,55)
55    FORMAT( /,10X,'OUTLET TEMPERATURES:')
      WRITE(5,66)
66    FORMAT( 9X,'---------------------')
      WRITE(5,77) T(4)
77    FORMAT( 15X,'HOT AIR=',F6.2,' DEGREES C.')
      WRITE(5,88) T(5)
88    FORMAT( 15X,'COLD AIR=',F6.2,' DEGREES C.')
      WRITE(5,99)
99    FORMAT( /,10X,'PERFORMANCE PARAMETERS:')
      WRITE(5,27)
27    FORMAT( 9X,'-------------------------')
      WRITE(5,37) Q
37    FORMAT( 15X,'HEAT EXCHANGE RATE=',F9.2,' WATTS.')
      WRITE(5,47) Q1F
47    FORMAT( 20X,F4.1,'%',' THROUGH DRY REGION.')
      WRITE(5,57) Q2F
57    FORMAT( 20X,F4.1,'%',' THROUGH WET REGION.')
      WRITE(5,67) EFF
67    FORMAT( 15X,'EFFECTIVENESS=',F4.2)
      WRITE(5,87) CF
87    FORMAT( 15X,'CORRECTION FACTOR=',F5.3)
      WRITE(5,97) LMTD
97    FORMAT( 15X,'LOG MEAN TEMPERATURE DIFFERENCE=',F5.2,'DEGREES C')
      WRITE(5,96) R
96    FORMAT( 15X,'RATIO OF HEAT CAPACITY RATES=',F5.3)
      WRITE(5,86) NTU
86    FORMAT( 15X,'NUMBER OF TRANSFER UNITS=',F4.2)
      WRITE(5,513)
513   FORMAT( /,10X,'EXCHANGE SURFACE CONDITIONS:')
      WRITE(5,514)
514   FORMAT( 9X,'----------------------------')
      WRITE(5,515) DRYFRA
515   FORMAT( 15X,'DRY AREA FRACTION=',F5.2,'%')
      WRITE(5,516) WETFRA
516   FORMAT( 15X,'WET AREA FRACTION=',F5.2,'%')
      WRITE(5,517)TEMPIN(4)
517   FORMAT( /,10X,'CORE TEMPERATURE = ',F5.1,' DEGREES C')
      IF(NFLPRT.EQ.0) GOTO 999
301   WRITE(5,302) TIME,T(4),T(5),Q,TEMPIN(4),TEMPIN(1),DRYFRA,MFRC,MFRH,
     #             FROSTP,TOTDP,FHMAX
302   FORMAT( F8.3,F6.2,2X,F6.2,2X,F7.0,2X,F6.2,2X,F6.2,2X,F6.2,
     #        1X,F5.4,1X,F5.4,1X,F5.4,1X,F6.1,F8.7)
      WRITE(22,302) TIME,T(4),T(5),Q,TEMPIN(4),TEMPIN(1),DRYFRA,MFRC,MFRH,
     #              FROSTP,TOTDP,FHMAX
      WRITE(22,311) (T(I),I=1,8)
311   FORMAT( 10X,'TEMPERATURES        ',8(2X,F8.2))
```

```
      WRITE(22,304) (C(I),I=1,8)
304   FORMAT( 10X,'HEAT CAPACITY RATES ',8(2X,F8.1))
      WRITE(22,305) (RE(I),I=1,8)
305   FORMAT( 10X,'REYNOLDS NUMBER     ',8(2X,F8.1))
      WRITE(22,306) (DENTDT(I),I=1,8)
306   FORMAT( 10X,'DI/DT               ',8(2X,F8.1))
      WRITE(22,307) (H(I),I=1,8)
307   FORMAT( 10X,'HEAT TRANSFER COEF  ',8(2X,F8.4))
      WRITE(22,308) (TEMPIN(I),I=1,4),(DHC(I),I=1,4)
308   FORMAT( 10X,'PLATE TEMPERATURES  ',4(1X,F8.2),' DHC ',
     #        4(1X,F8.5))
      WRITE(22,312) (TEMPSU(I),I=1,4),(ENHH(I),I=1,4)
312   FORMAT( 10X,'SURFACE TEMPERATURES',4(1X,F8.2),' ENHH',
     #        4(1X,F8.5))
      WRITE(22,315) (W(I),I=1,8)
315   FORMAT( 10X,'HUMIDITY RATIOS     ',8(1X,F8.6))
      WRITE(22,316) (WW(I),I=1,4)
316   FORMAT( 10X,'PLATE HUMIDITY RATIO',4(1X,F8.6))
      WRITE(22,317) (PW(I),I=1,8)
317   FORMAT( 10X,'PW                  ',8(1X,F8.6))
      WRITE(22,318) (PWS(I),I=1,8)
318   FORMAT( 10X,'PW2                 ',8(1X,F8.6))
      WRITE(22,319) (PWSW(I),I=1,4)
319   FORMAT( 10X,'PWSW                ',8(1X,F8.6))
      WRITE(22,310) FHMAX,XOMAX,(DHCEND(I),I=1,4)
310   FORMAT( 10X,'FHMAX ',F8.7,' XOMAX ',F8.6,' DHCEND ',
     #        4(1X,F8.6))
      WRITE(22,320) (PROP(1,I),I=1,8)
320   FORMAT( 10X,'CONDUCTIVITY        ',8(1X,F8.7))
      WRITE(22,321) (PROP(2,I),I=1,8)
321   FORMAT( 10X,'VISCOSITY           ',8(1X,E9.3))
      WRITE(22,322) (PROP(3,I),I=1,8)
322   FORMAT( 10X,'PRANDTL NUMBER      ',8(1X,F8.6))
      WRITE(22,323) (PROP(4,I),I=1,8)
323   FORMAT( 10X,'SPECIFIC HEAT       ',8(1X,F8.1))
      WRITE(22,324) (PROP(5,I),I=1,8)
324   FORMAT( 10X,'DENSITY             ',8(1X,F8.5))
      T(4)=T(4)+273.16
      T(5)=T(5)+273.16
      IF(TIME.EQ.0.0.AND.TEMPIN(4).GT.0.0) GOTO 998
999   CALL CONTROL
1000  CONTINUE
998   WRITE(22,303)OMFRC,T(8),RLHMCI,OMFRH,T(1),RLHMHI,PATM,FSCOND,PFAN
303   FORMAT( 9(2X,F10.4))
      CLOSE(UNIT=22)
      END
*****************************************************************
*                                                               *
*            SUBROUTINE:SATVAP                                  *
*       THIS SUBROUTINE CALCULATES THE SATURATION               *
*    VAPOR PRESSURE AT EACH POINT IN THE HEAT                   *
```

```
*                    EXCHANGER.                                          *
*                                                                        *
**************************************************************************
*                                                                        *
*                                                                        *
      SUBROUTINE SATVAP
      COMMON/CBLK1/T(8),PROP(5,8),PWS(8),PW(8),DPWSDT(8)
     #          ,DWDT(8),DENTDT(8),C(8),RE(8),H(8),F(8),SVAPP(61)
      COMMON/CBLK7/NS,L,DW,KW,TEMPIN(4),TEMPSU(4)
      COMMON/CBLK13/PWSW(4),PWW(4),WW(4),ENHH(4)
      REAL L,KW
      DO 10 I=1,8
      TT=T(I)-273.16+31.0
      J=INT(TT)
      PWS(I)=(TT-J)*SVAPP(J+1)+(J+1-TT)*SVAPP(J)
10    CONTINUE
      DO 40 I=3,4
      TT=TEMPSU(I)+31.0
      J=INT(TT)
      PWSW(I)=(TT-J)*SVAPP(J+1)+(J+1-TT)*SVAPP(J)
40    CONTINUE
      RETURN
      END
**************************************************************************
*                                                                        *
*                SUBROUTINE:HUMRAT                                       *
*          THIS SUBROUTINE FINDS THE HUMIDITY RATIO AT                   *
*               EACH POINT IN THE HEAT EXCHANGER.                        *
*                                                                        *
**************************************************************************
*                                                                        *
*                                                                        *
      SUBROUTINE HUMRAT
      COMMON/CBLK1/T(8),PROP(5,8),PWS(8),PW(8),DPWSDT(8)
     #          ,DWDT(8),DENTDT(8),C(8),RE(8),H(8),F(8),SVAPP(61)
      COMMON/CBLK4/W(8),PATM,RLHMHI,RLHMCI
      COMMON/CBLK6/DEWPT
      COMMON/CBLK13/PWSW(4),PWW(4),WW(4),ENHH(4)
      DO 10 I=5,8
            PW(I)=PWS(8)*RLHMCI
            W(I)=.62198*(PW(I)/(PATM-PW(I)))
10    CONTINUE
      DO 20 I=1,2
            PW(I)=PWS(1)*RLHMHI
            W(I)=.62198*(PW(I)/(PATM-PW(I)))
20    CONTINUE
      DO 30 I=3,4
            IF(T(I).LE.DEWPT) PW(I)=PWS(I)
            IF(T(I).GT.DEWPT) PW(I)=PWS(1)*RLHMHI
            W(I)=.62198*(PW(I)/(PATM-PW(I)))
30    CONTINUE
```

```
      DO 40 I=3,4
            PWW(I)=PWSW(I)
            WW(I)=.62198*(PWW(I)/(PATM-PWW(I)))
            IF(WW(I).GT.W(I)) WW(I)=W(I)
40    CONTINUE
      RETURN
      END
*****************************************************************************
*                                                                           *
*                  SUBROUTINE:PROPS                                         *
*            THIS SUBROUTINE CALCULATES THE FOLLOWING PROPERTIES            *
*              AT EACH POINT IN THE HEAT EXCHANGER:                         *
*                        DENSITY                                            *
*                   KINEMATIC VISCOSITY                                     *
*                   PRANDTL NUMBER                                          *
*                   THERMAL CONDUCTIVITY                                    *
*                   HEAT CAPACITY                                           *
*                                                                           *
*****************************************************************************
*                                                                           *
*                                                                           *
      SUBROUTINE PROPS
      COMMON/CBLK1/T(8),PROP(5,8),PWS(8),PW(8),DPWSDT(8)
     #          ,DWDT(8),DENTDT(8),C(8),RE(8),H(8),F(8),SVAPP(61)
      COMMON/CBLK3/KTA,KTW,KVA,KVW,PRA,PRW,CPA,CPW
      COMMON/CBLK4/W(8),PATM,RLHMHI,RLHMCI
      REAL KTA,KTW,KVA,KVW
      DO 10 I=1,8
            CALL PRPINT(T(I))
            PROP(1,I)=(KTA+W(I)*KTW)/(1+W(I))
            PROP(2,I)=(KVA+W(I)*KVW)/(1+W(I))
            PROP(3,I)=(PRA+W(I)*PRW)/(1+W(I))
            PROP(4,I)=(CPA+W(I)*CPW)/(1+W(I))
            PROP(5,I)=PATM*1000.0/(287.0*T(I)*(1.0+1.6078*W(I)))
10    CONTINUE
      RETURN
      END
*****************************************************************
*                                                               *
*                  SUBROUTINE ENHANCE                           *
*          SUBROUTINE TO CACULATE THE HEAT TRANSFER             *
*          FOR MASS TRANSFER,THE PLATE TEMPERATURE              *
*           AND THE FROST WATER INTERFACE TEMPERATURE           *
*                                                               *
*****************************************************************
*                                                               *
      SUBROUTINE ENHANCE
      COMMON/CBLK1/T(8),PROP(5,8),PWS(8),PW(8),DPWSDT(8)
     #          ,DWDT(8),DENTDT(8),C(8),RE(8),H(8),F(8),SVAPP(61)
      COMMON/CBLK4/W(8),PATM,RLHMHI,RLHMCI
      COMMON/CBLK7/NS,L,DW,KW,TEMPIN(4),TEMPSU(4)
```

```
      COMMON/CBLK13/PWSW(4),PWW(4),WW(4),ENHH(4)
      REAL L,KW
      DO 10 I=3,4
      TB=T(I)-273.16
      TW=TEMPSU(I)
      HB=1006*TB+W(I)*(2501000+1775*TB)
      HW=1006*TW+WW(I)*(2501000+1775*TW)
      ENHH(I)=(HB-HW)/(PROP(4,I)*(TB-TW))
10    CONTINUE
      RETURN
      END
*********************************************************************
*                                                                   *
*              SUBROUTINE:ENTHAL                                    *
*         THIS SUBROUTINE FINDS THE RATE OF CHANGE OF               *
*         ENTHALPY AT EACH POINT IN THE HEAT EXCHANGER.             *
*                                                                   *
*********************************************************************
*                                                                   *
*                                                                   *
      SUBROUTINE ENTHAL
      COMMON/CBLK1/T(8),PROP(5,8),PWS(8),PW(8),DPWSDT(8)
     #          ,DWDT(8),DENTDT(8),C(8),RE(8),H(8),F(8),SVAPP(61)
      COMMON/CBLK4/W(8),PATM,RLHMHI,RLHMCI
      COMMON/CBLK13/PWSW(4),PWW(4),WW(4),ENHH(4)
      DO 10 I=3,4
      TT=T(I)-273.16+31.0
      J=INT(TT)
      DPWSDT(I)=SVAPP(J+1)-SVAPP(J)
10    CONTINUE
      DO 40 I=1,8
            DWDT(I)=.62198*PATM*DPWSDT(I)/((PATM-PWS(I))**2)
            DENTDT(I)=1006+1775*W(I)+1775*DWDT(I)*(T(I)-273.16
     #                )+2501000*DWDT(I)
40    CONTINUE
100   RETURN
      END
*********************************************************************
*                                                                   *
*                SUBROUTINE:HTCPRT                                  *
*           THIS SUBROUTINE FINDS THE HEAT CAPACITY                 *
*           AT EACH POINT IN THE HEAT EXCHANGER.                    *
*                                                                   *
*********************************************************************
*                                                                   *
*                                                                   *
      SUBROUTINE HTCPRT
      COMMON/CBLK1/T(8),PROP(5,8),PWS(8),PW(8),DPWSDT(8)
     #          ,DWDT(8),DENTDT(8),C(8),RE(8),H(8),F(8),SVAPP(61)
      COMMON/CBLK5/MFRH,MFRC,NH,NC,WDTH,S,OMFRH,OMFRC
      REAL MFRH,MFRC
```

```
      DO 10 I=1,8
              IF(I.LE.4) GOTO 20
              C(I)=MFRC*DENTDT(I)
              GOTO 10
20            C(I)=MFRH*DENTDT(I)
10    CONTINUE
      RETURN
      END
*************************************************************************
*                                                                       *
*                 SUBROUTINE:REYNLD                                     *
*           THIS SUBROUTINE FINDS THE REYNOLDS NUMBER                   *
*            AT EACH POINT IN THE HEAT EXCHANGER.                       *
*                                                                       *
*************************************************************************
*                                                                       *
*                                                                       *
      SUBROUTINE REYNLD
      COMMON/CBLK1/T(8),PROP(5,8),PWS(8),PW(8),DPWSDT(8)
     #          ,DWDT(8),DENTDT(8),C(8),RE(8),H(8),F(8),SVAPP(61)
      COMMON/CBLK4/W(8),PATM,RLHMHI,RLHMCI
      COMMON/CBLK5/MFRH,MFRC,NH,NC,WDTH,S,OMFRH,OMFRC
      REAL MFRH,MFRC
      DO 10 I=1,4
              RE(I)=MFRH/NH*(1+W(I))*2/(PROP(5,I)*PROP(2,I)*WDTH)
10    CONTINUE
      DO 20 I=5,8
              RE(I)=MFRC/NC*(1+W(I))*2/(PROP(5,I)*PROP(2,I)*WDTH)
20    CONTINUE
      RETURN
      END
*************************************************************************
*                                                                       *
*             SUBROUTINE:FRICFC                                         *
*          THIS SUBROUTINE FINDS THE FRICTION FACTOR AT                 *
*             EACH POINT IN THE HEAT EXCHANGER.                         *
*                                                                       *
*************************************************************************
*                                                                       *
*                                                                       *
      SUBROUTINE FRICFC
      COMMON/CBLK1/T(8),PROP(5,8),PWS(8),PW(8),DPWSDT(8)
     #          ,DWDT(8),DENTDT(8),C(8),RE(8),H(8),F(8),SVAPP(61)
      DO 10 I=1,8
      IF(RE(I).LT.2300.0) GOTO 2
      IF(RE(I).GT.10000.0) GOTO 1
*                                                                       *
*------THE TRANSITION FROM LAMINAR TO TURBULENT IS ASSUMED--------------*
*      TO OCCUR FROM RE 2300-10000 : IN THIS REGION A LINEAR            *
*      INTERPOLATION IS DONE                                            *
*                                                                       *
```

```
*----------FRICTION FACTOR TRANSITIONAL LIMITS--------------------*
*                                                                  *
      FL=24.0/2300
      FU=(1.82*ALOG10(10000.0)-1.64)**-2
      IF(FU.LT..033) FU=.033
*                                                                  *
*----------TRANSITIONAL FRICTION FACTOR---------- ---------- ----*
*                                                                  *
      F(I)=(RE(I)-2300.0)/7700.0*FU+(10000.0-RE(I))/7700.0*FL
      GOTO 10
*                                                                  *
*---------TURBULENT FRICTION FACTOR------------- ---------------*
*                                                                  *
1     F(I)=(1.82*ALOG10(RE(I))-1.64)**-2
      IF(F(I).LT..033) F(I)=.033
      GOTO 10
*                                                                   *
*----------LAMINAR HEAT TRANSFER------------------ ---------------*
*                                                                   *
2     F(I)=24.0/RE(I)
10    CONTINUE
      RETURN
      END
**********************************************************************
*                                                                    *
*              SUBROUTINE:TRNCOF                                     *
*         THIS SUBROUTINE FINDS THE HEAT TRANSFER                    *
*       COEFFICIENT AT EACH POINT IN THE HEAT EXCHANGER.             *
*                                                                    *
**********************************************************************
*                                                                    *
*                                                                    *
      SUBROUTINE TRNCOF
      COMMON/CBLK1/T(8),PROP(5,8),PWS(8),PW(8),DPWSDT(8)
     #          ,DWDT(8),DENTDT(8),C(8),RE(8),H(8),F(8),SVAPP(61)
      COMMON/CBLK4/W(8),PATM,RLHMHI,RLHMCI
      COMMON/CBLK5/MFRH,MFRC,NH,NC,WDTH,SH,OMFRH,OMFRC
      COMMON/CBLK10/FROSTH(0:41),FROSTT(0:41),DHC(4),PFAN,FSCOND,
     #          DHTC(0:41),DHCEND(4),FHMAX,XOMAX,FROSTP,DPO,TOTDP
      COMMON/CBLK13/PWSW(4),PWW(4),WW(4),ENHH(4)
      REAL MFRH,MFRC
      DO 10 I=1,8
*                                                                   *
*------CORRECT PASSAGE SIZE FOR FROST ACCUMULATION---------------*
*                                                                   *
      IF(I.EQ.1) S=SH-2*FROSTH(5)
      IF(I.EQ.2) S=SH-2*FROSTH(15)
      IF(I.EQ.3) S=SH-2*FROSTH(25)
      IF(I.EQ.4) S=SH-2*FROSTH(35)
      IF(I.GE.5) S=SH
      IF(RE(I).LT.2300.0) GOTO 2
```

```
      IF(RE(I).GT.10000.0) GOTO 1
*                                                                     *
*-----THE TRANSITION FROM LAMINAR TO TURBULENT IS ASSUMED-----------*
*     TO OCCUR FROM RE 2300-10000 : IN THIS REGION A LINEAR         *
*     INTERPOLATION IS DONE                                         *
*                                                                     *
*----------HEAT TRANSFER TRANSITIONAL LIMITS----------------------*
*                                                                     *
      HL=PROP(1,I)*7.888/(2*S)
      FU=(1.82*ALOG10(10000.0)-1.64)**-2
      IF(FU.LT..033) FU=.033
      HU=PROP(1,I)*(FU/8)*10000.0*
     #          PROP(3,I)/(2*S*(1.07+12.7*(FU/8)**.5*
     #          (PROP(3,I)**.66666-1)))
*                                                                     *
*----------TRANSITIONAL HEAT TRANSFER COEFFICIENT-----------------*
*                                                                     *
      H(I)=(RE(I)-2300.0)/7700.0*HU+(10000.0-RE(I))/7700.0*HL
      GOTO 10
*                                                                     *
*---------TURBULENT HEAT TRANSFER--------------------------------*
*                                                                     *
1     H(I)=PROP(1,I)*(F(I)/8)*RE(I)*
     #          PROP(3,I)/(2*S*(1.07+12.7*(F(I)/8)**.5*
     #          (PROP(3,I)**.66666-1)))
      GOTO 10
*                                                                     *
*----------LAMINAR HEAT TRANSFER----------------------------------*
*                                                                     *
2     H(I)=PROP(1,I)*7.888/(2*S)
10    CONTINUE
      DO 20 I=3,4
            H(I)=H(I)*ENHH(I)
20    CONTINUE
*                                                                     *
*-----ENHANCE THE HEAT TRANSFER COEFFICIENT FOR ENTRANCE EFFECTS---*
*                                                                     *
      H(1)=H(1)*1.3
      H(8)=H(8)*1.3
      RETURN
      END
**********************************************************************
*                                                                     *
*           SUBROUTINE:PRPINT                                         *
*       THIS SUBROUTINE INTERPOLATES TO FIND THE FOLLOWING            *
*       PROPERTIES OF AIR AND WATER AT ANY TEMPERATURE                *
*          BETWEEN 200 K AND 350 K INCLUSIVE:                         *
*                THERMAL CONDUCTIVITY                                 *
*                KINEMATIC VISCOSITY                                  *
*                PRANDTL NUMBER                                       *
*                HEAT CAPACITY                                        *
```

```
*                                                                      *
************************************************************************
*                                                                      *
*                                                                      *
      SUBROUTINE PRPINT(T)
      COMMON/CBLK3/KTA,KTW,KVA,KVW,PRA,PRW,CPA,CPW
      REAL KTA,KTW,KVA,KVW
      IF(T.GT.250) GOTO 10
            CPA=(T-200)/50*-.8+1006.1
            KVA=((T-200)/50*2+7.49)*1E-6
            KTA=(T-200)/50*.00418+.01809
            PRA=(T-200)/50*-.017+.739
      GOTO 20
10    IF(T.GT.300) GOTO 30
            CPA=(T-250)/50*.4+1005.3
            KVA=((T-250)/50*6.19+9.49)*1E-6
            KTA=(T-250)/50*.00397+.02227
            PRA=(T-250)/50*-.014+.722
      GOTO 20
30          CPA=(T-300)/50*3.3+1005.7
            KVA=((T-300)/50*5.08+15.68)*1E-6
            KTA=(T-300)/50*.00379+.02624
            PRA=(T-300)/50*-.011+.708
*                                                                      *
*--------PROPERTIES OF STEAM : NBS/NRC TABLES---------------------- ----*
*                                                                      *
20          CPW=1896.0
            KTW=0.01777
            IF(T.LE.273.17) KVW=1.899E-3
            IF(T.GT.273.17) KVW=(T-273.17)/30.0*-1.570E-3+1.899E-3
            PRW=1.006
60    RETURN
      END
************************************************************************
*                                                                      *
*          SUBROUTINE:DESCRP                                           *
*        THIS SUBROUTINE DESCRIBES THE DATA FILE WHICH                 *
*        CONTAINS THE NECESSARY GEOMETRIC AND PHYSICAL DATA            *
*        FOR THE FLAT PLATE COUNTER-FLOW HEAT EXCHANGER.               *
*                                                                      *
************************************************************************
*                                                                      *
*                                                                      *
      SUBROUTINE DESCRP
      WRITE(5,10)
10    FORMAT( /,/,/,4X,'THE GEOMETRIC AND PHYSICAL DATA OF THE'
     # ' HEAT EXCHANGER IS DESCRIBED IN A DATA FILE')
      WRITE(5,20)
20    FORMAT( 'NAMED XCHGR.DAT.  REVISIONS ARE MADE TO THIS DATA'
     # ' BY EDITTING THIS DATA FILE.')
      WRITE(5,30)
```

```
30      FORMAT( /,/,7X,'EDIT LINE #',28X,'QUANTITY ',31X,'UNITS')
        WRITE(5,40)
40      FORMAT( 6X,'------------',26X,'---------',29X,'-------')
        WRITE(5,50)
50      FORMAT( 11X,'100',23X,'SPACING OF X''CHGR SURFACES',21X,
     #  'METERS')
        WRITE(5,60)
60      FORMAT( 11X,'200',23X,'FOULING FACTOR',36X,'-')
        WRITE(5,70)
70      FORMAT( 11X,'300',23X,'THICKNESS OF X''CHGR SURFACES',10X,
     #  9X,'METERS')
        WRITE(5,80)
80      FORMAT( 11X,'400',23X,'CONDUCTIVITY OF SURFACES',25X,
     #  8X,'W/(M©2 K)')
        WRITE(5,90)
90      FORMAT( 11X,'500',23X,'LENGTH OF X''CHGR SURFACES',13X,
     #  9X,'METERS')
        WRITE(5,100)
100     FORMAT( 11X,'600',23X,'WIDTH OF X''CHGR SURFACES',14X,
     #  9X,'METERS')
        WRITE(5,110)
110     FORMAT( 11X,'700',23X,'NUMBER OF HOT PASSAGES',16X,
     #  12X,'-')
        WRITE(5,120)
120     FORMAT( 11X,'800',23X,'NUMBER OF COLD PASSAGES',15X,
     #  12X,'-')
        WRITE(5,130)
130     FORMAT( 11X,'900',23X,'NUMBER OF X''CHGR SURFACES',13X,
     #  12X,'-')
        RETURN
        END
*                                                                      *
************************************************************************
*                                                                      *
*          SUBROUTINE TO CACULATE THE CORE                             *
*          TEMPERATURE AT LOCATION 4 TO                                *
*          DETERMINE IF FROST IS FORMING                               *
*                                                                      *
************************************************************************
*                                                                      *
        SUBROUTINE ITEMP
        COMMON/CBLK1/T(8),PROP(5,8),PWS(8),PW(8),DPWSDT(8),
     1              DWDT(8),DENTDT(8),C(8),RE(8),H(8),F(8),SVAPP(61)
        COMMON/CBLK2/XX,XXLOW,XXHIGH
        COMMON/CBLK5/MFRH,MFRC,NH,NC,WDTH,S,OMFRH,OMFRC
        COMMON/CBLK7/NS,L,DW,KW,TEMPIN(4),TEMPSU(4)
        COMMON/CBLK8/RF,Q,DC,KC,NFLPRT
        COMMON/CBLK10/FROSTH(0:41),FROSTT(0:41),DHC(4),PFAN,FSCOND,
     #          DHTC(0:41),DHCEND(4),FHMAX,XOMAX,FROSTP,DPO,TOTDP
        REAL KW,L,MFRH,MFRC,KC
*                                                                      *
```

```
*--------CACULATE THE PLATE TEMPERATURE-------------------------------*
*                                                                      *
        DO 1 I=1,4
                RES=1/H(I+4)+DW/KW
                REST=RES+1/H(I)+DHCEND(I)
                IF(I.GT.2) REST=REST+DC/KC
                DT=(T(I)-T(I+4))*(RES/REST)
                TEMPIN(I)=DT+T(I+4)-273.16
*                                                                      *
*--------CACULATE SURFACE TEMPERATURE OF THE FROST--------------------*
*                                                                      *
                RES=RES+DHCEND(I)
                IF(I.GT.2) RES=RES+DC/KC
                DT=(T(I)-T(I+4))*(RES/REST)
                TEMPSU(I)=DT+T(I+4)-273.16
1       CONTINUE
        DO 2 I=1,4
                IF(MFRC.LE.0.007) TEMPIN(I)=0.1
2       CONTINUE
        IF(XX.EQ.L) TEMPIN(3)=TEMPIN(2)
        IF(XX.EQ.L) TEMPIN(4)=TEMPIN(2)
        IF(XX.EQ.L) TEMPSU(3)=TEMPSU(2)
        IF(XX.EQ.L) TEMPSU(4)=TEMPSU(2)
        RETURN
        END
**********************************************************************
*                                                                      *
*               SUBROUTINE:DRY                                         *
*       THIS SUBROUTINE CACULATES THE PARAMETERS FOR THE               *
*       DRY PORTION OF THE HEAT EXCHANGER                              *
*                                                                      *
**********************************************************************
*                                                                      *
        SUBROUTINE DRY
        COMMON/CBLK1/T(8),PROP(5,8),PWS(8),PW(8),DPWSDT(8)
     #          ,DWDT(8),DENTDT(8),C(8),RE(8),H(8),F(8),SVAPP(61)
        COMMON/CBLK2/XX,XXLOW,XXHIGH
        COMMON/CBLK5/MFRH,MFRC,NH,NC,WDTH,S,OMFRH,OMFRC
        COMMON/CBLK7/NS,L,DW,KW,TEMPIN(4),TEMPSU(4)
        COMMON/CBLK8/RF,Q,DC,KC,NFLPRT
        COMMON/CBLK9/TIME,TISTEP,TIEND,CT,DLMASS,CONERR,PEAKQ,CONDIR,
     #          NSTFLG,CNTIME,CNTSTP,CGAIN,NS2FLG
        COMMON/CBLK10/FROSTH(0:41),FROSTT(0:41),DHC(4),PFAN,FSCOND,
     #          DHTC(0:41),DHCEND(4),FHMAX,XOMAX,FROSTP,DPO,TOTDP
        COMMON/CBLK11/UDRY,UWET,QDRY,QWET
        COMMON/CBLK12/ISTFLG
        REAL KW,L,NTU,KC,MFRH,MFRC,LMTD
        IF(ISTFLG.EQ.1) GOTO 6
        IF(TIME.GT.0.0) CALL ITEMP
        CALL SATVAP
        CALL HUMRAT
```

```
      CALL PROPS
      CALL ENTHAL
      CALL HTCPRT
      CALL REYNLD
      CALL FRICFC
      CALL TRNCOF
6     HH=(H(1)+H(2))/2.0
      HC=(H(5)+H(6))/2.0
      CH=(C(1)+C(2))/2.0
      CC=(C(5)+C(6))/2.0
      DHCH=(DHC(1)+DHC(2))/2.0
      IF(CH.GT.CC) GOTO 2
      CMIN=CH
      CMAX=CC
      GOTO 3
2     CMIN=CC
      CMAX=CH
3     R=CMIN/CMAX
      UDRY=1/(1/HH+1/HC+RF+DW/KW+DHCH)
      NTU=UDRY*NS*WDTH*XX/CMIN
      EFF=(1-EXP(-NTU*(1-R)))/(1-R*EXP(-NTU*(1-R)))
      QDRY=EFF*CMIN*(T(1)-T(6))
      THO=T(1)-QDRY/CH
      TCO=QDRY/CC+T(6)
      T(2)=THO
      T(5)=TCO
      RETURN
      END
*****************************************************************
*                                                               *
*              SUBROUTINE:WET                                   *
*       THIS SUBROUTINE CACULATES THE PARAMETERS FOR THE        *
*       WET PORTION OF THE HEAT EXCHANGER                       *
*                                                               *
*****************************************************************
*                                                               *
      SUBROUTINE WET
      COMMON/CBLK1/T(8),PROP(5,8),PWS(8),PW(8),DPWSDT(8)
     #          ,DWDT(8),DENTDT(8),C(8),RE(8),H(8),F(8),SVAPP(61)
      COMMON/CBLK2/XX,XXLOW,XXHIGH
      COMMON/CBLK5/MFRH,MFRC,NH,NC,WDTH,S,OMFRH,OMFRC
      COMMON/CBLK7/NS,L,DW,KW,TEMPIN(4),TEMPSU(4)
      COMMON/CBLK8/RF,Q,DC,KC,NFLPRT
      COMMON/CBLK10/FROSTH(0:41),FROSTT(0:41),DHC(4),PFAN,FSCOND,
     #          DHTC(0:41),DHCEND(4),FHMAX,XOMAX,FROSTP,DPO,TOTDP
      COMMON/CBLK11/UDRY,UWET,QDRY,QWET
      COMMON/CBLK12/ISTFLG
      REAL KW,L,NTU,KC,MFRH,MFRC,LMTD
      IF(ISTFLG.EQ.1) GOTO 6
      CALL ITEMP
      CALL SATVAP
```

```
      CALL HUMRAT
      CALL PROPS
      CALL ENTHAL
      CALL HTCPRT
      CALL REYNLD
      CALL FRICFC
      CALL ENHANCE
      CALL TRNCOF
6     HH=(H(3)+H(4))/2.0
      HC=(H(7)+H(8))/2.0
      CH=(C(3)+C(4))/2.0
      CC=(C(7)+C(8))/2.0
      DHCH=(DHC(3)+DHC(4))/2.0
      IF(CH.GT.CC) GOTO 2
      CMIN=CH
      CMAX=CC
      GOTO 3
2     CMIN=CC
      CMAX=CH
3     R=CMIN/CMAX
      UWET=1/(1/HH+1/HC+RF+DW/KW+DC/KC+DHCH)
      NTU=UWET*NS*WDTH*(L-XX)/CMIN
      EFF=(1-EXP(-NTU*(1-R)))/(1-R*EXP(-NTU*(1-R)))
      QWET=EFF*CMIN*(T(3)-T(8))
      THO=T(3)-QWET/CH
      TCO=QWET/CC+T(8)
      T(4)=THO
      T(7)=TCO
      RETURN
      END
*****************************************************************
*                                                               *
*           SUBROUTINE REINIT                                   *
*      IF THE EXIT PLATE TEMPERATURE IS GREATER THAN OC         *
*      FOR THE CONDENSING PORTION BUT THE EXCHANGER IS DRY      *
*      SET THE FROST HEIGHT AND TIME TO ZERO                    *
*****************************************************************
*                                                               *
      SUBROUTINE REINIT
      COMMON/CBLK10/FROSTH(0:41),FROSTT(0:41),DHC(4),PFAN,FSCOND,
     #          DHTC(0:41),DHCEND(4),FHMAX,XOMAX,FROSTP,DPO,TOTDP
      DO 1 I=0,41
      FROSTH(I)=0.0
      FROSTT(I)=0.0
      DHTC(I)=0.0
1     CONTINUE
      RETURN
      END
*****************************************************************
*                                                               *
*             SUBROUTINE FROST                                  *
```

```
*       A SUBROUTINE TO CACULATE THE FROST HEIGHT, THE                *
*       CHANCE IN HEAT TRANSFER COEFFICIENT AND THE CHANGE            *
*       IN MASS FLOW RATE                                             *
*                                                                     *
***********************************************************************
*                                                                     *
        SUBROUTINE FROST
        COMMON/CBLK1/T(8),PROP(5,8),PWS(8),PW(8),DPWSDT(8)
     #          ,DWDT(8),DENTDT(8),C(8),REN(8),H(8),F(8),SVAPP(61)
        COMMON/CBLK2/XX,XXLOW,XXHIGH
        COMMON/CBLK3/KTA,KTW,KVA,KVW,PRA,PRW,CPA,CPW
        COMMON/CBLK4/W(8),PATM,RLHMHI,RLHMCI
        COMMON/CBLK5/MFRH,MFRC,NH,NC,WDTH,S,OMFRH,OMFRC
        COMMON/CBLK7/NS,L,DW,KW,TEMPIN(4),TEMPSU(4)
        COMMON/CBLK8/RF,Q,DC,KC,NFLPRT
        COMMON/CBLK9/TIME,TISTEP,TIEND,CT,DLMASS,CONERR,PEAKQ,CONDIR,
     #          NSTFLG,CNTIME,CNTSTP,CGAIN,NS2FLG
        COMMON/CBLK10/FROSTH(0:41),FROSTT(0:41),DHC(4),PFAN,FSCOND,
     #          DHTC(0:41),DHCEND(4),FHMAX,XOMAX,FROSTP,DPO,TOTDP
        REAL KW,L,MFRH,MFRC,KC,K,KV,KTA,KTW,KVA,KVW,IWT,M,M2,M3,
     #       DHTCT(4),IT(4)
*                                                                     *
*---------INITIALIZE VARIABLES-----------------------------------------*
*                                                                     *
        WO=0.62198*(0.61117/(PATM-0.61117))
        TO=273.16
        TPLAST=273.17
        FHMAX=0.0
        XOMAX=0.0
        DP=0.0
        TPFLG=0.0
        FROSTP=0.0
        RE=0.0
        KV=0.0
        DEN=0.0
        DO 24 I=1,4
        IT(I)=0
        DHTCT(I)=0.0
        DHC(I)=0.0
24      CONTINUE
*                                                                     *
*---------DO LOOP TO CACULATE FROST CONDITIONS AT A--------------------*
*         NUMBER OF POINTS IN THE HEAT EXCHANGER                      *
*                                                                     *
        DO 1 I=0,41
        IF(I.LE.20) DELXO=XX/20.0
        IF(I.GT.20) DELXO=(L-XX)/20.0
        IF(DELXO.EQ.0.0) GOTO 1
        IF(I.LE.20) XO=DELXO*I
        IF(I.GT.20) XO=DELXO*(I-21)+XX
*                                                                     *
```

```
*---------ESTIMATE THE PLATE TEMPERATURE------------------------ -*
*                                                                  *
      IF(I.LE.20) TP=(TEMPIN(2)*XO+TEMPIN(1)*(XX-XO))/XX
      IF(I.GT.20) TP=(TEMPIN(4)*(XO-XX)+TEMPIN(3)*(L-XO))/(L-XX)
      TP=TP+273.16
*                                                                  *
*----------CACULATE THE HOT AIR TEMPERATURE-----------------------*
*                                                                  *
      IF(I.LE.20) TA=(T(2)*XO+T(1)*(XX-XO))/XX
      IF(I.GT.20) TA=(T(4)*(XO-XX)+T(3)*(L-XO))/(L-XX)
*                                                                  *
*----------CACULATE THE COLD AIR TEMPERATURE----------------------*
*                                                                  *
      IF(I.LE.20) TC=(T(6)*XO+T(5)*(XX-XO))/XX
      IF(I.GT.20) TC=(T(8)*(XO-XX)+T(7)*(L-XO))/(L-XX)
*                                                                  *
*----------CACULATE THE HOT SIDE HEAT TRANSFER COEFFICIENT--------*
*                                                                  *
      IF(I.LE.20) HH=(H(2)*XO+H(1)*(XX-XO))/XX
      IF(I.GT.20) HH=(H(4)*(XO-XX)+H(3)*(L-XO))/(L-XX)
*                                                                  *
*----------CACULATE THE COLD SIDE HEAT TRANSFER COEFFICIENT-------*
*                                                                  *
      IF(I.LE.20) HC=(H(6)*XO+H(5)*(XX-XO))/XX
      IF(I.GT.20) HC=(H(8)*(XO-XX)+H(7)*(L-XO))/(L-XX)
*                                                                  *
*----------CACULATE THE LOCAL HUMIDITY RATIO----------------------*
*                                                                  *
      TT=TA-273.16+31.0
      J=INT(TT)
      PWSF=(TT-J)*SVAPP(J+1)+(J+1-TT)*SVAPP(J)
      IF(I.EQ.0) PWF=PWSF*RLHMHI
      IF(I.GT.20) PWF=PWSF
      WA=.62198*(PWF/(PATM-PWF))
*                                                                  *
*---------CHECK IF PLATE TEMPERATURE OC OR GREATER----------------*
*                                                                  *
18    IF(TP.GE.273.16) FROSTH(I)=0.0
      IF(TP.GE.273.16) FROSTT(I)=0.0
      IF(TP.GE.273.16) DHTC(I)=0.0
      IF(TP.GE.273.16) GOTO 5
*                                                                  *
*---------FOR THE PLATE TEMPERATURE LESS THAN 0C------------------*
*                                                                  *
*---------CACULATE THE THERMAL CONDUCTIVITY----------------------*
*                      KINEMATIC VISCOSITY                         *
*                      PRANDTL NUMBER                              *
*                      DENSITY                                     *
*                      REYNOLDS NUMBER                             *
*        OF THE FREE STREAM AIR                                    *
*                                                                  *
```

```
      CALL PRPINT(TA)
            K  =(KTA+WA*KTW)/(1+WA)
            KV =(KVA+WA*KVW)/(1+WA)
            PR =(PRA+WA*PRW)/(1+WA)
            DEN=PATM*1000.0/(287.0*TA*(1.0+1.6078*WA))
*                                                                      *
*----------REYNOLDS NUMBER IS CACULATED ON THE PAST MFRH----------*
*                                                                      *
            RE=MFRH/NH*(1+WA)*2/(DEN*KV*WDTH)
*                                                                      *
*---------CHECK IF DEWPOINT BELOW FREEZING : IF THE----------------*
*         CASE THEN THE FROST COVER REMAINS UNCHANGED                  *
*                                                                      *
      IF(WA.LE.WO) GOTO 9
*                                                                      *
*--------CACULATE THE FROST TIME ---------------------------------*
*                                                                      *
      FROSTT(I)=FROSTT(I)+TISTEP
*                                                                      *
*---------CHECK IF PLATE TEMPERATURE OC OR GREATER----------------*
*                                                                      *
9     IF(TP.GE.273.16) FROSTH(I)=0.0
      IF(TP.GE.273.16) FROSTT(I)=0.0
      IF(TP.GE.273.16) DHTC(I)=0.0
      IF(TP.GE.273.16) GOTO 5
*                                                                  *
*    A) FROST HEIGHT                                               *
*                                                                  *
      IF(WA.LE.WO) FH=FROSTH(I)
      IF(WA.LE.WO) GOTO 19
      FH=0.466*(FROSTT(I)**0.663)*(RE**0.393)*
     #      (((TO-TP)/TO)**0.705)*(((WA-WO)/WO)**0.098)/1000.0
*                                                                  *
*    B) FROST DENSITY                                              *
*                                                                  *
*                                                                  *
*    C) FROST THERMAL CONDUCTIVITY                                 *
*                                                                  *
19    COND=FSCOND
*                                                                  *
*    D) FROST THERMAL RESISTANCE                                   *
*                                                                  *
      DHTC(I)=FH/COND
      RES=1/HC+DW/KW
      IF(I.LE.20) REST=RES+1/HH+DHTC(I)
      IF(I.GT.20) REST=RES+1/HH+DHTC(I)+DC/KC
      DT=(TA-TC)*(RES/REST)
      TPNEW=DT+TC
      IF(ABS(TP-TPNEW).LT.0.10) GOTO 12
      IF(TP.LT.273.16.AND.TPNEW.GT.273.16) TPFLG=1.0
      IF(TPFLG.EQ.1.0) TPHOLD=TP
```

```
        TP=TPNEW
        GOTO 9
*                                                                      *
*---------LOCATION OF FROST FRONT-----------------------------------*
*                                                                      *
12      IF(FROSTP.EQ.0.0) FROSTP=XO
*                                                                      *
*--------ENSURE FROST CANNOT GO BACKWARD IN TIME---------------------*
*        EXCEPT DURING DEFROST                                         *
*                                                                      *
        IF(NSTFLG.EQ.0.AND.FH.LT.FROSTH(I)) FROSTH(I)=FH
        IF(NSTFLG.EQ.0.AND.TIME.GT.1.0) GOTO 16
        IF(FH.GT.FROSTH(I)) FROSTH(I)=FH
16      DHTC(I)=FROSTH(I)/COND
5       CIT=1.0
        IF(I.EQ.0.OR.I.EQ.20.OR.I.EQ.21.OR.I.EQ.41) CIT=0.5
        IF(I.EQ.0.OR.I.EQ.20.OR.I.EQ.21.OR.I.EQ.41) DHTC(I)=DHTC(I)*0.5
*                                                                      *
*--------CACULATE AN AVERAGE HEAT TRANSFER RESISTANCE-------------------*
*                                                                      *
        IF(TPFLG.EQ.1.0) TP=TPHOLD
        TPFLG=0.0
        IF(I.LT.10) MC=1
        IF(I.GE.10.AND.I.LE.20) MC=2
        IF(I.GE.21.AND.I.LE.30) MC=3
        IF(I.GT.30) MC=4
        DHTCT(MC)=DHTCT(MC)+DHTC(I)
        IT(MC)=IT(MC)+CIT
*       IF((TIME-2.58).GT.0.0) WRITE(22,853) I,TP,TA,TC,HH,HC,WA,DEN,
*     #                              KV,RE,DHTC(I),FROSTT(I),FROSTH(I)
*853    FORMAT( 1X,'I ',I2,' TP ',F6.2,' TA ',F6.2,' TC ',F6.2,' HH ',
*     #          F6.2,' HC ',F6.2,' WA ',F6.5,' D ',F6.4,' V ',E9.3,
*     #           ' RE ',F6.1,' DHTC ',F6.5,' FT ',F6.4,' FH ',F6.5)
        IF(I.EQ.0)  DHCEND(1)=DHTC(0)*2.0
        IF(I.EQ.20) DHCEND(2)=DHTC(20)*2.0
        IF(I.EQ.21) DHCEND(3)=DHTC(21)*2.0
        IF(I.EQ.41) DHCEND(4)=DHTC(41)*2.0
        IF(FROSTH(I).GT.FHMAX) FHMAX=FROSTH(I)
        IF(FROSTH(I).EQ.FHMAX) XOMAX=XO
        TPLAST=TP
1       CONTINUE
        LMT=4
        IF(DELXO.EQ.0) LMT=2
        DO 7 I=1,LMT
        DHC(I)=DHTCT(I)/IT(I)
7       CONTINUE
        IF(DELXO.EQ.0) DHCEND(4)=DHCEND(2)
*                                                                      *
*-------CACULATE A NEW MASS FLOW RATE ON THE HOT SIDE-----------------*
*                                                                      *
        V1=1.0/PROP(5,1)
```

```
      V2=1.0/PROP(5,4)
      C9=9.5
      O9=OMFRH
*                                                                     *
*--------CACULATE AN AVERAGE PASSAGE SPACING----------------------*
*                                                                     *
      FHAVE=FHMAX
      A1=WDTH*(S-FHAVE)*NH
      A=WDTH*L*2.0*NH
      DO 22 M=OMFRH,0,-0.0005
      G=M*(1+W(1))/A1
      F9=(F(1)+F(2)+F(3)+F(4))/4.0
      Z1=1.05*C9
      Z2=2.0*(V2/V1-1.0)
      Z3=F9*(A/A1)*((V1+V2)/(2.0*V1))
      Z4=-0.35*V2/V1
      DP=(G**2.0*V1/2.0)*(Z1+Z2+Z3+Z4)
      IF(TIME.EQ.TISTEP) DPO=DP
      DP=DP-DPO
      IF(DP.GE.(PFAN-DPO)) GOTO 22
      M2=(((PFAN-DPO)-DP)/(PFAN-DPO))**0.5*OMFRH*(1+W(1))
      IF(ABS(M*(1+W(1))-M2).LT.O9) O9=ABS(M*(1+W(1))-M2)
      IF(ABS(M*(1+W(1))-M2).LT.09) TOTDP=DP+DPO
      IF(ABS(M*(1+W(1))-M2).EQ.O9) M3=M
      IF(ABS(M*(1+W(1))-M2).GT.O9) GOTO 23
22    CONTINUE
23    MFRH=M3
      RETURN
      END
*********************************************************************
*                                                                   *
*          SUBROUTINE CONTROL                                       *
*      OPTIMIZATION SUBROUTINE                                      *
*                                                                   *
*********************************************************************
*     SUBROUTINE CONTROL
*     COMMON/CBLK5/MFRH,MFRC,NH,NC,WDTH,S,OMFRH,OMFRC
*     COMMON/CBLK7/NS,L,DW,KW,TEMPIN(4),TEMPSU(4)
*     COMMON/CBLK8/RF,Q,DC,KC,NFLPRT
*     COMMON/CBLK9/TIME,TISTEP,TIEND,CT,DLMASS,CONERR,PEAKQ,CONDIR,
*    #          NSTFLG,CNTIME,CNTSTP,CGAIN,NS2FLG
*     REAL KW,L,MFRH,MFRC,KC
**                                                                  *
**--------PROPORTIONAL CONTROL SECTION-----------------------------*
**                                                                  *
*     IF(NSTFLG.EQ.1) GOTO 1
*     IF(TEMPIN(4).GT.0.0) NSTFLG=1
*     IF(NSTFLG.EQ.1) CNTIME=TIME
*     IF(NSTFLG.EQ.1) GOTO 2
*     DMASS=(1.0-TEMPIN(4))*CGAIN*OMFRC
*     IF(DMASS.GE.MFRC) DMASS=MFRC/2.0
```

```
*       MFRC=MFRC-DMASS
*       GOTO 11
**                                                                    *
**-------------OPTIMALIZING CONTROL SECTION-----------------------*
**                                                                    *
*       IF((TIME-CNTIME).LT.CNTSTP) GOTO 11
*       CNTIME=CNTIME+CNTSTP
*2      WRITE(5,5) Q,PEAKQ
*5      FORMAT( 5X,'Q= ',F12.2,' PEAKQ= ',F12.2)
*       IF(Q.GT.PEAKQ) PEAKQ=Q
*       DELTA=PEAKQ-Q
*       IF(DELTA.GT.CONERR) CONDIR=CONDIR*-1.0
*       IF(DELTA.GT.CONERR) PEAKQ=Q
*       MFRC=MFRC+DLMASS*CONDIR
*       IF(MFRC.GT.OMFRC) MFRC=OMFRC
*11     RETURN
*       END
*********************************************************************
*                                                                   *
*        SUBROUTINE CONTROL                                         *
*     MONITORS THE CHANGE OF THE SUPPLY AIR TEMPERATURE             *
*     THROUGH THE HEAT EXCHANGER AND DEFROSTS THE EXCHANGER IF      *
*     IT INCREASES OR DECREASES SIGNIFICANTLY                       *
*                                                                   *
*********************************************************************
       SUBROUTINE CONTROL
       COMMON/CBLK1/T(8),PROP(5,8),PWS(8),PW(8),DPWSDT(8)
     #          ,DWDT(8),DENTDT(8),C(8),RE(8),H(8),F(8),SVAPP(61)
       COMMON/CBLK2/XX,XXLOW,XXHIGH
       COMMON/CBLK5/MFRH,MFRC,NH,NC,WDTH,S,OMFRH,OMFRC
       COMMON/CBLK7/NS,L,DW,KW,TEMPIN(4),TEMPSU(4)
       COMMON/CBLK8/RF,Q,DC,KC,NFLPRT
       COMMON/CBLK9/TIME,TISTEP,TIEND,CT,DLMASS,CONERR,HOLDT,CONDIR,
     #          NSTFLG,CNTIME,CNTSTP,CGAIN,NS2FLG
       REAL KW,L,MFRH,MFRC,KC
*                                                                     *
*--------CHECK IF DEFROST IS REQUIRED-----------------------------*
*                                                                     *
*         NSTFLG INDICATES DEFROST IS REQUIRED                        *
*         NS2FLG INDICATES IF EXHAUST TEMPERATURE MUST BE RAISED      *
*                                                                     *
       IF(TIME.LT.CNTIME) GOTO 3
       CNTIME=CNTIME+CNTSTP
       IF(TIME.EQ.0.0) GOTO 1
       IF(NSTFLG.EQ.0) GOTO 1
2      IF(NS2FLG.EQ.0) GOTO 4
       IF(CONDIR.EQ.1.0) HOLDT=T(5)-T(8)
       IF(CONDIR.EQ.1.0) CONDIR=0.0
       DT=(T(5)-T(8))-HOLDT
       IF(DT.LT.CONERR) NSTFLG=0
       IF(DT.GT.2.0)  NSTFLG=0
```

```
      IF(NSTFLG.EQ.0) GOTO 1
      GOTO 3
*                                                                     *
*------ASSURE EXHAUST OUTLET TEMPERATURE IS GREATER THAN 0.5C-- ---*
*                                                                     *
4     DMASS=(2.5-(T(4)-273.16))*CGAIN*OMFRC
      MFRC=MFRC-DMASS
      IF(MFRC.GT.OMFRC) MFRC=OMFRC
      IF(MFRC.EQ.OMFRC) NS2FLG=1
      IF(ABS(275.66-T(4)).LT.1.0) NS2FLG=1
      GOTO 3
*                                                                     *
*---------DEFROST CYCLE-----------------------------------------------*
*                                                                     *
1     NS2FLG=0
      IF(TEMPIN(4).GT.0.0.OR.MFRC.LE.0.007) NSTFLG=1
      IF(TEMPIN(4).GT.0.0.OR.MFRC.LE.0.007) CONDIR=1.0
      IF(NSTFLG.EQ.1) GOTO 2
      WRITE(5,11)
11    FORMAT( 10X,'DEFROST CYCLE')
      DMASS=(1.0-TEMPIN(4))*CGAIN*OMFRC
      IF(DMASS.GE.MFRC) DMASS=MFRC/2.0
      MFRC=MFRC-DMASS
3     RETURN
      END
```